



Republic of Iraq

Ministry of Higher Education & Scientific Research

University of Kerbala

College of Engineering

Mechanical Engineering Department

Theoretical and Experimental Investigations of 3D-Printed Sandwich Panels Used in Aircraft Structure

A Thesis Submitted to the Council of the Faculty of the College of the Engineering/University Of Kerbala in Partial Fulfillment of the Requirements for the Master Degree in Mechanical Engineering

By:

Hayder Abduljabbar Sabah

BSc. Mechanical Engineering / University of Babylon 2002

Supervisors

Prof. Dr. Muhsin J. Jweeg

Lect. Dr. Ahmed K. Hassan

July 2023

Dhu al-Hijjah 1444

بِسْمِ اللَّهِ الرَّحْمَنِ الرَّحِيمِ

يَرْفَعِ اللَّهُ الَّذِينَ آمَنُوا مِنْكُمْ وَالَّذِينَ أُوتُوا

الْعِلْمَ دَرَجَاتٍ

صدق الله العلي العظيم

(المجادلة: من الآية 11)

Examination committee certification

We certify that we have read the thesis entitled " **Theoretical and Experimental Investigations of 3D-Printed Sandwich Panels Used in Aircraft Structure** " and as an examining committee, we examined the student " **Hayder Abduljabbar Sabah** " in its content and in what is connected with it and that, in our opinion, it is adequate as a thesis for the degree of Master of Science in Mechanical Engineering.

Supervisor

Signature: M. J. Jweeg

Prof. Dr. Muhsin J. Jweeg

Date: / / 2023

Supervisor

Signature: Ahmed K. Hassan

Lect. Dr. Ahmed K. Hassan

Date: / / 2023

Member

Signature: A.M. Aboud

Assist. Prof. Dr. Amjad

Al-Hamood

Date: / / 2023

Member

Signature: Muslim

Assist. Prof. Dr. Muslim

Muhsin Ali

Date: / / 2023

Chairman

Signature: Mohsin

Prof. Dr. Mohsin A. Al-Shammari

Date: / / 2023

Signature: H. J. K.

Assist. Prof. Dr. Hayder Jabber Kurji
Head of the Department of Mechanical
Engineering

Date: / / 2023

Signature: h. Sh. Rasheed

Prof. Dr. Laith Shakir
Rasheed
Dean of the Engineering College

Date: / / 2023

Supervisor certificate

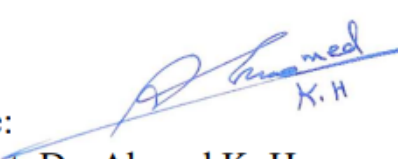
We certify that the thesis entitled "**Static and Dynamic Effectiveness of A Core Density of Sandwich Panels used in A/C Structures - Theoretical and Experimental Investigations**" was prepared by **Hayder Abduljabbar Sabah**, under our supervision at the Department of Mechanical Engineering, Faculty of Engineering, University of Kerbala as a partial of fulfilment of the requirements for the Degree of Master of Science in Mechanical Engineering.

Signature:

Prof. Dr. Muhsin J. Jweeg

Date: / / 2023

Signature:


Lect. Dr. Ahmed K. Hassan

Date: 5/ 6 / 2023

Linguistic certificate

I certify that the thesis entitled "**Static and Dynamic Effectiveness of A Core Density of Sandwich Panels used in A/C Structures - Theoretical and Experimental Investigations**" which has been submitted by **Hayder Abduljabbar Sabah**, has been proofread, and its language has been amended to meet the English style.

Signature:



Assist. Prof. Dr Ashwan A. Abdulmunem

Date: 5 / 6 / 2023

Undertaking

I certify that research work titled " Theoretical and Experimental Investigations of 3D-Printed Sandwich Panels Used in Aircraft Structure " is my own work. The work has not been presented elsewhere for assessment. Where material has been used from other sources, it has been properly acknowledged / referred.

Signature:

Hayder Abduljabbar Sabah

Date: / / 2023

Acknowledgments

I would like to express my thanks to "Allah", the Most Gracious and Most Merciful, his prophet "Mohammad", and to the family of the Prophet (Muhammad), may God's prayers and peace be upon them, for enabling me to complete this study. I introduce my thanks to my supervisors, Prof. Dr. Muhsin J. Jweeg and Dr. Ahmed K. Hassan, for their valuable guidance, assistance, cooperation, and motivation throughout preparing my thesis. I would like to thank Assistant Prof. Dr. Laith Shakir Rasheed, the Dean of the College of Engineering at Karbala University. Also, I would like to thank the Head of the Department of Mechanical Engineering, Dr. Hayder Jabber Kurji, Dr. Mohammad Wahab, and the teaching staff in the Department of Mechanical Engineering for their help and support throughout my year of study. Also, I extend my heartfelt thanks to my family, all my friends, and anyone who helped me with this work.

Hayder Abduljabbar Sabah

Abstract

Sandwich panels, which often consist of two face sheets attached to a honeycomb or foam core. Sandwiches have been utilized in a variety of applications, such as wind energy systems, ships, and aircraft. In this study, the regular hexagonal honeycomb core type is studied utilizing the available analytical solutions that involve finding the relation between core density and the total deflection of sandwiches under bending loads. Whereas, in a practical study, sandwich samples with various core densities were manufactured in regular hexagonal, triangular, and overlapped octagonal core configurations, utilizing 3D printing technology with the PLA (polylactic acid) material by adjusting the core density value to three magnitudes (105 kg/m³, 132 kg/m³, and 160 kg/m³) using cell size as the sole governing parameter in density value. These samples are subjected to a flexural test according to the standard (ASTM C393-00) to find deflection, stiffness, and consequently the effect of variation in core density for each type. Then, the theoretical conclusions, followed by experimental test results, are compared with the numerical results generated by the simulation software "Ansys" to provide a clear idea of how the density of the core will impact the mechanical characteristics of the sandwich and reveal the superior core type. Additionally, impact resistance is significantly influenced by core density variation, so to explore that, samples with different core densities were subjected to the simulation of a tower drop test. Moreover, a numerical evaluation was carried out to determine the effect of core density on natural frequencies and explore the behavior of sandwiches under repeated loads. Finally, the experimental results demonstrate that an increase in core density by 25.7% and 52.4% leads to more stiffness by 8.14% and 16.75% in a hexagonal core, 8.43% and 28.1% in a triangular core, and 10.94% and 19.04% in an

octagonal core. Besides, the overlapped octagonal and triangular cores are more stiff than hexagonal. Regarding impact exploration, it can be deduced that increasing the density of the core increased the sandwich's resistance to impacts and that the regular hexagonal core has greater impact resistance than the triangular core. Additionally, the results show that increases in core density of 25.7% and 52.4% lead to a slight drop in the value of natural frequencies, at least in the first mode.

Keywords:

Sandwich Panel, A/C, Core Density, Stiffness, 3D Printing, 3-Point Bending, ASTM C393-00, Impact, and Natural Frequency.

Table of Contents

Examination committee certification.....	3
Supervisor certificate	iv
Linguistic certificate	v
Undertaking	vi
Acknowledgments	vii
Abstract.....	viii
Table of Contents.....	x
List of Tables	xvi
List of Figures.....	xviii
List of Abbreviations	xxiii
List of Symbols.....	xxiv
Chapter One: Introduction	1
1.1 General.....	1
1.2 Aircraft Structure.....	2
1.3 Sandwich Panel.....	3
1.3.1 Skins.....	6
1.3.2 Core.....	7
1.4 Cellular Materials	8
1.5 Sandwich Structure Optimization	9
1.6 Honeycomb Sandwich in A/C.....	10
1.7 The aim of study	11
1.8 Objectives of work.....	11
Chapter Two: Literature Review	13

2.1	Introduction	13
2.2	Static Conditions.....	13
2.3	Dynamic Conditions	19
2.4	Concluding Remarks	22
Chapter Three: Theoretical and Numerical Analysis		23
3.1	Introduction	23
3.2	Honeycomb Core.....	23
3.2.1	Hexagonal core	24
3.2.1.1	Core Density.....	25
3.2.2	Triangular Core.....	27
3.2.2.1	Core Density.....	28
3.2.3	Overlapped Octagonal Core.....	29
3.2.3.1	Core Density of Overlapped Octagonal Configuration	29
3.3	Theoretical Solution to Find Deflection of Sandwich Structure	31
3.4	Numerical Solution to Find Deflection of Sandwich Structure	35
3.4.1	Boundary Conditions of flexural loading	35
3.4.2	Regular Hexagonal Core Meshing.....	36
3.4.3	Triangular Core Meshing.....	36
3.4.4	Overlapped Octagonal Core Meshing.....	37
3.5	Numerical Solution of the Other Orientation.....	37
3.5.1	Regular Hexagonal Honeycomb Core Orientation.....	38

3.5.2	Triangular Honeycomb Core Orientation	39
3.5.3	Overlapped Octagonal Core Orientation	41
3.6	Free Vibration Analysis.....	43
3.6.1	Boundary Conditions For Free Vibration Analysis	43
3.7	Impact Analysis	45
3.7.1	Boundary Conditions For Impact Analysis	45
3.7.2	Impact Test of Regular Hexagonal Honeycomb Core...	46
3.7.3	Impact Test of Triangular Honeycomb Core.....	47
3.8	Wing Analysis	48
3.8.1	Airfoil.....	48
3.8.2	Wing Structure	48
3.8.3	Boundary Conditions For Wing.....	49
3.8.4	Wing Meshing.....	50
Chapter Four: Experimental Work		51
4.1	General.....	51
4.2	Core Configurations	51
4.3	Experimental test	53
4.3.1	The standard (ASTM C393-00) Scope.....	53
4.3.2	Test Specimen Dimensions.....	54
4.4	Prepare samples	55
4.4.1	3D Printing.....	55
4.4.2	3D Printer	56
4.4.3	Filament	56
4.4.4	CAD Program	57

4.4.5	Slicing program.....	57
4.4.6	Specimens printing process	58
4.4.6.1	Regular Hexagonal Honeycomb Core Manufacturing 59	
4.4.6.2	The Triangular Honeycomb Core Manufacturing ...	64
4.4.6.3	The Overlapped Octagonal Core Manufacturing.....	68
4.5	Specimens testing	72
4.6	Filament Material Mechanical Properties	74
4.6.1	Experimental Test	74
4.6.1.1	Samples preparing	74
4.6.2	Tensile Specimens testing.....	77
4.7	Filament Material's Physical Properties	79
4.7.1	Filament Material's Density	79
Chapter Five: Results and Discussion.....		80
5.1	General.....	80
5.2	Properties Results	80
5.2.1	Tensile Test Results	80
5.2.2	Density Determination Results	81
5.3	Results of Regular Hexagonal Honeycomb Core Tests	82
5.3.1	Theoretical Results of Regular Hexagonal Honeycomb Core	82
5.3.2	Numerical Results of Regular Hexagonal Honeycomb Core	85
5.3.3	Experimental Results of Regular Hexagonal Honeycomb Core	87

5.4	Results of Triangular Honeycomb Core Tests	89
5.4.1	Numerical Results of Triangular Honeycomb Core Tests	90
5.4.2	Experimental Results of Triangular Honeycomb Core Tests	92
5.5	Results of Overlapped Octagonal Core Tests	94
5.5.1	Numerical Results of Overlapped Octagonal Core Tests	95
5.5.2	Experimental Results of Overlapped Octagonal Core Tests	97
5.6	Variation in mechanical properties according to the orientation	100
5.6.1	Results of hexagonal core tests according to the orientation	101
5.6.2	Results of Triangular core tests according to the orientation	102
5.6.3	Results of Overlapped Octagonal Core tests according to the orientation	103
5.7	Results of a Free Vibration Analysis.....	105
5.8	Results of Impact Simulation Tests.....	106
5.8.1	Results of Impact of Regular Hexagonal Honeycomb Core	106
5.8.2	Results of Impact Triangular Honeycomb Core	109
5.9	Wing Simulation.....	111
Chapter Six:	Conclusions and Recommendations.....	113

6.1	Core density effects on the stiffness.....	113
6.2	Core density effects on the natural frequencies	113
6.3	Core density effects on the impact resistance (Numerically) 114	
6.4	Core type effect on results.....	114
6.5	Suggestions for Future Work.....	114
	References.....	115

List of Tables

Table 1.1:Comparing honeycomb to other options.....	10
Table 4.1:Samples attributes.....	63
Table 4.2:Samples attributes.....	67
Table 4.3:Samples Attributes	71
Table 5.1:Tensile test results for (PLA).	81
Table 5.2:Density test results for (PLA).....	81
Table 5.3:Deflections of (122, 154.5, and 187 Kg/m ³) density specimens theoretically	82
Table 5.4:Deflections of (105, 132, and 160 Kg/m ³) density specimens numerically with Ansys 2021 R2	85
Table 5.5:Deflections of (105, 132, and 160 Kg/m ³) density specimens Experimentally.....	87
Table 5.6:Theoretical, Numerical, and Experimental Stiffness values for each core density.....	89
Table 5.7:Deflections of (105, 132, and 160 Kg/m ³) density specimens numerically with Ansys 2021 R2	90
Table 5.8:Deflections of (105, 132, and 160 Kg/m ³) density specimens Experimentally.....	92
Table 5.9:Numerical, and Experimental Stiffness values for each core density.....	94
Table 5.10:Deflections of (105, 132, and 160 Kg/m ³) Density Specimens Numerically	95
Table 5.11:Deflections of (105, 132, and 160 Kg/m ³) density specimens Experimentally.....	97
Table 5.12:Numerical, and Experimental Stiffness values for each core density.....	99

Table 5.13:Numerically calculated stiffnesses specimens with single and double web thicknesses in various orientation loadings	101
Table 5.14:Numerically calculated stiffnesses in various orientation loadings.....	102
Table 5.15:Numerically calculated stiffnesses in various orientation loadings.....	104
Table 5.16: Natural Frequencies for specimens with various core densities	105
Table 5.17:Core density effect on dent depth due to impact for Regular hexagonal honeycomb core sandwiches.....	107
Table 5.18:Core density effect on dent depth due to impact for Triangular honeycomb core sandwiches.	109
Table 5.19:Wing Deflection of Each Core Type and Density	111

List of Figures

Figure 1.1:Composite Sandwich Structures in ATR 72 Airframe [4].....	1
Figure 1.2: Wing Structure[6]	3
Figure 1.3:Sandwich Panels Construction [10].....	4
Figure 1.4:The Sandwich Panel in Comparison to an I beam [11]	4
Figure 1.5:Sandwich Panel Stresses During Bending [11]	5
Figure 1.6:Failure modes of sandwich structures [17].	6
Figure 1.7:An Example of How an Increase in thickness will magnify Strength and Stiffness (by using a honeycomb core) [22].	7
Figure 1.8:Different types of sandwich structures [25].....	8
Figure 1.9:Natural cellular structures (a) Human bone, (b) Honeycomb, and, (c) Fungi mushrooms)[27].	9
Figure 1.10:Boeing 727 Elevator[32].....	10
Figure 3.1:different types of honeycombs [22]	23
Figure 3.2:Hexagonal honeycomb [30]	24
Figure 3.3:Hexagonal Honeycomb [9], [64].	24
Figure 3.4:Basic Geometrical Elements of Hexagonal Honeycomb.....	25
Figure 3.5:Basic Geometrical Elements Analysis	25
Figure 3.6:Element Analysis for Hexagonal.	26
Figure 3.7:Basic Geometrical Elements Analysis for doubled web thickness.....	27
Figure 3.8:Basic Geometrical Elements of Triangular Honeycomb	28
Figure 3.9:Basic Geometrical Elements Analysis	28
Figure 3.10: Basic Geometrical Elements of Overlapped Octagonal Core	29
Figure 3.11:Basic Geometrical Elements Analysis	30
Figure 3.12:Stresses in sandwich structure [9].....	31
Figure 3.13:Flexural Test.	31

Figure 3.14:Produced Deflection [9]	32
Figure 3.15:Shear deflection of core.	33
Figure 3.16:Boundary Conditions.	35
Figure 3.17:Orientation (a) L-Direction (b) W-Direction for hexagonal core.....	38
Figure 3.18:Orientation (a) L-Direction (b) W-Direction for triangular core	40
Figure 3.19:Loading in (a) L or W, and (b) diagonal directions.	42
Figure 3.20:Boundary Conditions for free vibration analyses.	44
Figure 3.21:Boundary Conditions for impact test.	45
Figure 3.22:Hexagonal Samples with (a) 105, (b) 132, and (c) 160 kg/m ³ densities.	46
Figure 3.23: Triangular Samples with (a) 105, (b) 132, and (c) 160 kg/m ³ densities.	47
Figure 3.24:NACA 0009 Airfoil [68].....	48
Figure 3.25:Wing Structure.	49
Figure 3.26:Boundary Condition.....	49
Figure 4.1:(a,b,c) The honeycomb configurations explored in this study.	52
Figure 4.2:Flexural Test	53
Figure 4.3:Sample geometry with selected dimensions.	54
Figure 4.4:The Fused deposition modeling (FDM) process [71].....	55
Figure 4.5:(Creality Ender 3 V2) 3D printer.	56
Figure 4.6:Polylactic acid (PLA) filament.	56
Figure 4.7:Create and export models with AutoCAD Mechanical.	57
Figure 4.8:The process of slicing a specimen.	58
Figure 4.9:Printing samples process.....	58
Figure 4.10:Regular hexagonal honeycomb core cell.	59

Figure 4.11:Regular hexagonal honeycomb core with doubled cell wall thickness in the L direction.....	59
Figure 4.12:The honeycomb fabrication process [30].....	60
Figure 4.13:First specimen with 9.5 mm cell size.....	61
Figure 4.14:Second specimen with 7.52 mm cell size.	61
Figure 4.15:Third specimen with 6.2 mm cell size.	61
Figure 4.16:First sliced specimen with 9.5 mm cell size.	62
Figure 4.17:First printed specimen with 9.5 mm cell size.	62
Figure 4.18:Second printed specimen with 7.52 mm cell size.....	62
Figure 4.19: Third printed specimen with 6.2 mm cell size.....	63
Figure 4.20: The triangular honeycomb core cell.	64
Figure 4.21:First specimen with 16.45 mm cell size.....	65
Figure 4.22:Second specimen with 13 mm cell size.	65
Figure 4.23:Third specimen with 10.74 mm cell size.	65
Figure 4.24:First sliced specimen with 16.45 mm cell size.	66
Figure 4.25:First printed specimen with 16.45 mm cell size.	66
Figure 4.26:Second printed specimen with 13 mm cell size.....	66
Figure 4.27:Third printed specimen with 10.74 mm cell size.....	67
Figure 4.28:The Overlapped Octagonal Honeycomb Core.....	68
Figure 4.29:First specimen with 23.6 mm cell size.....	69
Figure 4.30:Second specimen with 18.7 mm cell size.	69
Figure 4.31:Third specimen with 15.4 mm cell size.	69
Figure 4.32:First sliced specimen with 23.6 mm cell size.	70
Figure 4.33:First printed specimen with 23.6 mm cell size.	70
Figure 4.34:Second printed specimen with 18.7 mm cell size.....	70
Figure 4.35:Third printed specimen with 15.4 mm cell size.....	71
Figure 4.36:The universal test machine (Max Load 5 KN)	72
Figure 4.37:The roller used with a universal test machine.....	73
Figure 4.38:The load-deflection curve.	73

Figure 4.39:(Type I) specimen.	75
Figure 4.40:Dimension of the specimen.....	75
Figure 4.41:Sliced specimen via (Ultimaker Cura).....	76
Figure 4.42:Printing samples by 3D printer.	76
Figure 4.43:Printed specimens before test.....	77
Figure 4.44:The universal testing machine (Max Load 5 KN).	77
Figure 4.45:Jigs of the testing machine.	78
Figure 4.46:Printed specimens after the test.....	78
Figure 4.47:Specimen, Density Tester, and Lab Environment.	79
Figure 5.1:Tensile test results for samples.	80
Figure 5.2:Theoretical Load-Deflection Curve	83
Figure 5.3:Theoretical Core density - Stiffness Curve.....	83
Figure 5.4:Relation Core density and Shear modulus of the core.....	84
Figure 5.5:Shear modulus effect on the value of deflection due to shear	84
Figure 5.6:Numerical Load-Deflection Curve	86
Figure 5.7:Numerical Core density - Stiffness Curve	86
Figure 5.8:Experimental Load-Deflection Curve.....	88
Figure 5.9:Experimental Core density - Stiffness Curve	88
Figure 5.10:Theoretical, Numerical, and Experimental Stiffness Comparison.....	89
Figure 5.11:Theoretical Load-Deflection Curve	91
Figure 5.12:Numerical Core density - Stiffness Curve	91
Figure 5.13:Experimental Load-Deflection Curve.....	93
Figure 5.14:Experimental Core density - Stiffness Curve	93
Figure 5.15:Numerical, and Experimental Core density - Stiffness Curves	94
Figure 5.16:Numerical Load-Deflection Curve	96
Figure 5.17:Numerical Core density - Stiffness Curve	96
Figure 5.18:Experimental Load-Deflection Curve.....	98

Figure 5.19:Experimental Core density - Stiffness Curve	98
Figure 5.20:Numerical, and Experimental Core density - Stiffness Curves	99
Figure 5.21:(Stiffness to core density) comparison for each core type..	100
Figure 5.22:Stiffness in various orientations for single and double web thickness.....	102
Figure 5.23:Stiffness in various loading orientations for Triangular core.	103
Figure 5.24:Stiffness in various loading orientations.....	104
Figure 5.25:Simulation of the impact test.	107
Figure 5.26:Relation between core density and dent depth due to impact for (Regular hexagonal honeycomb core).	108
Figure 5.27:Relation between core density and dent depth due to impact for (Triangular honeycomb core).	110
Figure 5.28:Comparison of (Core density - dent depth due to impact) for Hexagonal and Triangular honeycomb cores.	110
Figure 5.29:Deflection in all cases with various core types and densities	112

List of Abbreviations

A/C	Aircraft
ABS	Acrylonitrile Butadiene Styrene
AM	Additive Manufacturing
ASTM	American Society for Testing Materials
CAD	Computer-Aided Design
FDM	Fused Deposition Modeling
GFRP	Glass-Fiber-Reinforced Polymer
HOBE	Honeycomb Before Expansion
NACA	National Advisory Committee for Aeronautics
PA	Polyamide
PC	Polycarbonate
PETG	Polyethylene Terephthalate Glycol
PLA	Polylactic Acid
PS	Polystyrene
PVC	Poly Vinyl Chloride
2D	Two Dimensions
3D	Three Dimensions

List of Symbols

Symbol	Description	unit
A_c	Area of core section	mm ²
B_1	constant	---
B_2	constant	---
C_2	constant	---
E_c	Modulus of elasticity of core material	Mpa
E_f	modulus of elasticity of facing material	Mpa
E_s	Modulus of elasticity of sold material	Mpa
G_s	Shear modulus of core material	Mpa
G_c	shear modulus of the core	Mpa
t_s	Skin thickness	mm
h	height of the octagonal	mm
L	L-Direction	---
S	Cell Size	mm
T	T-Direction	---
W	W-Direction	---
a	cell wall length, hexagon side length in the W-direction	mm
b	cell wall length, hexagon side length in the L-direction.	mm
c	core height	mm
l	length of triangular side	mm
p	load	KN
t	web thickness	mm
$\delta_{bending}$	sandwich deflection due to bending	mm
δ_c	Core deflection	mm
δ_{shear}	sandwich deflection due to shear	mm
δ_{total}	total sandwich deflection under bending load	mm
ρ_c	core density	Kg/m ³
ρ_s	sold web material density	Kg/m ³
τ_c	shear stress of the core	MPa
γ	Angle of Shear deflection	Degree
θ	Angle of Hexagonal cell	Degree

Chapter One: Introduction

1.1 General

Strength, weight, and reliability are the most important influencing factors in aircraft construction. These criteria govern the requirements that any material used to build an aircraft must satisfy. Airframes must be both strong and light. All materials used in the manufacture of an aircraft should be reliable to prevent a disaster. Early airplanes were built of wood, while both metallic and non-metallic materials are now employed in the aerospace and aviation industry [1]. But reducing weight without a loss in strength is still the main problem facing design engineers in that industry, so searching for new materials with unique properties becomes necessary, and sandwiched composites have developed into among the most effective options [2]. Due to their exceptional mechanical properties and multifunctionality, sandwiches have been used in a wide range of applications, including satellites, aircraft, ships, automobiles, train vehicles, wind energy systems, and bridge construction. Even so, the use of composite sandwich constructions is now limited mostly to secondary constructions, see Figure (1.1) [3].



Figure 1.1: Composite Sandwich Structures in ATR 72 Airframe [4]

For commercial airplanes (for instance, Airbus), composite sandwich constructions are used in multiple ways; for example, aerodynamic fairings, coverings, doors, Radomes, belly fairings, landing gear doors, engine cowlings, and leading and trailing edges are common structures. Furthermore, spoilers, ailerons, and rudders are even inside aircraft, like floor panels in the passenger compartment. The near-and mid-term future of aviation holds significant promise for the advancement and implementation of sandwiches, but also challenges and difficulties that must be solved to further advance the more reliable use of sandwich structures [5].

1.2 Aircraft Structure

The fuselage, wings, tailplane, and control surfaces are major components of the aircraft's structure. They are made of various materials and designed professionally to bear the maximum expected loads in extreme service conditions according to the material's mechanical properties which they are made from [6]. The structure of an aircraft is responsible for transferring and resisting applied loads, providing an aerodynamic shape, and keeping the crew, payload, and other components safe from the ambient conditions encountered during flight. The airframe must withstand two types of loads: ground loads and air loads. Ground loads are any loads encountered by an airplane while traveling or transporting on the ground as a result of gravitational and inertial effects. These loads act on the whole structure, while the generated pressure distribution on the skins is what causes all air loads. Which causes direct stress, bending, shear, and torsion in all areas of the structure. Furthermore, the skin is already subjected to local normal pressure loads [7]. On the other hand, the challenge of manufacturing a structure as light as possible without losing the strength necessary to endure those stresses is extremely

important. In earliest works and recently, traditional aircraft structural design overcomes this challenge by using longitudinal stiffeners connected to stabilizing rings covered by thin plates forming the fuselage. Besides the wings, which take a shape designed according to aerodynamic requirements, consisting of skin made of a thin plate reinforced by stringers riveted to supported ribs by main spars attached to the fuselage, as shown in Figure (1.2). However, this is not a particularly elegant or efficient option. Sandwich panels are a creative technology that can provide stabilized surfaces, making them resistant to deforming stresses and represent a noteworthy solution that provides multifunctional materials with a wide range of configurations and has various characteristics that are unbeatable, especially in terms of a higher stiffness and strength-to-weight ratio [8].

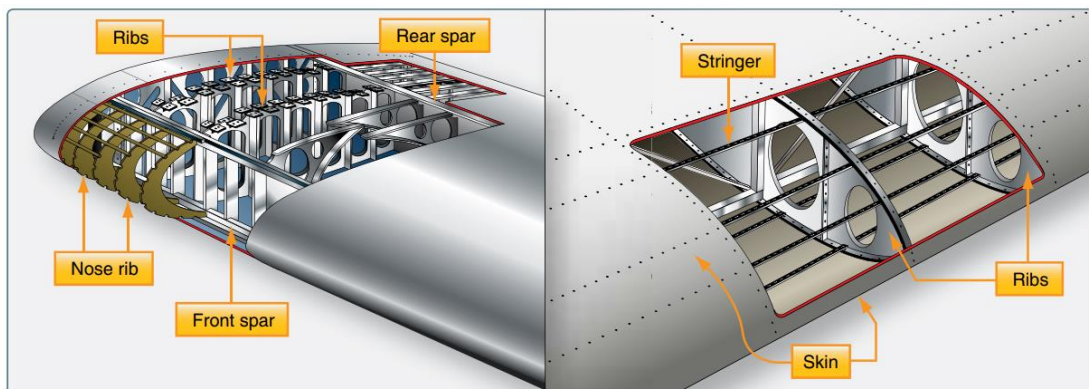


Figure 1.2: Wing Structure[6] .

1.3 Sandwich Panel

A sandwich structure is a thick, lightweight core adhered to two thin, strong-facing layers, composing material with high resistance to bending stress due to layer spacing, which increases the moment of inertia. On the other hand, the lower density core, which is usually a cellular material, causes a minor increase in total weight, figure (1.3). The core by itself is rather flexible and weak, and the face sheets are not strong enough. That

option facilitates forming it to the desired flat or curved shape, but when they are bonded together, they give significant stiffness. Sandwich panels' mechanical properties will have various values depending on how they are manufactured, which means they do not have specific mechanical properties like other materials. Rather, their properties could be intelligently designed to be appropriate for certain purposes by specifying their materials, configurations, and governing dimensions [9].

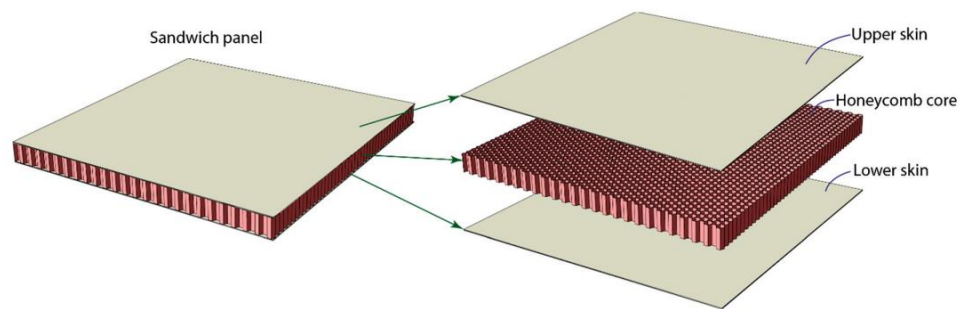


Figure 1.3: Sandwich Panels Construction [10]

Sandwich panels have an effective structural design similar to an I-beam. The faces replace the flanges, and the core replaces the web, see fig (1.4).

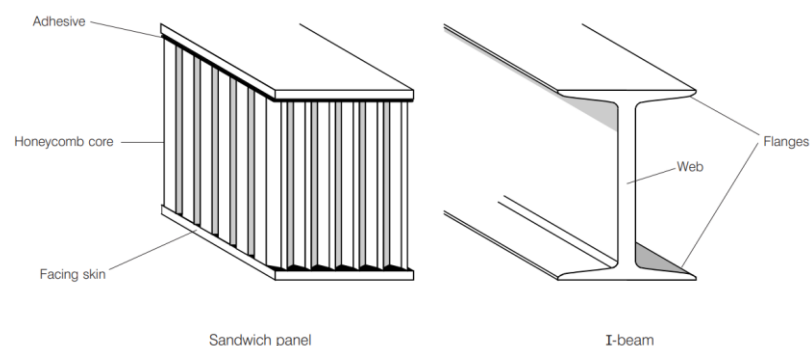


Figure 1.4: The Sandwich Panel in Comparison to an I beam [11]

Additionally, the core may be made of a different material than the faces and distributed to provide full support for the faces against wrinkling or buckling instead of being concentrated in a tight web [12]. Hence, there is

a serious need for strong bonding between the sandwich's elements (skins and core). Often, powerful adhesives meet that requirement, which means more weight and additional limitations to their usability and design [13]. When sandwich panels are subjected to flexural loading, the skins effectively handle the tensile and compressive stresses. On the other hand, the core's task is to endure shear stress and maintain the fixed spacing between two skins and prevent the movement of the skins relative to each other, see figure (1.5). The core can effectively carry out these tasks although it has a low density, which gives sandwich panels significant lightness besides the fundamental features of its high stiffness-to-weight and strength-to-weight ratios [14].

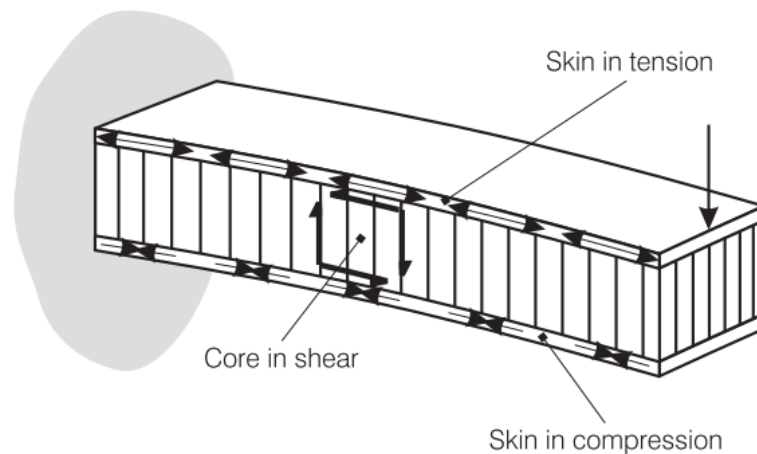


Figure 1.5: Sandwich Panel Stresses During Bending [11]

Besides strength and weight improvements, the potential economic benefits from low-cost core materials employment are significant, which makes sandwich construction an opportunity to be used in limited-budget applications [15]. Nonetheless, sandwich structures have complicated behavior and a variety of complex failure modes, see figure (1.6), making it difficult to predict how they will fail. Consequently, specifying materials for the skins and core with proper configurations is challenging [16].

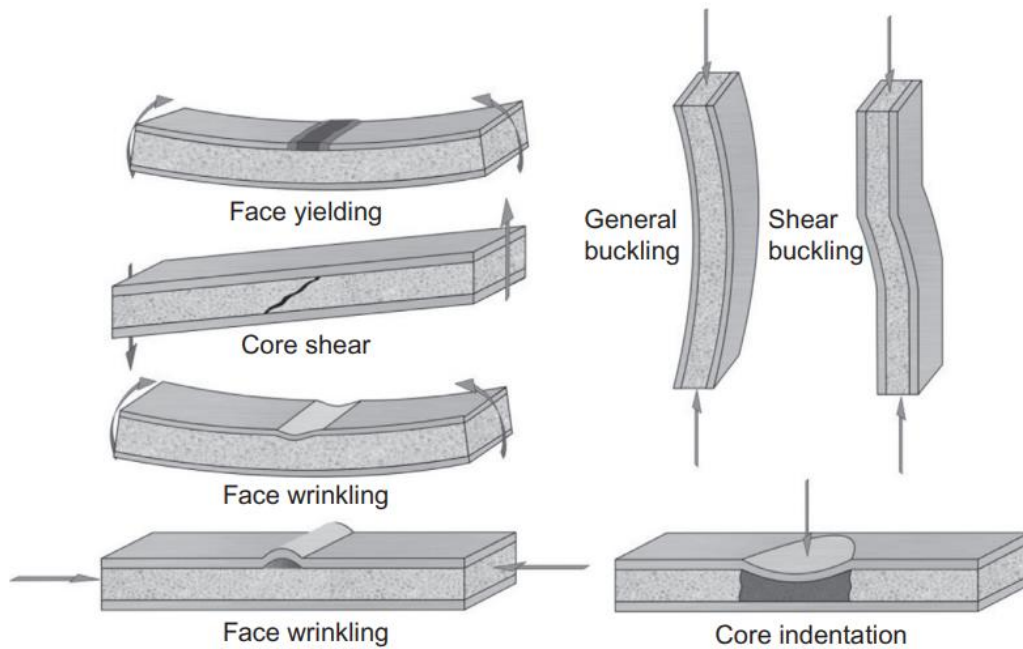


Figure 1.6: Failure modes of sandwich structures [17].

1.3.1 Skins

Almost any material that can be formed into thin sheets can be used as the sandwich panel's facing material, whether it is metallic (like steel, titanium, and aluminum alloys) or non-metallic, which are often used (like reinforced plastics, plywood, and composites based on glass, aramid, carbon, or Kevlar fibers), these materials have strength characteristics that are even better than those of metals and are easier to fabricate. Even with double curvature [18]. In general, whatever the material is, it must be stiff to contribute to the structural rigidity of the sandwich structure and have excellent resistance to tension, compression, and impact loads. Finally, it should have an appropriate surface finish to withstand various environmental conditions and wear [19]. On the other hand, usually, faces are identical in material and thickness (a symmetric sandwich), but in other situations, the thickness or material of the faces may vary, or perhaps both (an asymmetric sandwich), because one face may be responsible for carrying the majority of the load or be exposed to low temperatures, while

the other face must endure higher temperatures or be exposed to corrosive conditions, etc. [20].

1.3.2 Core

There are no limitations on the type of material utilized in sandwich core fabrication. Where there are different materials can be used such as polymers, metals, wood, paper, aramid, and composites are among the materials to manufacture various cores. As long as such fabrication produces a core with the lowest density possible, consequently, whatever the required core thickness is, it will magnify the sandwich's stiffness value with a slight increase in its overall weight, as shown in figure (1.7) [21].

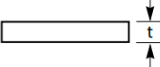
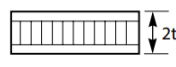

	Solid Metal Sheet	Sandwich Construction	Thicker Sandwich
			
Relative Stiffness	100	700 7 times more rigid	3700 37 times more rigid!
Relative Strength	100	350 3.5 times as strong	925 9.25 times as strong!
Relative Weight	100	103 3% increase in weight	106 6% increase in weight

Figure 1.7: An Example of How an Increase in thickness will magnify Strength and Stiffness (by using a honeycomb core) [22].

Main requirements of the sandwich core, it must be stiff enough in the direction perpendicular to the faces to maintain the spacing between them fixed during loading. Furthermore, it must also be stiff enough in shear to prevent skins from slipping over one another. These criteria must be satisfied, or else the skins will just operate as two separate beams, so the sandwich's influence will vanish. Another need, the core must also have enough flexural stiffness to provide a meaningful contribution to the overall bending stiffness of the sandwich structure [23]. Various core types can be included in sandwich construction, such as wood like balsa, foams,

and honeycomb, which all have a cellular structure, as well as corrugated, Waffle-Type, Cross-banded, web, and truss core, figure (1.8) shows some of these types [24].

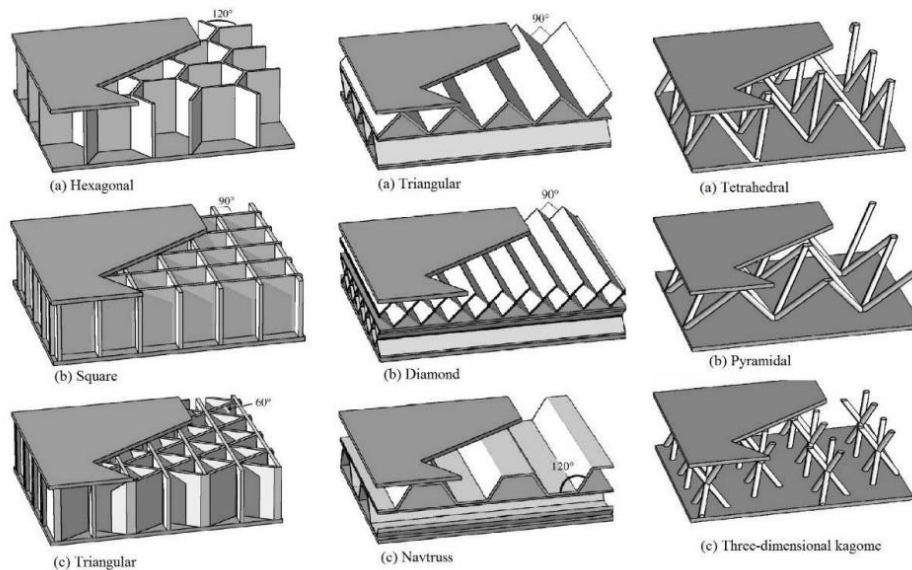


Figure 1.8: Different types of sandwich structures [25].

1.4 Cellular Materials

Cellular materials, whether human-made or natural, are composed of a network of linked plates or solid struts arranged in two or three dimensions, periodically or randomly, forming open or closed cells. Naturally, such materials are frequently found, including wood, bone, cork, sponges, and other similar materials, as shown in figure (1.9) [26]. They are designed to achieve structural and functional optimal solutions with minimal material. Those principles inspired the creation of numerous manufactured cellular solids with superior physical and mechanical properties, like foams and honeycombs, which are utilized in different sectors. The most important feature of those materials is relative density, which is the ratio of a cellular material's density to the density of the solid material from which it is constructed. On the other hand, the density of cellular materials is

determined by cell size, wall thickness, material density from which they are made, and the regularity, repetition, and connectivity of unit cells [27].

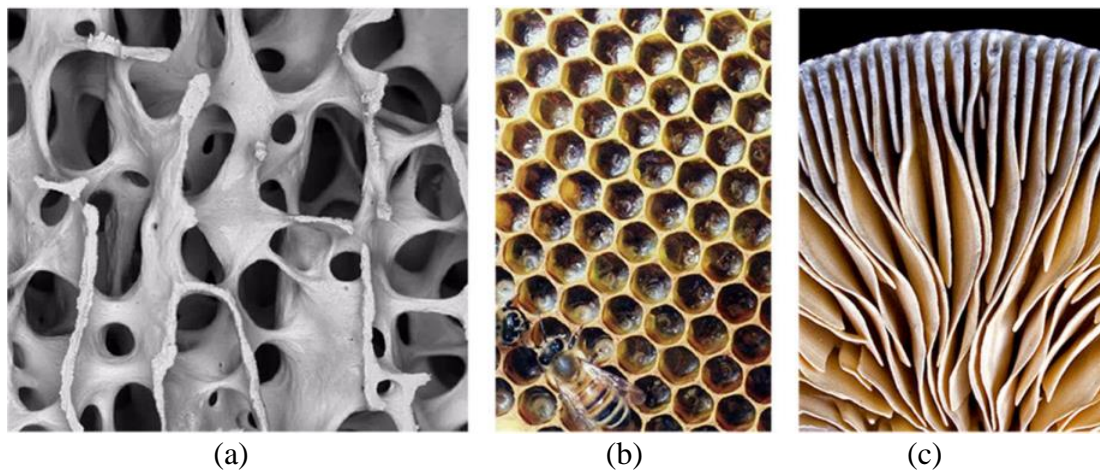


Figure 1.9:Natural cellular structures (a) Human bone, (b) Honeycomb, and, (c) Fungi mushrooms)[27].

1.5 Sandwich Structure Optimization

Optimal performance while utilizing minimal materials is the fundamental concept of structural optimization [5]. For sandwich structure optimization, it is necessary to keep it as light and rigid as possible. Starting with skins, utilizing high-strength metals or maybe materials with multiple design variables, such as fiber-reinforced composites, contributes to that optimization due to their expected excellent strength [28]. However, various cellular cores have been analyzed and optimized to provide a lightweight one with optimum performance, which requires an understanding of the core's behavior and the effect of its design and its mechanical properties on the overall sandwich structure behavior. Whereas, changes in the core type and geometric dimensions can have a major impact on how the core behaves, and therefore how the sandwich structure behaves [29]. Generally, the use of balsa wood or foam cores in airplanes is uncommon. Consequently, metal and non-metal hexagonal honeycomb sandwiches are widely used in aerospace applications where

light weight is a priority due to their high stiffness-to-weight and strength-to-weight efficiency, see table (1.1) [9].

Table 1.1: Comparing honeycomb to other options [30].

	Relative Strength	Relative Stiffness	Relative Weight
Honeycomb	100%	100%	3%
Foam Sandwich	26%	68%	
Structural Extrusion	62%	99%	
Sheet & Stringer	64%	86%	
Plywood	3%	17%	100%

The total weight of the sandwich construction is perfectly influenced by the relative core density. Additionally, sandwich characteristics including maximum load, maximum deflection, and energy absorption are significantly influenced by honeycomb parameters like cell size, cell wall thickness, and core height[29].

1.6 Honeycomb Sandwich in A/C

One example of the use of honeycomb sandwiches in the A/C sector [31], the Boeing (727) which utilizes hexagonal Nomex honeycomb with composite skins in many important parts of its airframe. For instance, by replacing the solid plates in the elevator with sandwiches, as illustrated in figure (1.10) which allows for a reduced number of supporting elements, this contributed to reducing the weight by 26% [32], and significantly reducing the overall flight costs, and making the Boeing 727 one of the most popular and marketable models in the seventies of the last century [33].

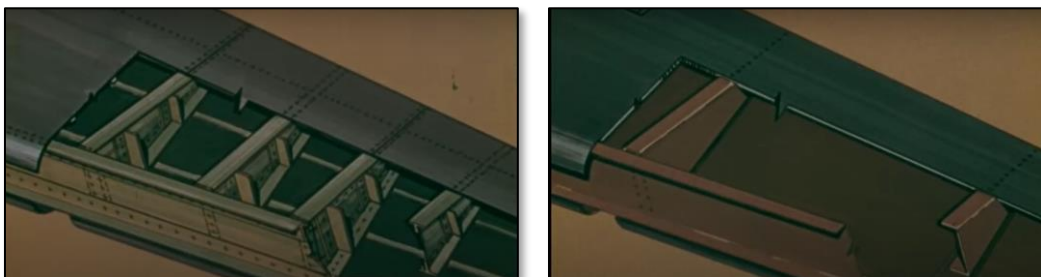


Figure 1.10: Boeing 727 Elevator [32]

1.7 The aim of study

The primary aim of this research is to examine how core density affects the mechanical characteristics of the core and, as a result, how the sandwich will behave both under static and dynamic loading conditions.

1.8 Objectives of work

To achieve the intended aims of the work, the procedures involved the following:

1. Core density depends mainly on the shape of the cell (hexagonal, triangular, etc.), the size of the cells, the thickness of their walls, and the density of the solid material from which the core is made.
 - **In this research**, the cell size will be the sole variable controlling density magnitude, while other parameters will be constant factors.
 - Cell size will have three values; consequently, there will be three densities.
2. Deciding what tests have to be done to explore the effects of core density on each required property.
 - First, bending tests are required to investigate the effect of core density on stiffness.
 - Bending tests are required to investigate the effect of core orientation on stiffness.
 - Second, impact tests are required to numerically investigate the effect of core density on impact resistance.
 - Third, free vibration tests are required to numerically investigate the effect of core density on natural frequencies.
 - Conduct the required test to specify the mechanical properties of the material that the samples will be made of.
 - Conduct the required test to specify the physical properties of the material that the samples will be made of.

3. Design models according to each test's requirements, for each density.
 - According to all tests, samples will be in three cell sizes, resulting in three densities.
4. Manufacturing samples by utilizing 3d printing.
 - Specifying one material to utilize in manufacturing all samples.
 - Specifying one magnitude for cell wall thickness for all samples of all tests
 - Manufacturing bending test samples only.
5. Conducting the experiments numerically, then experimentally.
 - Conducting all tests numerically using Ansys simulating software.
 - Conducting bending test experimentally only.
6. Comparing the results.
 - Comparing the experimental results with the numerical and theoretical (if available).
7. Designing and numerically testing a virtual case to explore the effect of variation in each core type's core density on the stiffness of sandwich panels used in A/C.
 - Specifying the wing airfoil
 - Specifying design and dimensions
 - Specifying boundary conditions
 - Specifying loading conditions
 - Conducting numerical test
8. Obtaining the conclusions and attempting to understand the geometrical factors that produced the variation in results from one core type to another, then showing each core's superiority over the others by highlighting their advantages.

Chapter Two: Literature Review

2.1 Introduction

The previous work published during the last decade included research and development of everything related to sandwich panels. But concerning the cores in particular, the literature included studies of the performance of the usually used types and the proposed core configurations; therefore, the articles can be arranged according to whether they deal with static conditions or dynamic conditions, which include impact and free vibrations, as follows:

2.2 Static Conditions

Salih N. Akour and Hussein Z. Maaitah (2010) [37] investigated how the stiffness of the core material affected the behavior of sandwich panels after the yield limit. They used aluminum face sheets and foam core (AirexR63.50), and they found that if a sandwich panel is loaded past its core yield limit, the load will be transferred to the face sheet as long as the core material is sufficiently soft. And so, this increased the sandwich panel's capacity to carry loads. In other words, when the core material's stiffness is increased to a certain level, the face sheet yields before the core material. So, it has been demonstrated that increasing core stiffness boosts the sandwich panel's ability to support more weight.

Kantha Rao et al. (2012) [34] calculated the strength of honeycomb sandwich panels made of various materials. Samples were honeycomb sandwich panels made of high-tensile steel, titanium, and aluminum, and they were subjected to the flexural test. The findings were that the core

height has no bearing on how the honeycomb core behaves when it is crushed. However, a crucial factor affecting the sandwich panels' ability to withstand crushing is the honeycomb core cell's wall thickness.

H. R. Ali et al. (2013) [35]. The critical bending stress of honeycomb sandwich panels examined in relation to the core shape, cell wall height, wall thickness, and skin thickness. Other sandwich panel parameters were assumed to remain constant. For conducting the finite element simulation, the ABAQUS software was used, and the outcomes were compared to those of the experiments. According to the findings, there was an approximate 50% skin thickness impact on the critical bending load. Wall thickness and core shape were shown to have respective effects of 17.85 and 14.92, respectively. When compared to other parameters, the impact of cell wall height was minimal, with an influence percentage of about 3.

Kazuyoshi Seto et al. (2014)[36] conducted an investigation of the bending stiffness of an adhesively bonded honeycomb sandwich panel, taking temperature fluctuations in the adhesive's Young's modulus into account. They found that temperature had a significant impact on an adhesive's Young modulus. Hence, with rising temperatures, the bending stiffness decreases. Additionally, it had been proposed that the adhesive's Young modulus only significantly affects the bending stiffness when it is below a particular limit.

Zheng Chen et al. (2014) [41] examined the effects of structural factors on the mechanical performance of lightweight sandwich panels made of kraft paper, including the core shape, cell size, core density, core and web thickness, and the material properties of the core and skin layers. Additionally, they discovered that, for the identical honeycomb core

configurations, the honeycomb core density directly influenced the stiffness of the panels under out-of-plane loading conditions.

Shokrgozar Navi et al. (2015)[37] suggested that the core could be considered to be a homogeneous anisotropic material. Changes were made in their study to the number and locations of nodes, the number of cell walls, and the size of the volume element. Additionally, by assuming an unconstrained core, the shear components of the elasticity tensor are derived for heterogeneous geometries using the homogenization method. The findings demonstrated that these changes in geometry improve shear stiffness and reduce weight for several core geometries that have not previously been evaluated.

Nick Bruffey et al. (2016)[38] investigated the hexagonal core and find that to determine the failure mode for a specific sandwich panel, the shear strength of the core must be computed and compared to the load predicted by the model. They found higher face sheet thickness and core thickness significantly increased the failure loads, which were essential variables in the model. Also, the right correction factors must be applied at the right times. It is crucial to constantly take into account how the sandwich panels were manufactured since this might result in early failures like debonding.

Doaa Fadhel (2016) [39] concentrated on the design and modeling of honeycomb sandwich panels with various core configurations (hexagonal, circular, and square) with various materials and facing thicknesses. Then those sandwiches were subjected to a three-point bending test to explore their durability. According to testing, the square core bears the maximum load and also has the highest strength-to-weight ratio, followed by the other types. Also, by raising the face thickness, the maximum load rose. Finally, depending on the results of the free vibration analysis, changing skin

thickness has a 3%–30% impact on natural frequencies. Moreover, the natural frequencies were altered by 19.7%–38.8% when the core configuration is changed.

Hazem E. Soliman's (2016) [40] introduced this study to cover three types of honeycomb cores: hexagonal, square, and triangular, and focused on configuration effects on stiffness. The investigation of the three cell cores led to some important conclusions; the most important was that the transverse shear stiffness of the triangular core is often higher, so it is stiffer in terms of in-plane stiffness. Also, he found that when the panel size to cell size ratio is less than 60, the findings' accuracy when employing homogenized characteristics for the cellular core is significantly affected.

Dorota et al. (2017) [41] investigated how core lattice geometry parameters affected plate stiffness. They discovered that the equivalent core material properties of a core structure are affected by its geometric parameters, and that a beam's bending stiffness is increased by the magnitude of the Poisson's ratio.

Udit B. Shah and Rakesh K. Kapania's (2018) [47] compare sandwich panels with a triangular core and a hexagonal core of equal cell size and relative density. They found that triangular core panels surpassed hexagonal in applications where in-plane loading predominated, but the triangular core panels tended to fail at lower loads and lower deflections when out-of-plane loading was present.

Cihan Kaboglu, et al. (2018) [42] provided a study with multiple sandwich structures with densities ranging from 60 to 100 kg/m³ have been created using glass-fiber-reinforced polymer (GFRP) skins but varied layers of poly vinyl chloride (PVC) foam as the core. They found that a

symmetric graded-density configuration and a uniform core configuration gives the best performance for the sandwich structures when subjected to quasi-static flexural loading.

Sajjad Raeisi and Andres Tovar (2018) [43] created three different types of cellular architecture. The first one was aluminum foam; the next structure was a regular hexagonal honeycomb; and finally, an optimized repetitive cellular core. According to the results, the honeycomb and the optimized structures were more rigid while the foam-based model had the lowest stiffness.

Lyes Azzouz et al. (2019) [44] reported in their research the viability of using additive manufacturing (AM) technology in the process of producing lightweight sandwich panels utilized in aerospace applications. Additionally, AM technology could also compete with traditional core structures.

Assmaa Sattar (2020) [45] focused on the preparation and testing of hexagonal, triangular, square, and circular honeycomb core configuration. The findings demonstrate that the flexural properties of honeycomb sandwich structures are significantly influenced by variations in the core shape, core material, and number of skin layers. So, the strongest and stiffest cell form was square, whereas the weakest was triangular.

Amin Farrokhbadi et al. (2020) [46] examined the mechanical behavior of multilayer corrugated core laminated composite sandwich panels exposed to quasi-static three-point bending. The results indicated that the quantity of energy absorbed rises in comparison to a non-reinforced specimen due to the multilayer method's enhancement of peak loads.

Penumaka Dhananandh et al. (2020) [47] found that the octagonal honeycomb structure performs better than the hexagonal structure in some regions, yet both honeycomb core designs have equivalent strength. It is possible to prefer an octagonal honeycomb structure in the production of aircraft and aerospace technologies to save weight because it has a lower weight ratio than hexagonal structures.

Hamid Abedzade Atar et al. (2020) [48] attempted to theoretically and experimentally examine the effect of core geometry on the flexural stiffness and transverse shear rigidity of corrugated core sandwich panels. By testing the trapezoidal, triangular, and rectangular cores, they found that the transverse shear rigidity and core shear modulus are dramatically reduced when the angle of the core wall is increased from a triangular form to a rectangular.

Sadiq E. Sadiq, M.J. Jweeg, et al. (2021)[49] evaluated the honeycomb core theoretically and experimentally based on failure mode maps. They find that the peak bending load is inversely correlated with cell size but directly correlated with cell wall thickness and core height. As well as The primary factor influencing sandwich panels' ability to withstand crashes is their core height.

Sridhar B. S. et al. (2021) [50] studied a hexagonal honeycomb sandwich in which, to increase strength and enhance the stiffness of the honeycomb material, polyurethane foam with different densities is utilized to fill the honeycomb core and explore its effect on the characteristics of the produced core. The results revealed that the compressive strength of the core slightly increased due to the increase in foam density. Also, adding foam improved the ability to absorb impact energy.

Alaa Al-Fatlawi (2021) [28] exhibited studies on honeycomb sandwiches, including the following: The most effective way to reduce deflection is to increase the core thickness of honeycomb sandwich panels. The thickness of the face sheets, as opposed to the honeycomb core, had an impact on the adhesive's resistance to peeling. Finally, increasing the honeycomb core thickness will result in higher natural frequencies for the honeycomb sandwich panels because of an improved stiffness-to-weight ratio.

Diogo Pereira, et al. (2022) [51] utilized additive manufacturing methods to create tailored cellular lattice cores in various characteristics. They used 3D printing to make the entire sandwich panel without the need to use adhesives, and founded the flexural behavior of the panels was significantly influenced by the core's relative density and geometrical characteristics, and the panels with the highest strut attained the highest values of strength, stiffness, and absorbed energy.

2.3 Dynamic Conditions

Remmelt Andrew Staal (2006) [52] studied the impact effect on sandwich panels. So, to precisely forecast and capture the localized wrinkling failure mechanism that takes place in the damaged region, analytical and finite element models were created. Analytical and numerical models demonstrated that impact-damaged panels were broken because of wrinkling instability rather than due to an early core crushing failure. Also, damage depth and damage diameter were shown to have an impact on the wrinkling failure load.

Amit Kumar (2007) [53] examined how the thickness and density of the sandwich core affect its natural frequencies. So it is found that increases in natural frequency occur as core thickness increases. Moreover, the

natural frequency of the sandwich is reduced by an increase in core density. Also, it was found that a sandwich plate had 1.4 times the fundamental frequency of a face plate of equal size. But at higher modes, there is a greater difference in frequency.

E.A. Flores-Johnson, and Q.M. Li (2011) [54] conducted experiments on the quasi-static indentation of a stiff indenter into sandwich panels having a polymeric foam core and a face reinforced with carbon fiber. It was discovered that the density of the core affects the difference in indentation resistance.

Parikh and Mahamuni (2015) [55] used an experimental setup and finite element analysis to study the modal analysis of the hexagonal honeycomb plate. On the sandwich plate made of honeycomb, a free vibration test was conducted, epoxy carbon, titanium, and aluminum were utilized to show how the kind of core and skin material affected the natural frequency. It was discovered that the epoxy carbon material had a high natural frequency.

Sunith Babu Loganathan, et al. (2015) [56] studied core density and thickness variations' effects on specific energy absorption capacity, and by using a drop test, they observed that energy absorption increased with an increase in core density, and core thickness has the same effect.

Sakar (2015) [65] conducted analytical and experimental research on the free vibration analysis of an aluminum honeycomb sandwich beam. The natural frequency and mode shapes with different parameters were found. Results show that the first natural frequency dropped as cell width rose. The first natural frequency rose along with the rise in foil thickness and

core height. Finally, the core height was found to be the parameter that had the greatest impact on the natural frequency increase of the sandwich beam.

Muhsin J. Jweeg (2016) [57] suggested an analytical solution. In order to determine the honeycomb sandwich's natural frequency with varied design parameters, the motion differential equation for vibration analysis of a honeycomb sandwich combination plate was solved. Numerous design factors were investigated, including how the fundamental natural frequency was impacted by the core height, cell size, and cell angle. The collected findings demonstrated that natural frequency is exactly proportional to the honeycomb parameter, with the exception that the proportionality is inverse for the thickness of the face.

Soraia Pimenta, Cihan Kaboglu, et al. (2017) [58] propose a better understanding of the impact behavior of sandwich structures with various core materials, and they found the density of the core material is a significant indicator of how they will respond to the impacts. By increasing the strength and density of the core, the impact behavior of the structure improves.

Rajesh Kumar, and Shivdayal (2019) [59] discovered how the honeycomb sandwich panel behaves structurally when exposed to blast loading. The minimal deflections for the top and back plates as well as the maximum energy absorption for the sandwich panel are calculated using square and octagonal core constructions. They discovered that the sandwich panel's octagonal shape exhibits less deformation than the square honeycomb core constructions.

Jiaqi Qi, Cheng Li, et al. (2021) [60] examined how the structural parameters of a new origami core affect the impact response and showed how this new sandwich structure performs better. By utilizing a drop tower instrument in an impact test, they found that the new origami core exceeded the properties of traditional honeycomb in absorbing energy.

Alejandra et al. (2021) [61] explained that exposure to freezing temperatures may negatively impact the mechanical properties of some materials, so they intended to examine the low-velocity impact behavior of sandwich composites at low temperatures by utilizing a drop tower impact system. And they found that the average bending stiffness values increased with decreasing temperatures, but the damage due to impact increased in intensity.

2.4 Concluding Remarks

As mentioned previously, the sandwich panel is a material that does not have specific characteristics but could be designed according to the required applications, which depend on the available materials, manufacturing capabilities, and the designer's intelligence in selecting and defining the correct geometrical parameters to achieve the required performance. Therefore, most of the research focused on increasing the stiffness and strength of sandwich panels in any possible way, either using materials with high-performance properties like composites or specifying optimized geometrical properties. So, researchers often combine two or more parameters to get the required characteristic. But in this research, core density would be the sole parameter governing the produced properties. As well, by studying more than one core type, the effect of geometrical parameters would be obvious.

Chapter Three: Theoretical and Numerical Analysis

3.1 Introduction

The effects of core density value on sandwich structure performance will be studied in this chapter by utilizing the literature's published theoretical solutions for the hexagonal honeycomb core type, which is usually used in aircraft structures. Those solutions involve determining the maximum loads and deflections that sandwiches with various density values can withstand under bending stresses. The results, then will be compared later with numerical and experimental solutions to specify the effective core parameters that control the sandwich performance, so their effects on other types of cores can be visualized.

3.2 Honeycomb Core

Various honeycomb types with different configurations and specific geometrical parameters could be manufactured using any thin flat sheet material [9]. The fundamental feature of honeycombs would be that both stiffness and density are partially dependent on geometrical parameters that are carefully chosen to achieve strong structural performance and a high weight-to-strength ratio [62]. As a result, there are more than 500 different types of honeycombs that have been created, see fig (3.1) but the most common type is the hexagonal one [9].

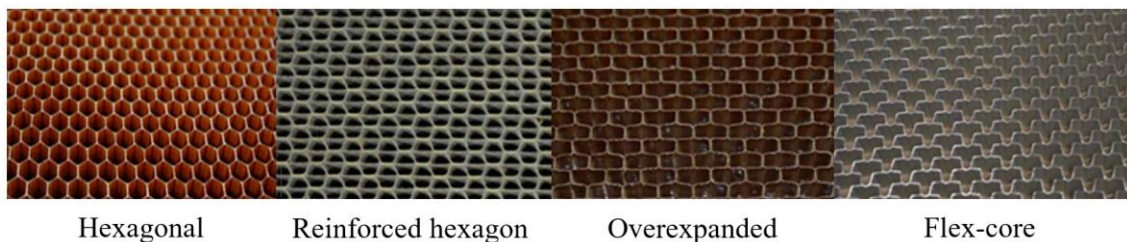


Figure 3.1: different types of honeycombs [22] .

3.2.1 Hexagonal core

The geometry of the hexagonal honeycomb core consists of identical prismatic hollow cells with a regular hexagonal section (identical sides in length and thickness crossed at 120° angles). By using that geometry, minimal material is utilized to achieve minimal weight [26]. The honeycomb also exhibits orthotropic behavior, meaning that its mechanical characteristics depend on the orientation of the structure, particularly in the "L" and "W" directions. Notably, "L" is the strongest and stiffest direction. Furthermore, due to the effective hexagonal structure, where the walls support one another, honeycomb cores usually have good compression strengths [63].

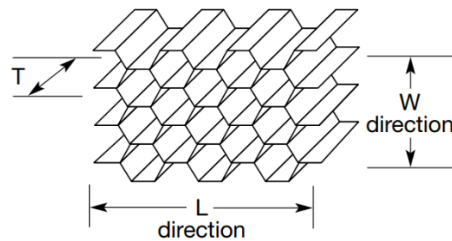


Figure 3.2:Hexagonal honeycomb [30] .

Due to the common manufacturing processes, honeycomb is made by gluing strips of material periodically, such that when pulled apart, or expanded, hexagonal cells are formed. So those bonded areas of strips produce double-thick bonded walls known as "nodes", whilst single remaining walls are known as "free walls"[9].

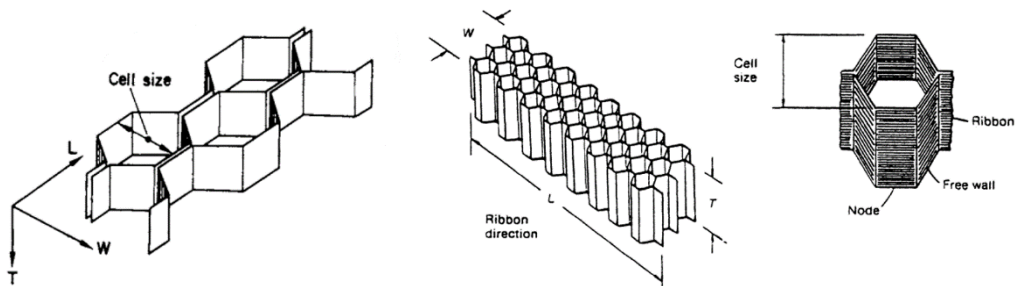


Figure 3.3:Hexagonal Honeycomb [9], [64].

3.2.1.1 Core Density

To compute the density of the honeycomb core, it has to be broken down into its basic geometrical elements figure (3.4) represents these elements.

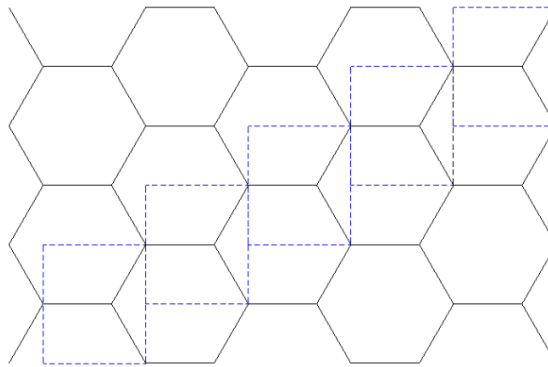


Figure 3.4: Basic Geometrical Elements of Hexagonal Honeycomb

So, that element could submit to geometric analysis, as shown in figure (3.5) and several key relationships can be derived from this analysis, including density, which represents the mass of the utilized material per unit volume.

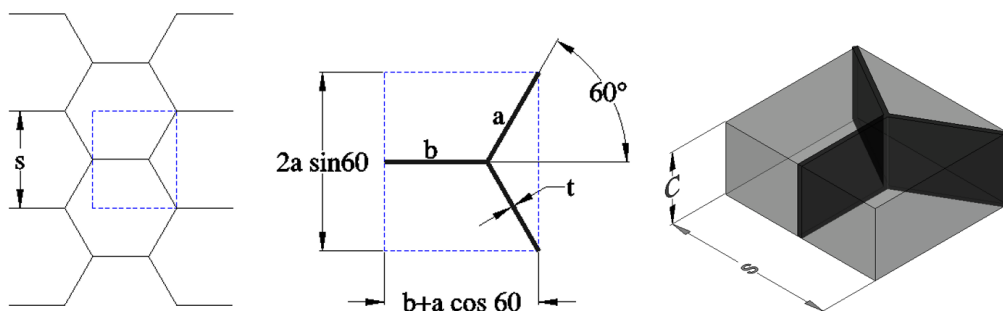


Figure 3.5: Basic Geometrical Elements Analysis

Where:

s : cell size ($s = a\sqrt{3}$)

a : cell wall length.

b : cell wall length.

t : web thickness

C : core height

- For a regular hexagonal honeycomb with a single web thickness, side length (a) is equal to (b), and the two intersect at 60° , as shown in figure (3.5).

$$\begin{aligned}
 \text{Honeycomb core density } (\rho_c) &= \frac{\text{mass}}{\text{volume}} \\
 &= \frac{(2a+b)t * C * \rho_s}{(2 a \sin 60) * (b+a \cos 60) * C} \\
 &= \frac{2}{\sqrt{3}} \frac{t * \rho_s}{a} \\
 &\approx 1.15 \frac{t * \rho_s}{a}
 \end{aligned}$$

Substitute (s) (3.1)

$$= 2 \frac{t * \rho_s}{s}$$

Equation (3.1) shows that the regular hexagonal honeycomb core density (ρ_c), depends on solid web material density (ρ_s) and geometrical parameters such as web thickness (t) and cell wall length (a or b), in other words, on cell size, equation (3.1) [26], [64].

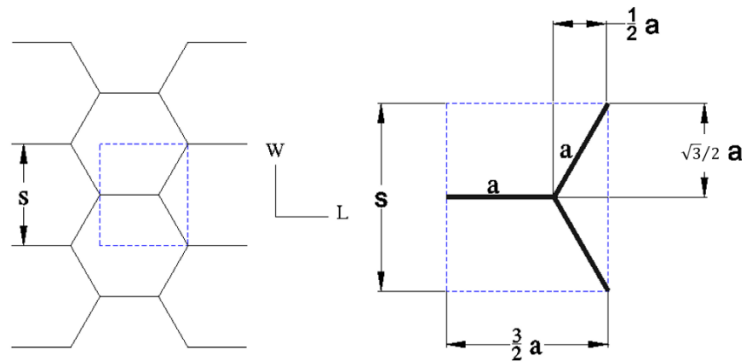


Figure 3.6:Element Analysis for Hexagonal.

It is worth noting that the sides of the hexagon that are parallel to the loading direction are the ones that will have the maximum resistance to the shear load resulting from the loading in that direction. On the other hand, the element analysis for hexagonal shown in figure (3.6) states that loading in the L-direction would act on one of the cell sides plus the components of the other two sides in the same direction (equal to $2 a$). While loading in the W-direction would act on the other components (equal to $\sqrt{3} a$). That

means the hexagonal shape made the L-direction more resistant to shear loads than the W-direction.

- For regular hexagonal honeycomb with doubled web thickness, side length (a) is equal to (b) and intersect at 60°, figure (3.7) depicts the analysis of double web thickness.

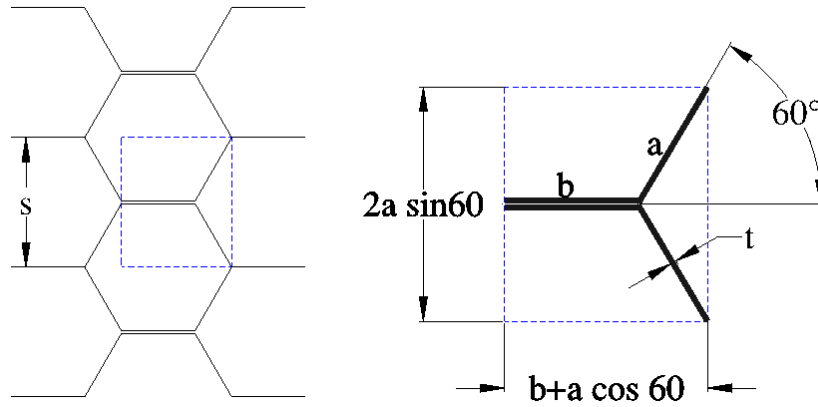


Figure 3.7: Basic Geometrical Elements Analysis for doubled web thickness

$$\begin{aligned}
 \text{Honeycomb core density } (\rho_c) &= \frac{\text{mass}}{\text{volume}} \\
 &= \frac{2(a+b)t * C * \rho_s}{(2a \sin 60) * (b+a \cos 60) * C} \\
 &= \frac{8}{3\sqrt{3}} \frac{t * \rho_s}{a} \\
 &\approx 1.54 \frac{t * \rho_s}{a} \tag{3.2}
 \end{aligned}$$

3.2.2 Triangular Core

The triangular honeycomb core is made up of identical prismatic hollow cells with a triangular section (identical length and thickness sides crossed at 60° angles), and it displays orthotropic behavior, which means that its mechanical properties are influenced by the direction in which the structure is oriented, particularly in the "L" and "W" directions.

3.2.2.1 Core Density

By utilizing the same technique that has been used in hexagonal honeycombs, the triangular honeycomb core must be divided into its fundamental geometric components in order to calculate its density. That explains in figure (3.8).

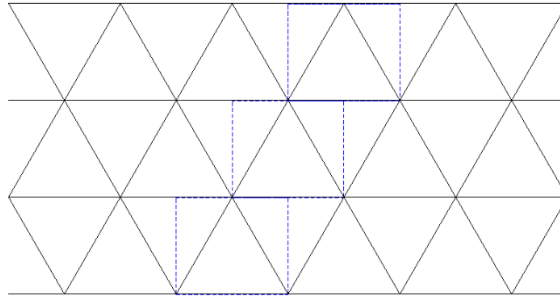


Figure 3.8: Basic Geometrical Elements of Triangular Honeycomb

In order to determine density, which is defined as the mass of the used material per unit volume, that element could be subjected to geometric analysis, as illustrated in figure (3.9).

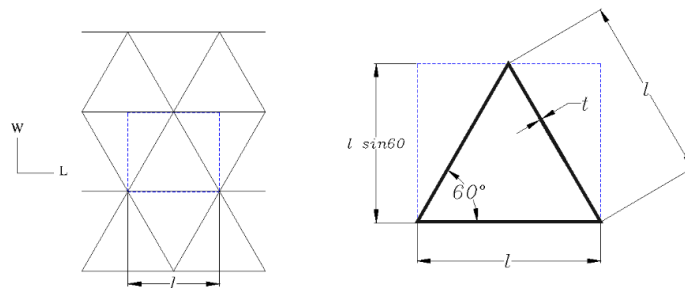


Figure 3.9: Basic Geometrical Elements Analysis

$$\begin{aligned}
 \text{Honeycomb core density } (\rho_c) &= \frac{\text{mass}}{\text{volume}} \\
 &= \frac{3 l * t * C * \rho_s}{l * (l \sin 60) * C} \\
 &= 2 \sqrt{3} \frac{t * \rho_s}{l} \\
 &\approx 3.46 \frac{t * \rho_s}{l} \tag{3.3}
 \end{aligned}$$

Where: (l : length of side)

It is noticeable that the sides of the triangles that are parallel to the loading direction will have the maximum resistance to the shear load resulting from the loading in that direction. Whereas, the element analysis for triangular shown in figure (3.9) states that loading in the L-direction would act on one of the cell sides plus the components of the other two sides in the same direction (equal to $2l$). In addition, loading in the W-direction would act on the other components (equal to $\sqrt{3}a$). That means the triangular shape made the L-direction more resistant to shear loads than the W-direction.

3.2.3 Overlapped Octagonal Core

The overlapped octagonal honeycomb core is made up of prismatic hollow cells with a multi-configuration section (hexagons and squares), and it displays orthotropic behavior too but has the same properties in both orthogonal axes (L and W).

3.2.3.1 Core Density of Overlapped Octagonal Configuration

The density of the overlapped octagonal core can be calculated by dividing it into its basic geometric parts using the same method as for the hexagonal and triangular honeycombs. Figure (3.10) shows the elements of Overlapped Octagonal Core.

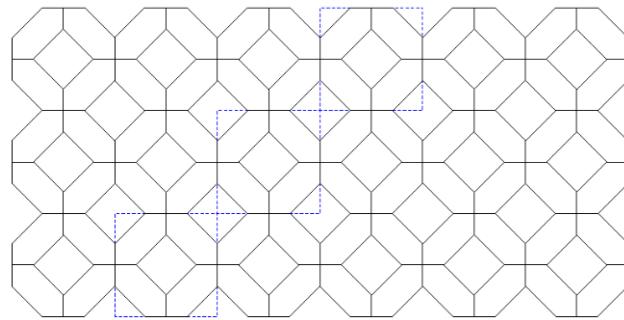


Figure 3.10: Basic Geometrical Elements of Overlapped Octagonal Core

The element could be submitted to geometric analysis to determine the density, which is the mass of the employed material per unit volume, as shown in figure (3.11).

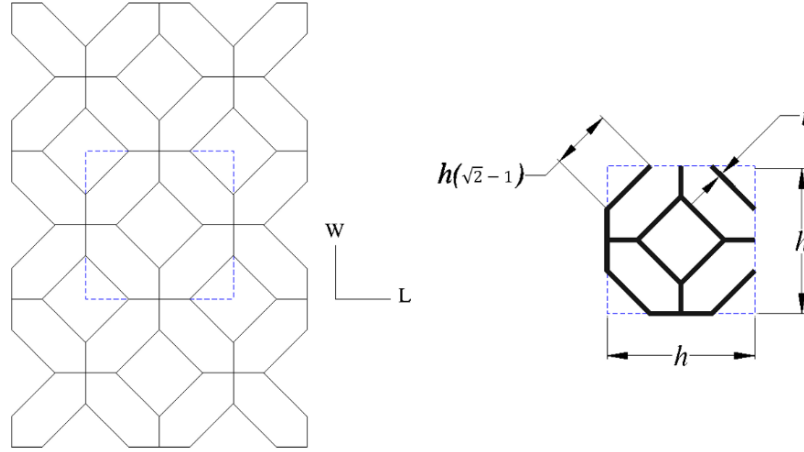


Figure 3.11: Basic Geometrical Elements Analysis

$$\begin{aligned}
 \text{Honeycomb core density } (\rho_c) &= \frac{\text{mass}}{\text{volume}} \\
 &= \frac{12 h(\sqrt{2}-1) * t * C * \rho_s}{h^2 * C} \\
 &= 12 (\sqrt{2} - 1) \frac{t * \rho_s}{h} \\
 &\approx 4.97 \frac{t * \rho_s}{h} \quad (3.4)
 \end{aligned}$$

Where:

h : height of the octagonal

On the other hand, the element analysis for the overlapped octagonal shown in figure (3.11) states that loading in the (L or W)-direction would act on the same number of elements plus the same components of others. That meant the overlapped octagonal shape made both the (L and W)-Directions have equally resistant to shear loads. This added a new feature that was not present in the hexagonal or triangular core.

3.3 Theoretical Solution to Find Deflection of Sandwich Structure

As previously stated, the behavior of the sandwich panel under bending load is based on the assumption that the skins hold the bending stresses while the core bears the shear stress, see figure (3.12)

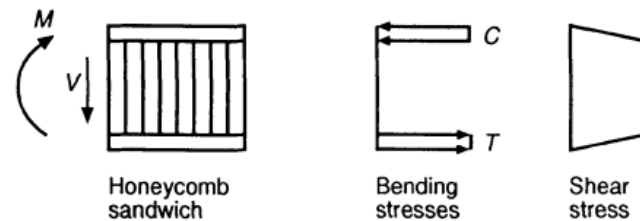


Figure 3.12: Stresses in sandwich structure [9].

So, to get a full understanding of how sandwich panels behave under bending loading conditions, it has to be assumed that a central load (p) is applied to a simply supported piece of sandwich that has a rectangular shape; its width is (b), its span is (l), its core thickness is (c), and its skin thickness is (t), as illustrated in figure (3.13).

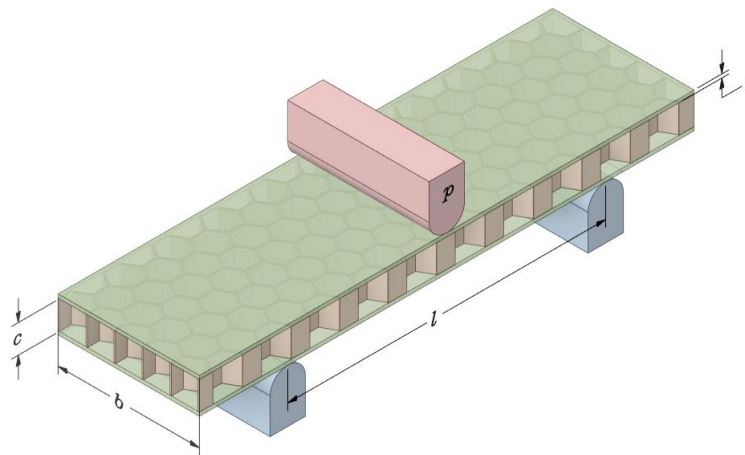


Figure 3.13: Flexural Test.

As a result, the total deflection (δ_{total}) produced in that sandwich is a combination of the bending deflection ($\delta_{bending}$) of skins and the shear deflection (δ_{shear}) of the core, as illustrated in figure (3.14).

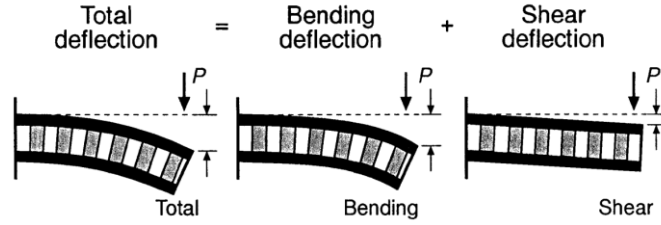


Figure 3.14: Produced Deflection [9] .

Equation (3.6) gives the total deflection (δ_{total}) value in that case [26]

$$\begin{aligned} \delta_{total} &= \delta_{bending} + \delta_{shear} \\ &= \frac{p l^3}{B_1 (EI)_{eq}} + \frac{p l}{B_2 (AG)_{eq}} \end{aligned} \quad (3.5)$$

And, based on the parallel axis theorem, for the rectangular section beam, bending stiffness:

$$(EI)_{eq} = \underbrace{\frac{E_c b c^3}{12}}_{\text{too small}} + \underbrace{\left(\frac{E_f b t_s^3}{12} \right) * 2}_{\text{too small}} + \underbrace{E_f b t \left(\frac{c + t_s}{2} \right)^2 * 2}_{t_s \approx \text{too small}}$$

the equivalent flexural rigidity $(EI)_{eq}$ will be,

$$(EI)_{eq} = \frac{E_f b t_s c^2}{2} \quad (3.6)$$

Because the first and second terms are too small in comparison with the third one, they were ignored, and skin thickness (t) was so thin in comparison with core thickness (c) that it was neglected, so we will get the bending term with an acceptable approximation in equation (3.5).

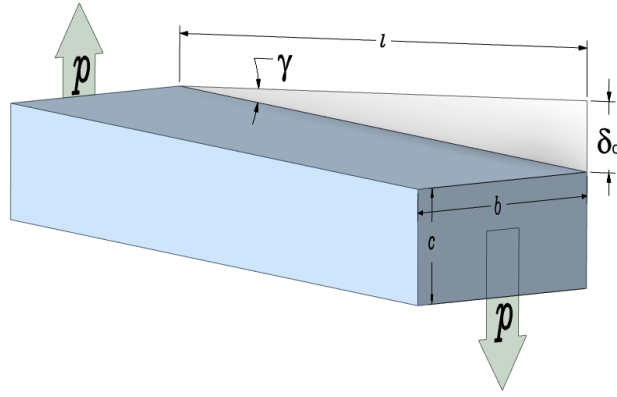


Figure 3.15: Shear deflection of core.

To determine the equivalent shear rigidity $(AG)_{eq}$, or the second term[65]:

$$\tau_c = G_c * \gamma$$

$$\frac{p}{A_c} \propto G_c * \frac{\delta_c}{l}$$

$$\therefore \delta_c = \frac{p l}{B_2 b c G_c}$$

Where: $(A_c = b c)$, $(\gamma = \frac{\delta_c}{l})$, as illustrated in figure (3.15).

$$(AG)_{eq} = b c G_c \quad (3.7)$$

Where $(B_1 = 48$ and $B_2 = 4)$ theoretical values in three-point bending with the central load (p) [26]

$$\therefore \delta_{total} = \frac{p l^3}{48 (EI)_{eq}} + \frac{p l}{4 (AG)_{eq}} \quad (3.8)$$

$$or \quad \delta_{total} = \underbrace{\frac{p l^3}{24 E_f b t_s c^2}}_{\delta_{bending}} + \underbrace{\frac{p l}{4 b c G_c}}_{\delta_{shear}} \quad (3.9)$$

$$and \quad \frac{\delta_{total}}{p} = \frac{l^3}{24 E_f b t_s c^2} + \frac{l}{4 b c G_c} \quad (3.10)$$

Where:

δ_{total} : total sandwich deflection under bending load

p : load

l : length of span sandwich beam

E_f : modulus of elasticity of facing

b : width of sandwich beam

t_s : skin thickness

c : core thickness

G_c : shear modulus for the core

Equation (3.9) shows that the core is responsible for the shear part of the total sandwich deflection, particularly its shear modulus value (G_c), which is a function of core density (ρ_c) and solid material properties (E_s, ρ_s), as in equation (3.11) [26].

$$G_c = C_2 E_s (\rho_c / \rho_s)^2 \quad (3.11)$$

Where:

ρ_c : core density

ρ_s : solid material density

E_s : Modulus of elasticity of solid material of core

C_2 : constant

Referring to the previous equation (3.1), which shows that the control parameters of the core density value (ρ_c) for a regular hexagonal honeycomb are solid material density (ρ_s), wall thickness (t), and cell size (s). Consequently, these parameters partially affect sandwich deflection, as in equation (3.9), and its compliance, as in equation (3.10), consequently, its stiffness.

$$G_c = \frac{2 t}{s \cos \theta (1 + \sin \theta)} G_s \quad (3.12)$$

Where equation (3.12) exhibits the effect of the geometrical parameters of regular hexagonal honeycomb cells (t or s) on the shear modulus of the core (G_c)[66]

3.4 Numerical Solution to Find Deflection of Sandwich Structure

To determine the deflection due to a bending load, the simulation software ANSYS 2021 R2 is used to build models and subject them to a three-point bending test experiment with graduated values of concentrated load (0 – 50 – 100- 150..... 400 N) to find out the resultant deflection and the stiffness of each sample of the three tested core types in this study and to compare the obtained results with the theoretical and experimental results.

3.4.1 Boundary Conditions of flexural loading

To simulate loading conditions in theoretical and experimental analyses, the geometric models have been designed and drawn by SpaceClaim 2021 software, which is the new default drawing software of Ansys 2021r2, the drawn models include the three types with three densities, and then the models have been subjected to three-point bending load boundary conditions, as illustrated in figure (3.16).

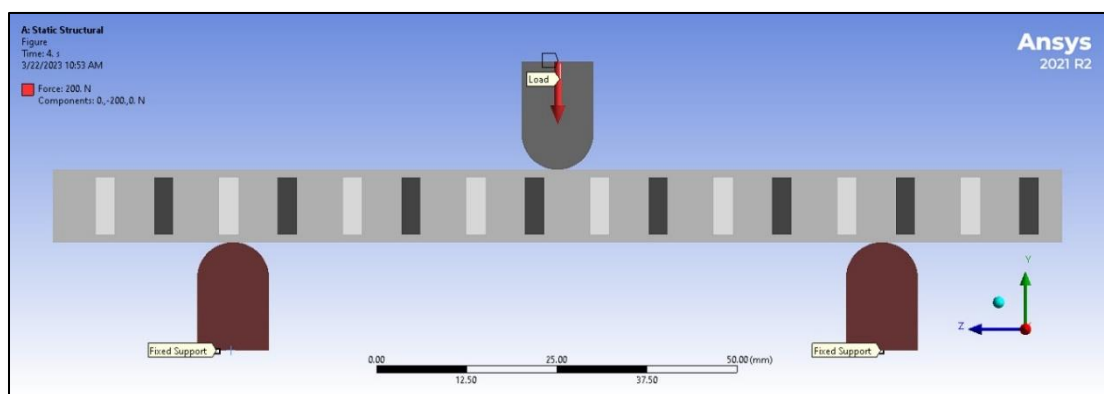
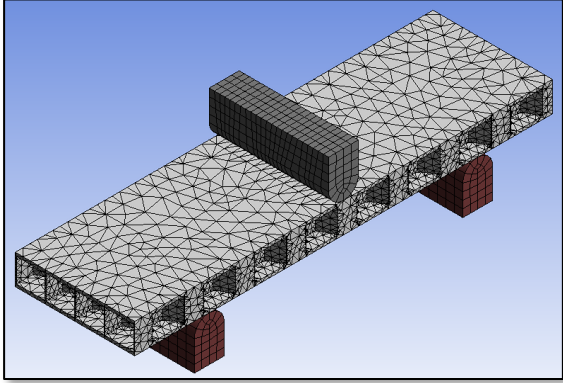


Figure 3.16:Boundary Conditions.

3.4.2 Regular Hexagonal Core Meshing

The regular hexagonal core samples, which have been designed in three densities, are then exported to the Static Structural, which is an analysis tool listed in Ansys 2021 R1 Simulation Software, and submitted to the meshing process; the resultant mesh statistics are listed in Table (3.1).

Table (3.1): Regular Hexagonal Cores Meshing.

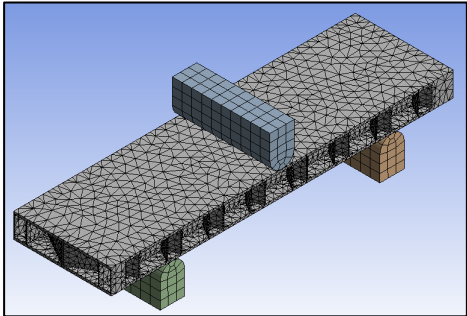
Densities	Meshing	Nodes	Elements
105 kg/m ³		103,475	52,430

After completing the meshing process, specifying the boundary conditions, setting the scheduled applied force values, and checking other simulation process settings, the program is ready for implementation and calculating the deflection values for each amount of the applied force.

3.4.3 Triangular Core Meshing

With the same previous procedures, the resultant triangular core mesh statistics are listed in Table (3.2).

Table (3.2): Triangular Cores Meshing.

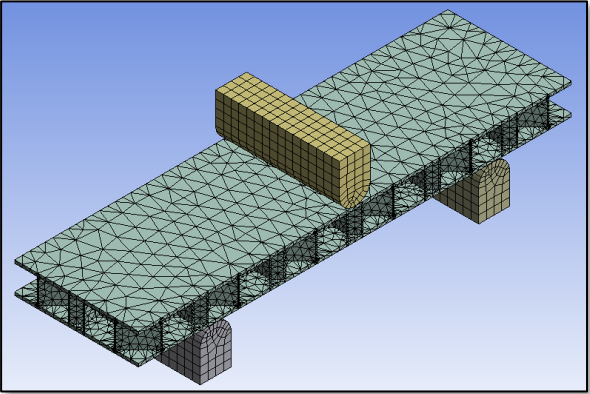
Densities	Meshing	Nodes	Elements
105 kg/m ³		94,438	48,839

After completing the meshing process, the program is ready for implementation and calculating the deflection values for each amount of the applied force.

3.4.4 Overlapped Octagonal Core Meshing

With the same previous procedures, the resultant Overlapped Octagonal Core mesh statistics are listed in Table (3.3).

Table (3.3): Overlapped Octagonal Cores Meshing.

Densities	Meshing	Nodes	Elements
105 kg/m ³		85,396	42,181

After completing the meshing process, the program is ready for implementation and calculating the deflection values for each amount of the applied force.

3.5 Numerical Solution of the Other Orientation

Depending on how the force is applied, the honeycomb core has different mechanical characteristics in various orientations. So, to determine the preferred loading direction, the variation must be examined. For the tested configurations in this study, it is required to conduct a numerical check using Ansys simulation software.

3.5.1 Regular Hexagonal Honeycomb Core Orientation

Regular hexagonal honeycomb core has two main loading directions (L and W). Thus, the required simulation contains two bending tests, the first loaded in the L-direction and the second loaded in the W-direction, as shown in figure (3.17).

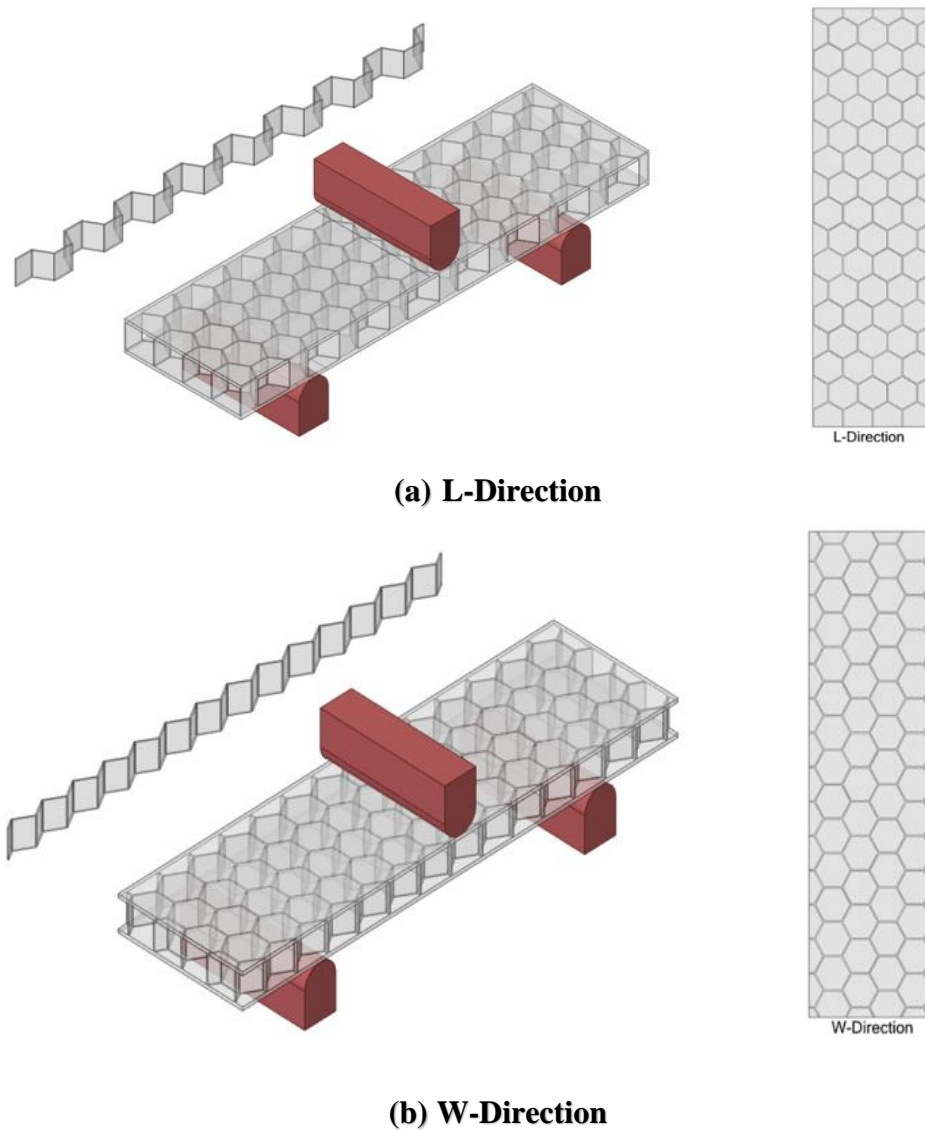
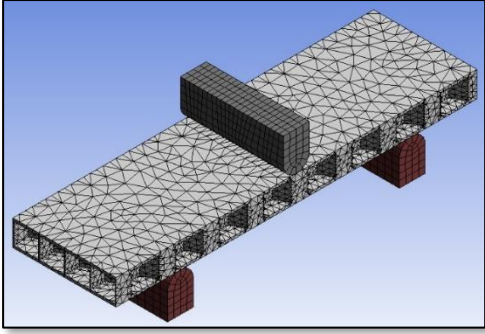
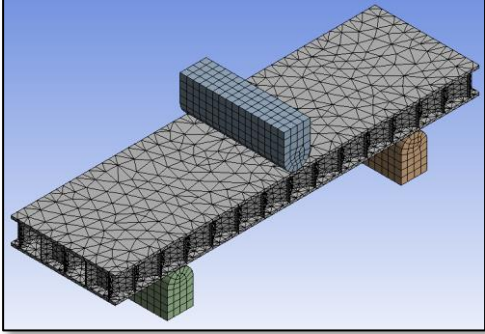


Figure 3.17: Orientation (a) L-Direction (b) W-Direction for hexagonal core

The regular hexagonal core samples, which have been designed in two orientation loading directions, are then exported to the static structural analysis tool listed in Ansys 2021 R1 simulation software and submitted to the meshing process; the resultant mesh statistics are listed in Table (3.4).

Table (3.4): Regular Hexagonal Cores Meshing.

Direction	Meshing	Nodes	Elements
L		103,475	52,430
W		107,016	54,168

After completing the meshing process, the program is ready for implementation and calculating the deflection values for each amount of the applied force.

3.5.2 Triangular Honeycomb Core Orientation

Triangular honeycomb core has two main loading directions (L and W). Thus, the required simulation contains two bending tests, the first loaded in the L-direction and the second loaded in the W-direction, as shown in figure (3.18).

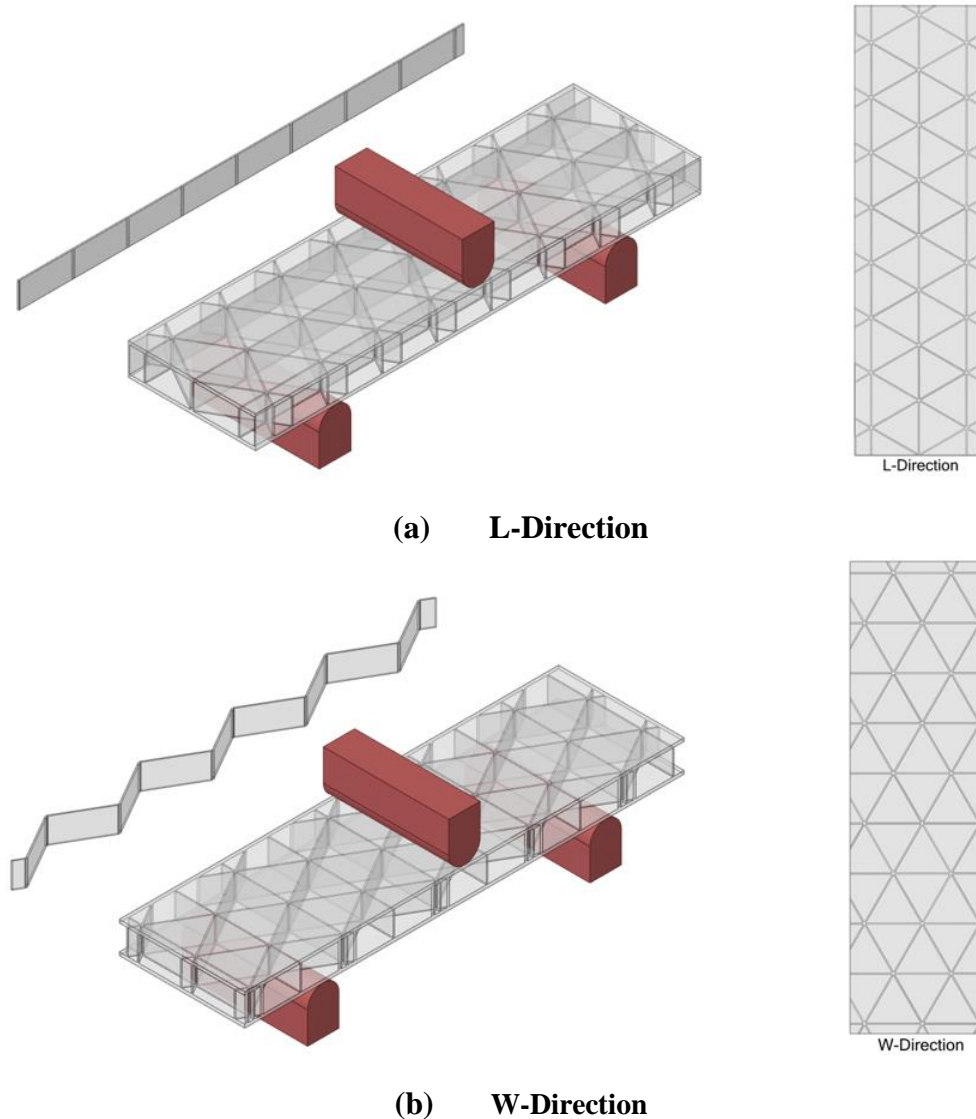
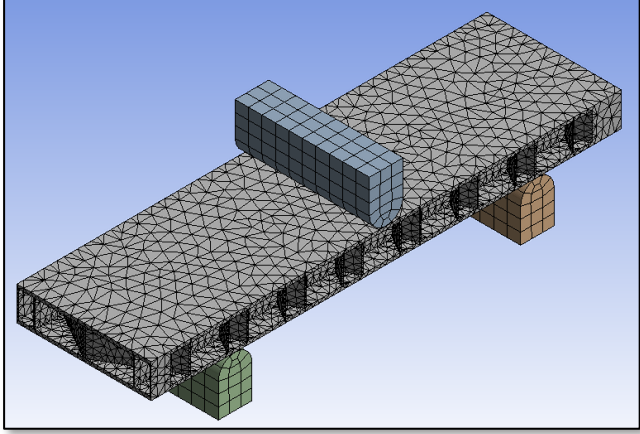
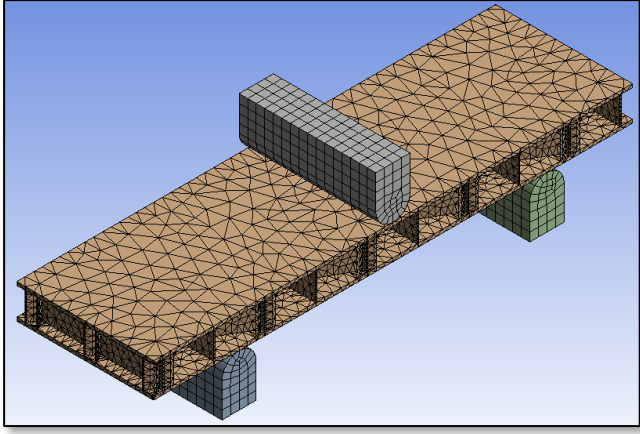


Figure 3.18:Orientation (a) L-Direction (b) W-Direction for triangular core

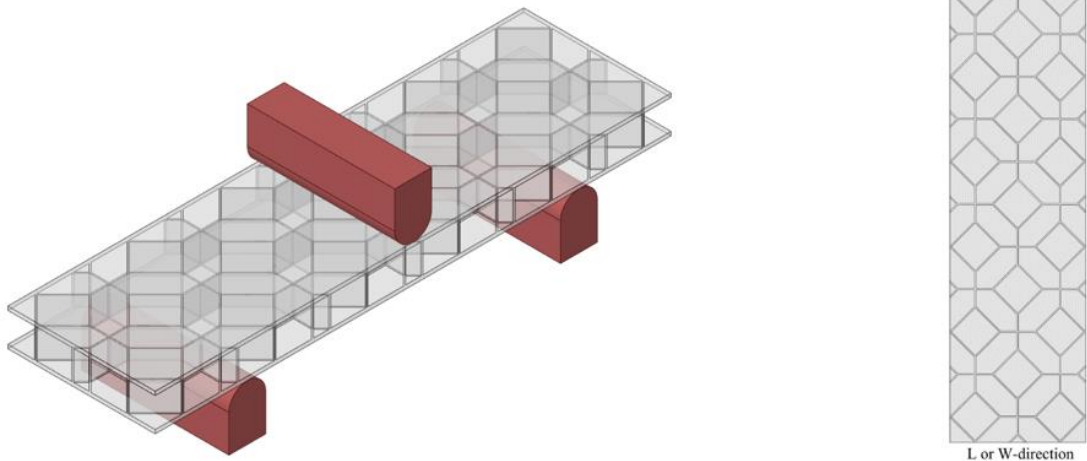
Triangular honeycomb core samples, which have been designed in two orientation loading directions, are then exported to the static structural analysis tool listed in Ansys 2021 R1 Simulation Software and submitted to the meshing process; the resultant mesh statistics are listed in Table (3.5). After completing the meshing process, the program is ready for implementation and calculating the deflection values for each amount of the applied force. By compare the results for each loading orientation (L or W) it would be clear the variation in properties. It's important to mention that the L and W directions are orthogonal, which means the mechanical properties would be different at 90° .

Table (3.5): Triangular honeycomb Cores Meshing.

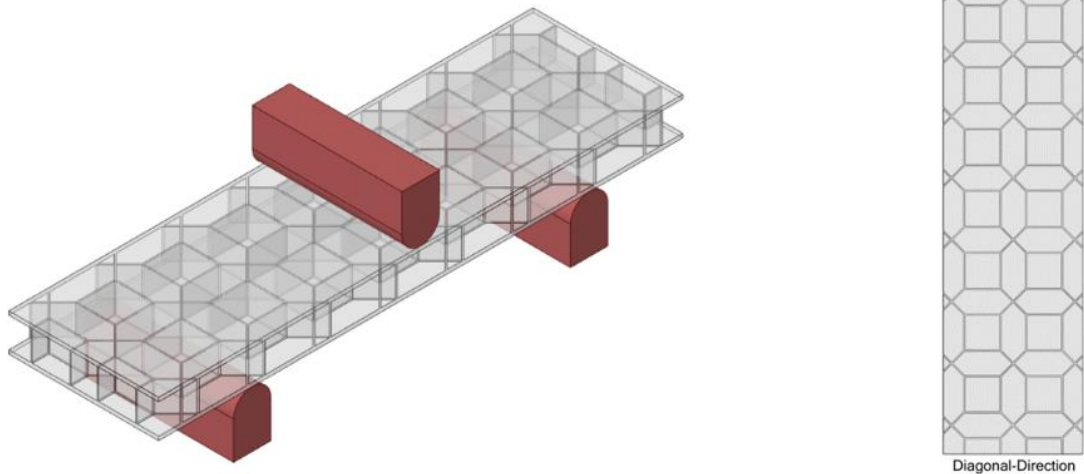
Direction	Meshing	Nodes	Elements
L		94,438	48,839
W		80,061	39,936

3.5.3 Overlapped Octagonal Core Orientation

Overlapped Octagonal Core has the same mechanical properties in both loading directions (L and W), but it is different diagonally; as a result, the simulation includes two bending tests for orientation varying at 45° , as shown in figure (3.19).



(a) L or W-Direction

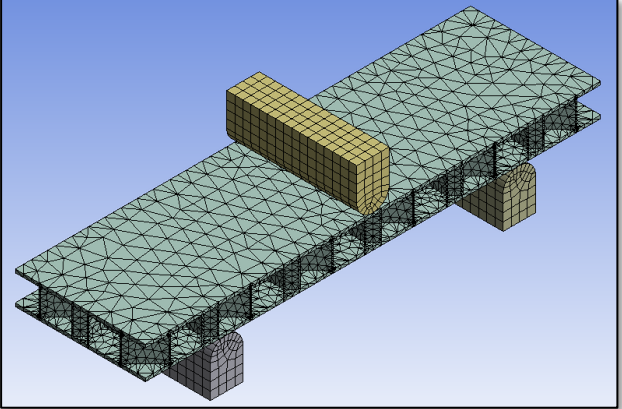
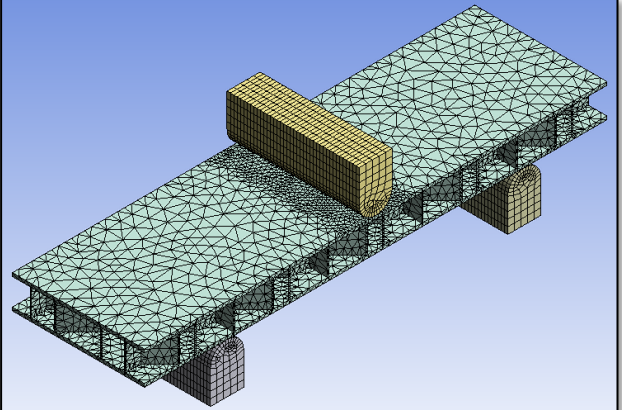


(b) Diagonal-Direction

Figure 3.19: Loading in (a) L or W, and (b) diagonal directions.

The Overlapped Octagonal Core samples, which have been designed in two orientation loading directions, are then exported to the static structural analysis tool listed in Ansys 2021 R1 simulation software and submitted to the meshing process; the resultant mesh statistics are listed in Table (3.6).

Table (3.6): Overlapped Octagonal Cores Meshing.

Direction	Meshing	Nodes	Elements
L or W		85,396	42,181
Diagonal		135,881	57502

3.6 Free Vibration Analysis

The impact of the core density value on the natural frequency of a sandwich would be clear by running a simulation with the Ansys software to determine the first four natural frequencies for specimens with different core densities.

3.6.1 Boundary Conditions For Free Vibration Analysis

To conduct a simulation of free vibration analysis, the geometric models have been designed and drawn by the SpaceClaim 2021 software. The models were (300*300) mm square boards of regular hexagonal sandwich

in three densities, as well as a fully solid one with the same dimensions, and then the boards were fully clamped, as illustrated in figure (3.20).

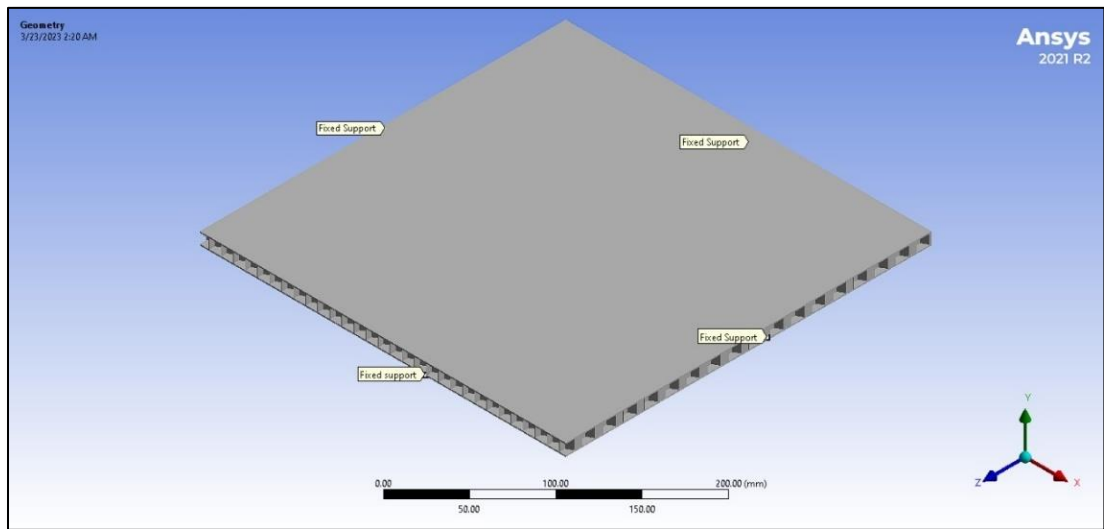
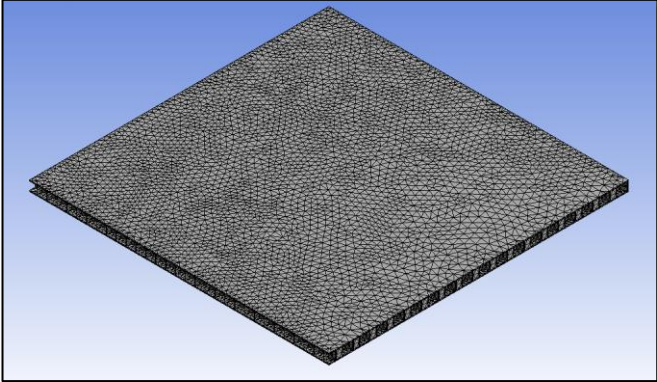


Figure 3.20: Boundary Conditions for free vibration analyses.

The models are then exported to Modal, which is an analysis tool listed in Ansys 2021 R1 Simulation Software, and submitted to the meshing process; the resultant mesh statistics are listed in Table (3.7). After completing the meshing process, specifying the boundary conditions, and checking other simulation process settings, the program is ready for implementation. Finally, find out the first four natural frequency values and their mode shapes.

Table (3.7): Sample of Boards Meshing.

Direction	Meshing	Nodes	Elements
FVHA		769,155	430,734

3.7 Impact Analysis

In order to simulate a low-velocity impact test and reveal the effect of core density magnitude on the sandwich's behavior under sudden dynamic loading, it has to conduct a simulation of an experiment that meets ASTM D7766 [67] requirements and involves dropping a cylindrical mass with a hemispherical head from a certain height [60]. This would leave a dent on the sandwich's surface, whose depth depends on the sandwich's resistance to impact and, consequently, the effect of the sandwich's core density on that depth value.

3.7.1 Boundary Conditions For Impact Analysis

To conduct a simulation of an impact analysis, the geometric models have been designed and drawn by the SpaceClaim 2021 software. The models are (100*150)mm rectangular sandwich boards in three densities, as well as a cylindrical (0.31164) kg mass with a (12.75) mm hemispherical head made of structural steel, hitting the tested board with (40) m/s dropping velocity. The boards are fully clamped by their four (12) mm of ribbon edges as shown in figure (3.21). It is worth noting that the analysis simulates the experiment using the Drop Tower device.

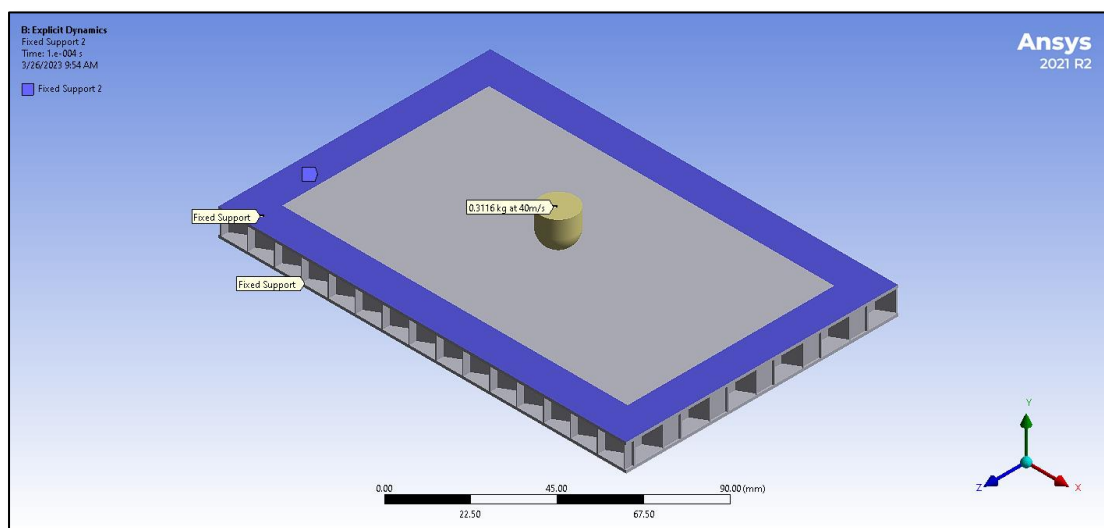
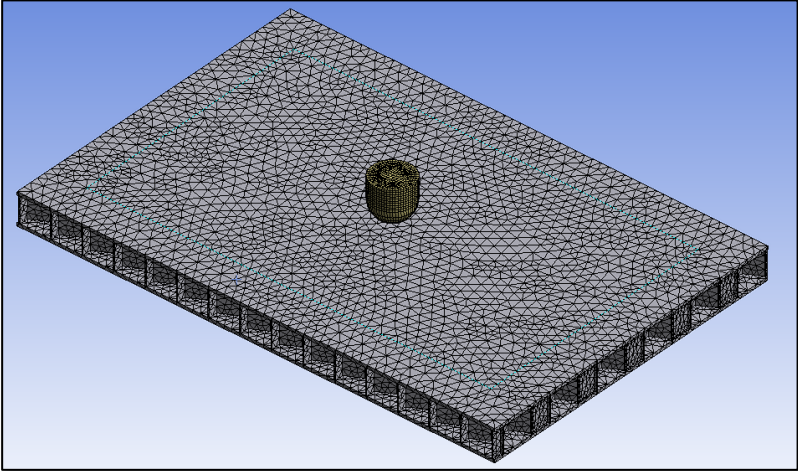


Figure 3.21: Boundary Conditions for impact test.

The resultant mesh statistics are listed in Table (3.8). After completing the meshing process, specifying the boundary conditions, and checking other simulation process settings, the program is ready for implementation.

Table (3.8): Sample of Meshing.

Meshing	Nodes	Elements
	43,896	143,442

3.7.2 Impact Test of Regular Hexagonal Honeycomb Core

An impact test was numerically performed on a regular hexagonal honeycomb core with three densities by exporting models to Explicit Dynamics, which is an analysis tool in Ansys simulation software. As shown in figure (3.22)

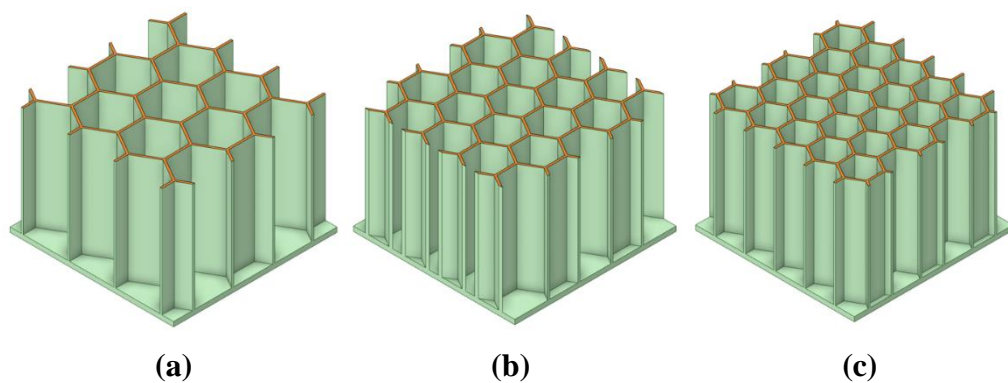


Figure 3.22: Hexagonal Samples with (a) 105, (b) 132, and (c) 160 kg/m³ densities.

After being subjected to dropping that cylindrical object at the same velocity, sandwich panel samples would have a particular dent, whose depth should indicate how the sandwich could withstand impact for each core density.

3.7.3 Impact Test of Triangular Honeycomb Core

An impact test is numerically performed on a Triangular Honeycomb Core with three densities by exporting models to Explicit Dynamics. As shown in figure (3.23)

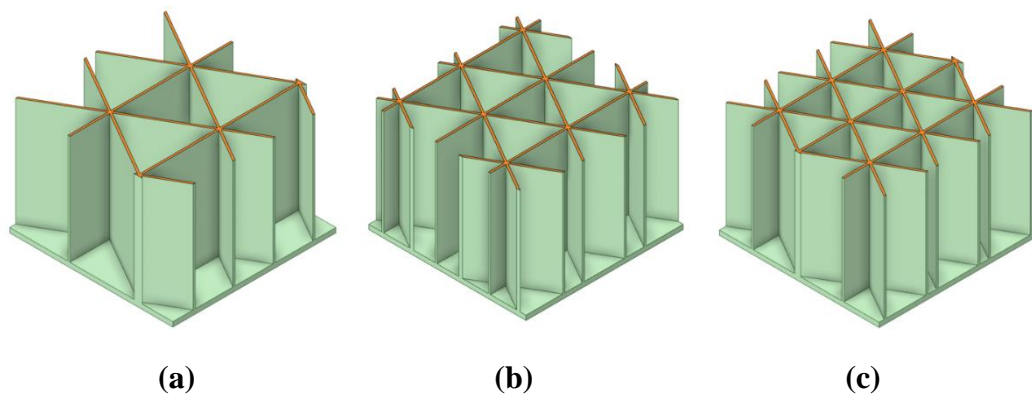


Figure 3.23: Triangular Samples with (a) 105, (b) 132, and (c) 160 kg/m³ densities.

After being subjected to dropping that cylindrical object at the same velocity, sandwich panel samples would have a particular dent, whose depth should indicate how the sandwich could withstand impact for each core density.

3.8 Wing Analysis

A wing made of honeycomb sandwich construction in three densities for regular hexagonal, triangular, and overlapped octagonal is used in a virtual case study to simulate the core type and density influence on wing overall performance during flight conditions.

3.8.1 Airfoil

To design a wing, the NACA 0009 airfoil data has to be specified and downloaded from the airfoil tool website [68], as shown in figure (3.24).

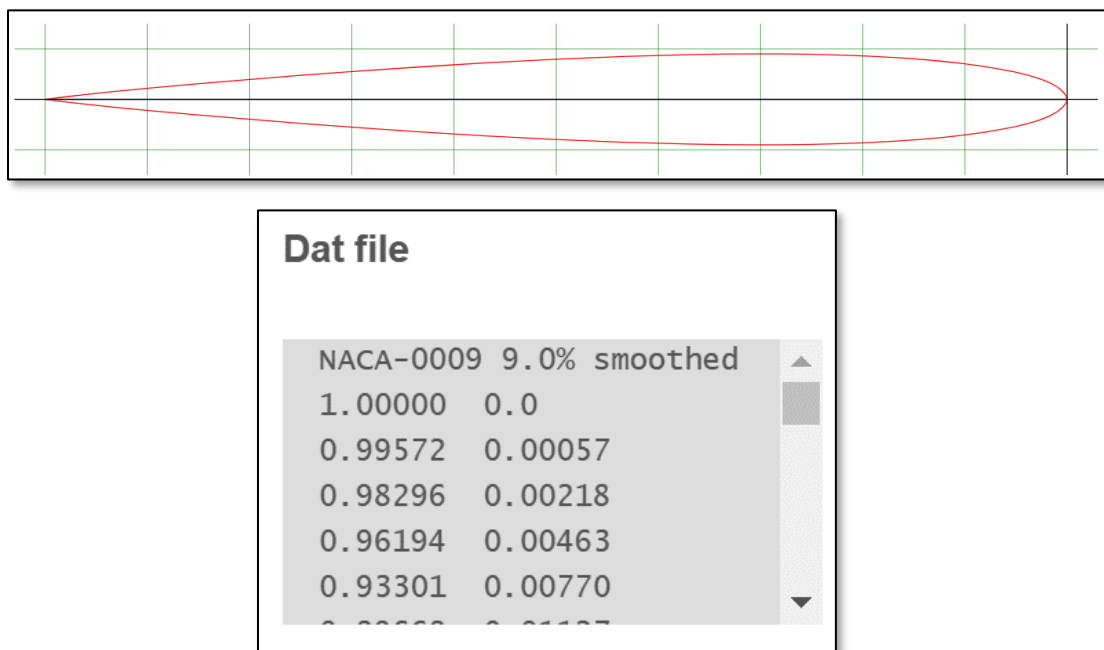


Figure 3.24:NACA 0009 Airfoil [68].

3.8.2 Wing Structure

Based on an airfoil, wing models are created in 250mm length, 92mm width, and 9mm thickness, involving an 8mm honeycomb core height and 5mm skin thickness. as shown in figure (3.25).

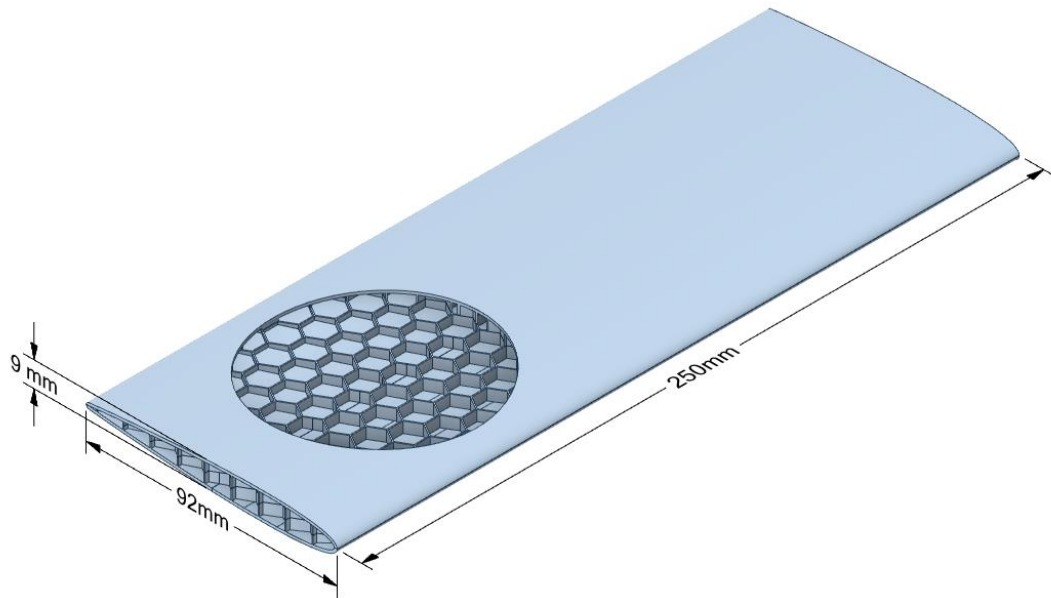


Figure 3.25:Wing Structure.

3.8.3 Boundary Conditions For Wing

To simulate flight conditions, the models were fixed at one end and subjected to distributed pressure on their lower surfaces (producing lift force) and line pressure on their front edges (producing drag force), as illustrated in figure (3.26).

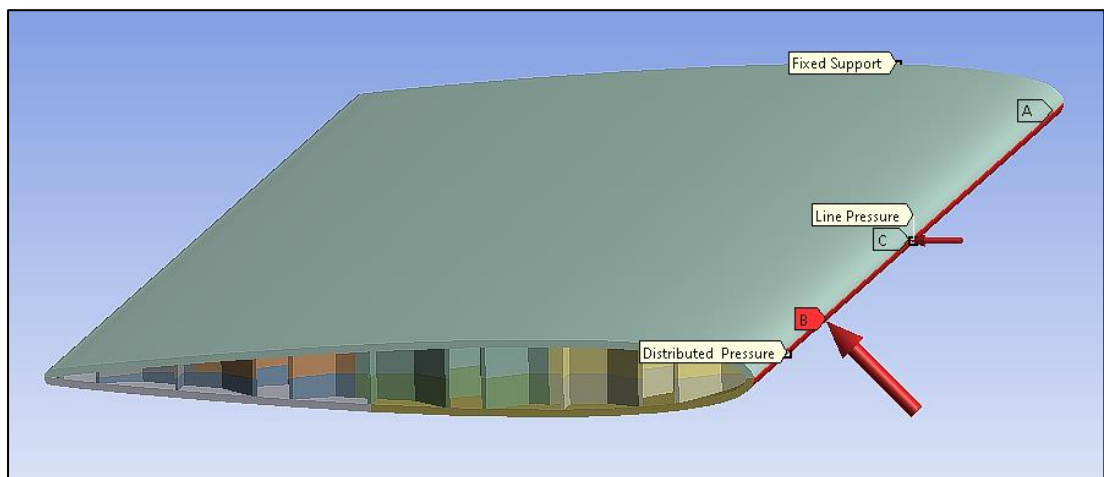
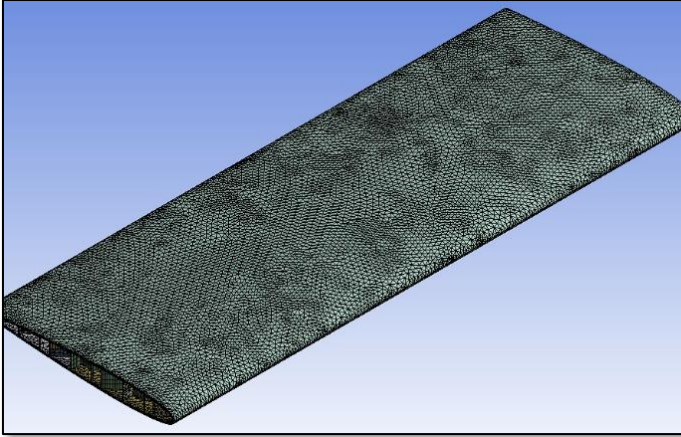


Figure 3.26:Boundary Condition.

3.8.4 Wing Meshing

The wing models, which have been designed in three densities for regular hexagonal, triangular, and overlapped octagonal cores, are then exported to the static structural tool and submitted to the meshing process; the resultant mesh statistics are listed in Table (3.9).

Table (3.9): Sample of Wing Meshing.

Meshing	Nodes	Elements
	784,511	438,309

Chapter Four: Experimental Work

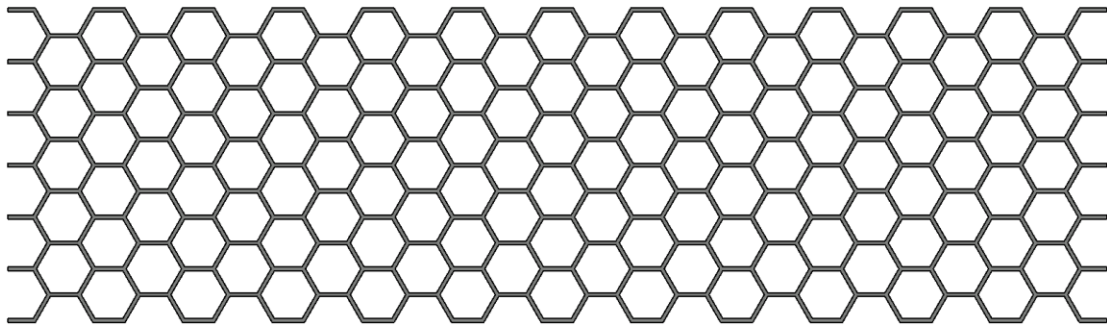
4.1 General

Firstly, to study the effects of a specific property of a material, it must specify parameters that govern this property's value. So, it will be possible to prepare and test samples with various magnitudes of that property. Consequently, the effects of property value variation on material behavior will be obvious. Here, with a honeycomb core of a certain configuration, the property is core density. The governing parameters are cell size, cell wall thickness, and density of the solid material from which the core is made, as previously shown in equation (3.1). To investigate the effect of core density, samples of sandwich panels with various core configurations have been prepared; each configuration has three cell size values, resulting in three core densities. In other words, controlling the density value by changing the cell size value, while the other affective factors are constant with no change. Finally, subjecting those samples to the right test with a specific standard may give a complete understanding of how core density affects sandwich behavior under static or dynamic loading conditions for each core configuration.

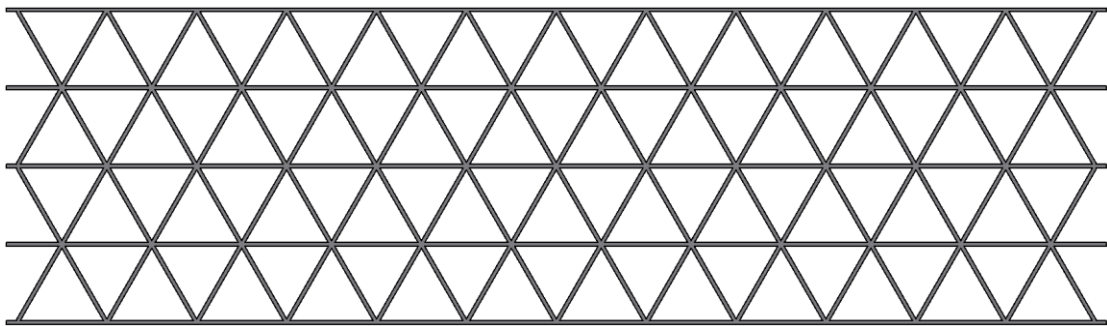
4.2 Core Configurations

Since the purpose of the research is to investigate the influence of the core density of sandwich panels used in aircraft structures. Therefore, high strength-to-weight and stiffness-to-weight ratios are fundamental requirements, so it is necessary to keep weight to a minimum while maintaining maximum strength to prevent structural failure. Otherwise, stiffness is also essential to avoid obstructing the aerodynamic functions of aircraft structures, especially the wings. So, the tested sandwiches will first

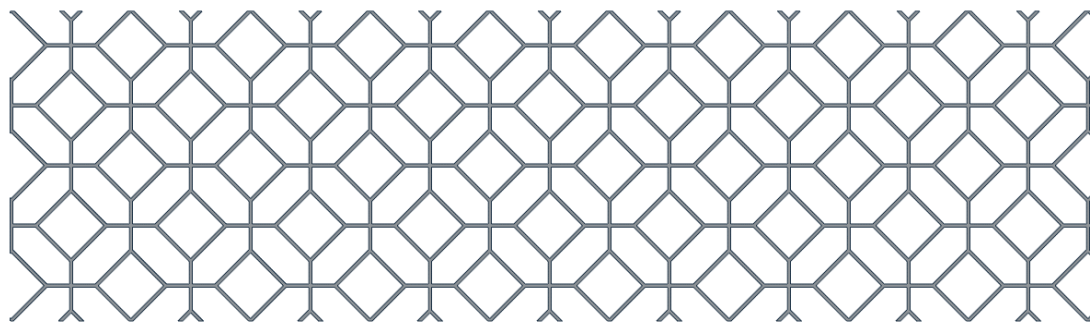
have the regular hexagonal honeycomb core configuration, which is widely used in aircraft structures. Secondly, the triangular core configuration, which is also mentioned in many research papers in its significant features, Finally, the overlapped octagonal core configuration. Figure (4.1) shows the tested configurations.



(a): Regular hexagonal honeycomb configuration.



(b): Triangular honeycomb configuration.



(c): Overlapped Octagonal honeycomb configuration.

Figure 4.1:(a,b,c) The honeycomb configurations explored in this study.

4.3 Experimental test

Utilizing the plate shear method is preferred to obtaining core shear strength and modulus, but the beam-flexure test with a three- or four-point method is often used to evaluate sandwich panel performance [22]. So, as shown in Figure (4.2) the three-point bending test is utilized in this research by investigation using a variety of samples with different core densities to that test, per the standard (ASTM C393-00) [69] by the American Society for Testing and Materials. This test gives a clear understanding of how the core density value impacts sandwich behavior under loading conditions.

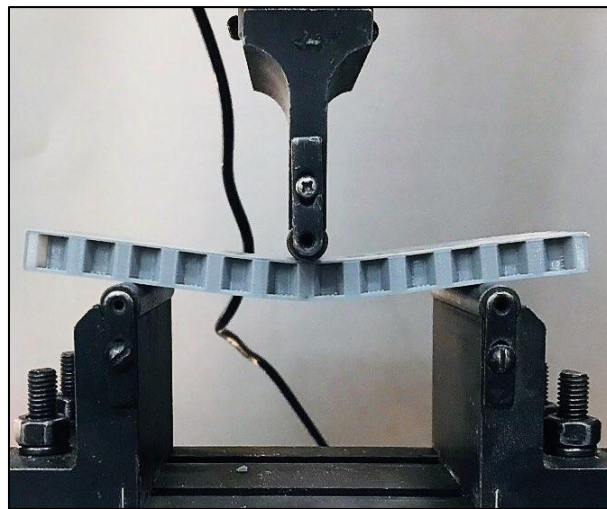


Figure 4.2: Flexural Test .

4.3.1 The standard (ASTM C393-00) Scope

The properties of flat sandwich structures are determined by subjecting simply supported beam samples with a specific geometry to a central load that causes the sandwich-facing planes to bend due to generated bending moments. Observed deflections of sandwich flexure specimens can be used to compute the flexural stiffness of the sandwich, the core shear strength, and shear modulus, or the compressive and tensile strengths of the facings [69], [70]

4.3.2 Test Specimen Dimensions

The test specimen's cross-section must be rectangular. The width must be at least twice as thick as the total thickness, not less than three times the size of a core cell and not more than half the length of the span (so the specimen will behave as a beam under bending). The specimen length must be longer than the span length by 50 mm (that prevents the sample from slipping). On the other hand, to determine core shear strengths, the specimens must have thicker facings and shorter support spans so that the facings are not stressed above the compressive or tensile stress limits of the facing material as a result of the moments created at the core collapse [70] So, the dimensions of the specimen in this research will be as shown in figure (4.3) below:

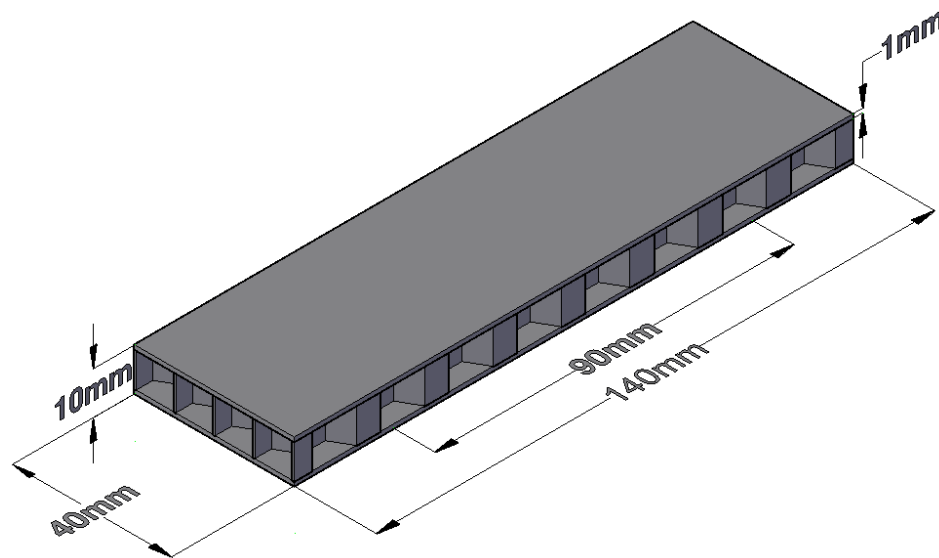


Figure 4.3: Sample geometry with selected dimensions.

Where:

- Specimen length = 140 mm
- Specimen width = 40 mm
- Specimen thickness = 10 mm
- Specimen span length = 90 mm
- Upper and lower Facing thickness = 1 mm

4.4 Prepare samples

Paper, aluminum, and Nomex honeycomb cores offered by manufacturers are often utilized to investigate the mechanical properties of specific types of them. But manufacturing and investigating new cores represented a challenge. So, 3D printing technology is one of the promising methods, which has enabled some researchers to design and investigate cores with complicated configurations that would have been difficult to create using conventional methods.

4.4.1 3D Printing

In this work, samples are prepared by an additive manufacturing technique utilizing a 3D printer, which works by fused deposition modeling (FDM) technology, in which the items are made by dividing the 3D design (drawn with any CAD program) into extremely thin layers using slicing programs, and then a 3D printer, via an extrusion heated nozzle, extrudes those layers with melted printing material (filaments) in horizontal and vertical controlled nozzle movements, as shown in Figure (4.4).

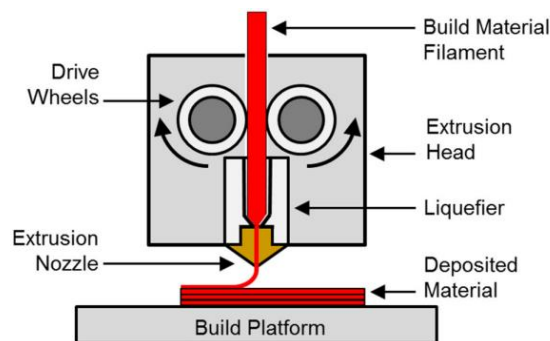


Figure 4.4: The Fused deposition modeling (FDM) process [71].

The printed layers then cool and solidify one on top of the other to create the final shape, according to the desired design [72]. Various polymers are used in 3D printing with fused deposition modeling (FDM)

technology, including acrylonitrile butadiene styrene (ABS), polylactic acid (PLA), polycarbonate (PC), polyamide (PA), polystyrene (PS), polyethylene terephthalate (PETG) [71].

4.4.2 3D Printer

The 3D printer utilized in this research is (Creality Ender 3 V2), as shown in Figure (4.5):

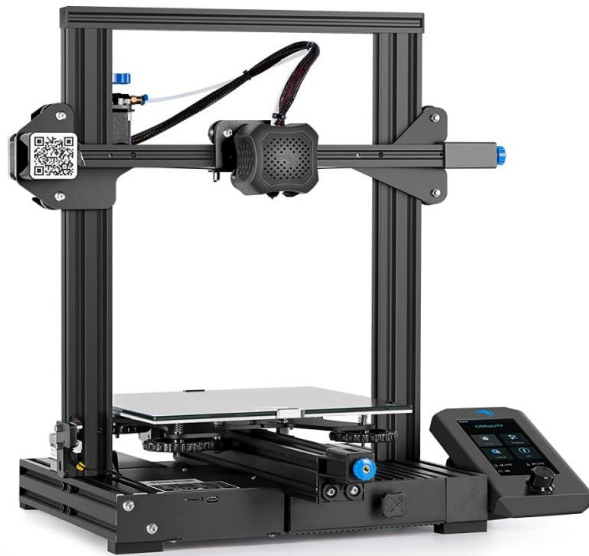


Figure 4.5:(Creality Ender 3 V2) 3D printer.

4.4.3 Filament

Printing material (filament) used in this research is polylactic acid (PLA), as shown in Figure (4.6):



Figure 4.6:Polylactic acid (PLA) filament.

4.4.4 CAD Program

The CAD program utilized to draw samples is (AutoCAD Mechanical 2023), which allows exporting a CAD file directly in a (.slt) format to the slicing program of a 3D printer, as shown in Figure (4.7).

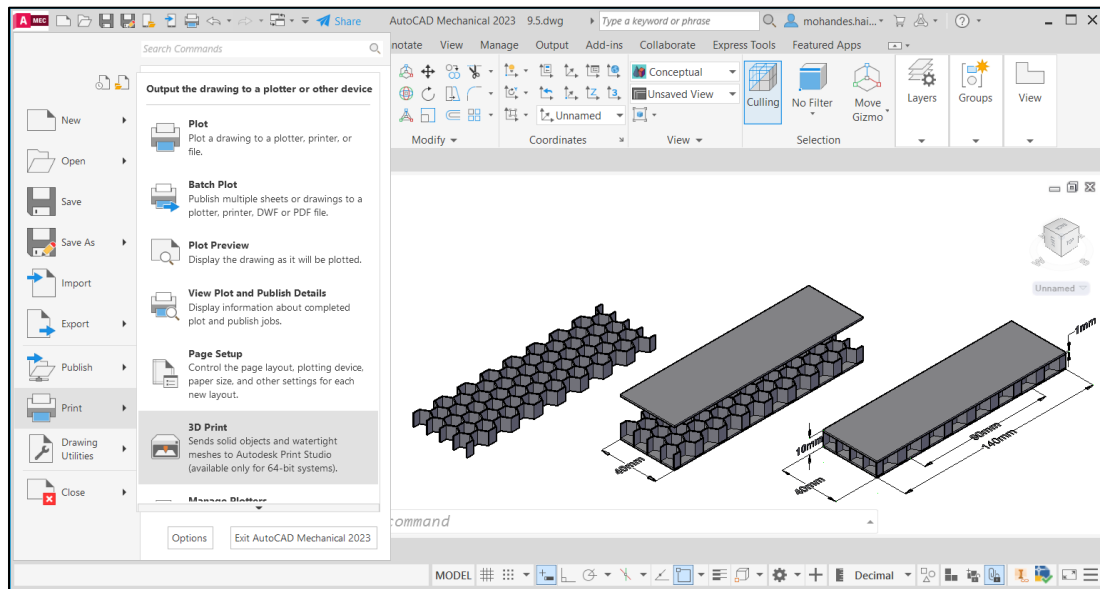


Figure 4.7: Create and export models with AutoCAD Mechanical.

4.4.5 Slicing program

In order to make a 3D model printable by a 3D printer, it has to be sliced into 2D-printable layers with a slicing program. The slicing program is utilized to do that job in this research is (Ultimaker Cura) which is a slicing software with various print settings. These settings must be carefully selected because they have effective impacts on the 3D-printed item's mechanical properties. To avoid having those impacts be negative on test results, it has to print all samples with the same settings. These settings include printing quality, number of layers, printing path and speed, and many other complex details, as well as heating temperatures appropriate for the type of used filament and its quantity. Figure (4.8) Shows the slicing process. Finally, the slicing software converts the file with (.slt) format into a (.gcode) format that can be printed on a 3D printer.

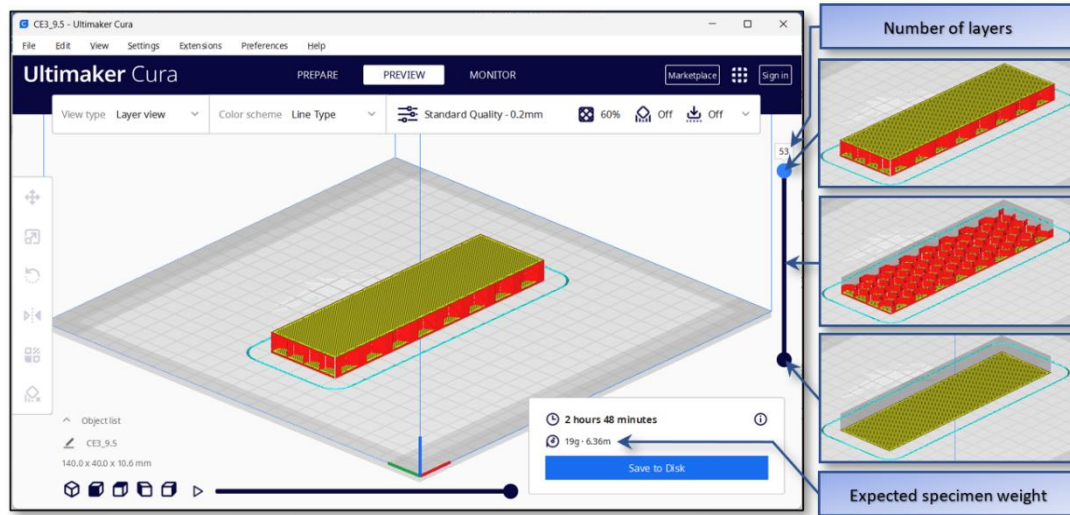


Figure 4.8:The process of slicing a specimen.

4.4.6 Specimens printing process

Honeycomb samples designed with AutoCAD Mechanical software and sliced with specific settings by the Ultimaker Cura slice program would finally be ready to be printed using the (Creality Ender 3 V2) 3D printer with PLA filament in the required quantity. But these procedures should be repeated each time to create honeycomb samples with any density for each cell configuration. Figure (4.9) Shows the printing samples.



Figure 4.9:Printing samples process.

4.4.6.1 Regular Hexagonal Honeycomb Core Manufacturing

Regular hexagonal means that all cell sides are equal and all internal corners are equal at 120° . So, manufacturing specimens with a core density of three different values will be dependent on their governing geometrical parameters, which are cell wall thickness and cell size. In this research, the cell walls will have the same thickness (0.4 mm) while cell size will be the sole governing parameter of core density magnitude, as shown in Figure (4.10).

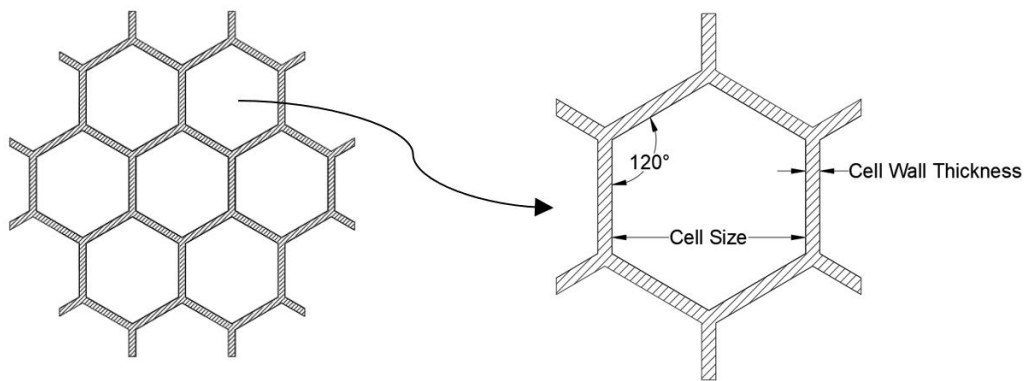


Figure 4.10: Regular hexagonal honeycomb core cell.

The majority of studies on the performance of the regular hexagonal core used cores provided by manufacturers or experimentally fabricated with the same technology (expansion or corrugated), which necessitated two adhered cell walls that would double the thickness of cell walls in the (L-direction), consequently more weight, as shown in Figure (4.11).

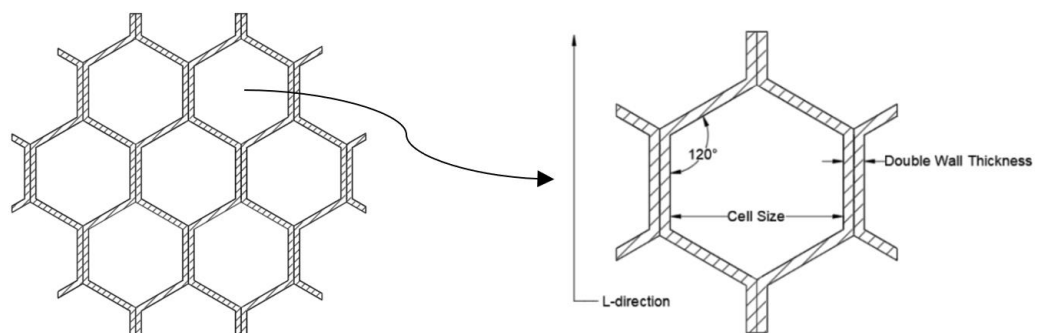


Figure 4.11: Regular hexagonal honeycomb core with doubled cell wall thickness in the L direction.

Fortunately, 3D printing technology provides the possibility of manufacturing the core identically without having to unnecessarily double the thickness of the cell walls. That allows for a more accurate exploration of the effect of core density on the overall performance of the sandwich panel, in contrast to the expansion or corrugated techniques, which are illustrated in figure (4.12).

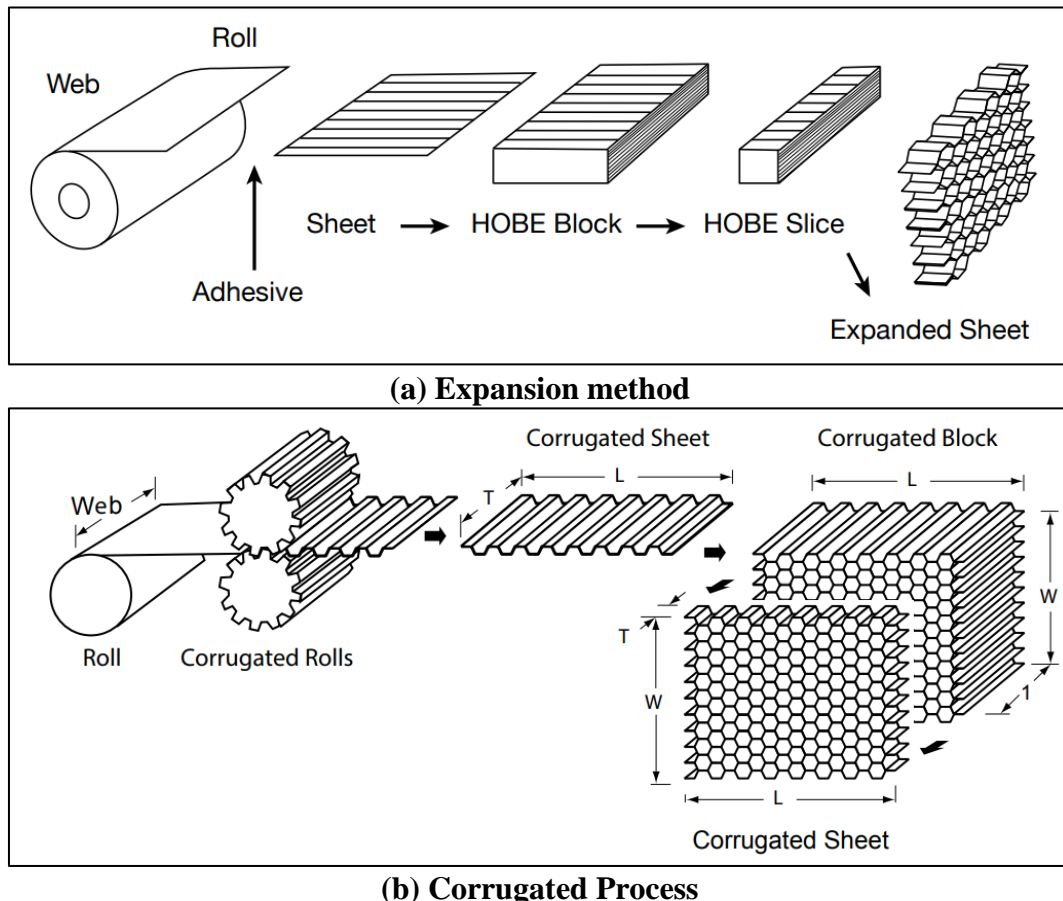


Figure 4.12: The honeycomb fabrication process [30].

So, according to the intended experiment requirements of manufacturing sandwich panel specimens that have a regular hexagonal honeycomb core with three different values of density. Samples will be in three values of cell size and, consequently, in three values of density, as follows: -

- The first specimen cell size value will be 9.5 mm, so the specimen will have four cells in its transverse cross-section, as shown in Figure (4.13).

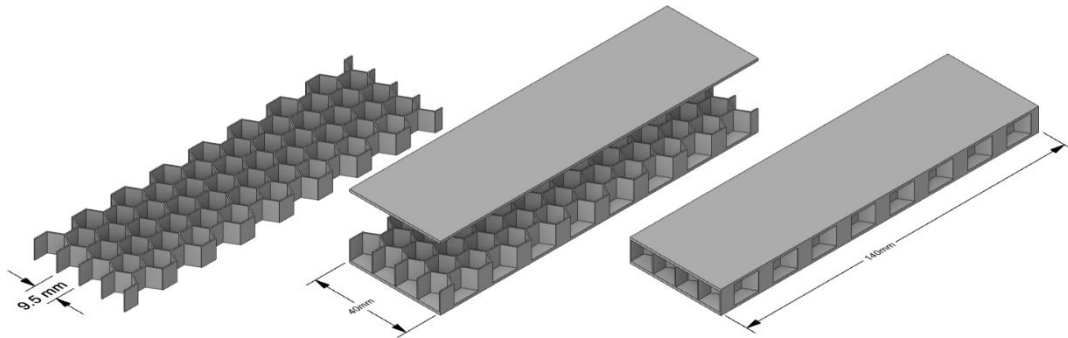


Figure 4.13: First specimen with 9.5 mm cell size.

- The second specimen cell size value will be 7.52 mm, so the specimen will have five cells in its transverse cross-section, as shown in Figure (4.14).

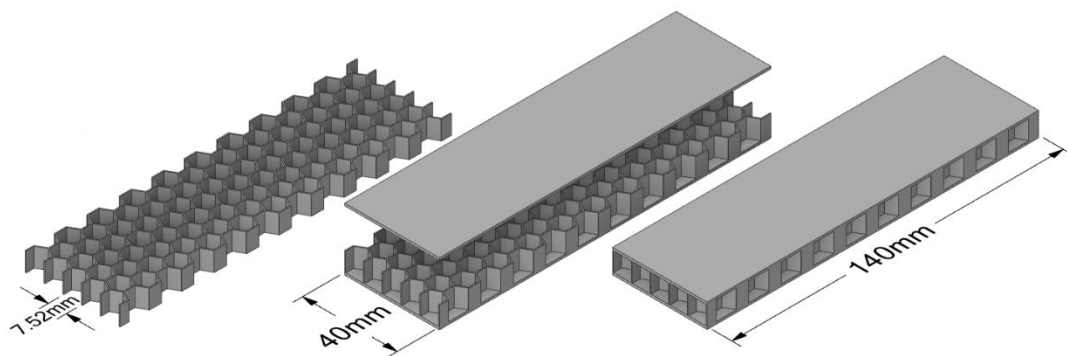


Figure 4.14: Second specimen with 7.52 mm cell size.

- The third specimen cell size value will be 6.2 mm, so the specimen will have six cells in its transverse cross section, as shown in Figure (4.15).

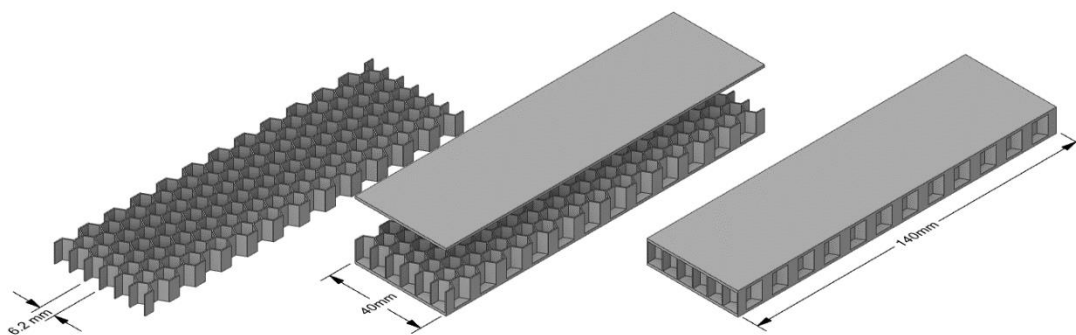


Figure 4.15: Third specimen with 6.2 mm cell size.

After utilizing AutoCAD Mechanical 2023 to draw the designed specimens, as illustrated in Figures (4.13), (4.14), and (4.15), 3D CAD files are exported to the (Ultimaker Cura) slicing program to convert 3D models

to 2D printable slices with appropriate settings for PLA material printing, as shown in Figures (4.16).

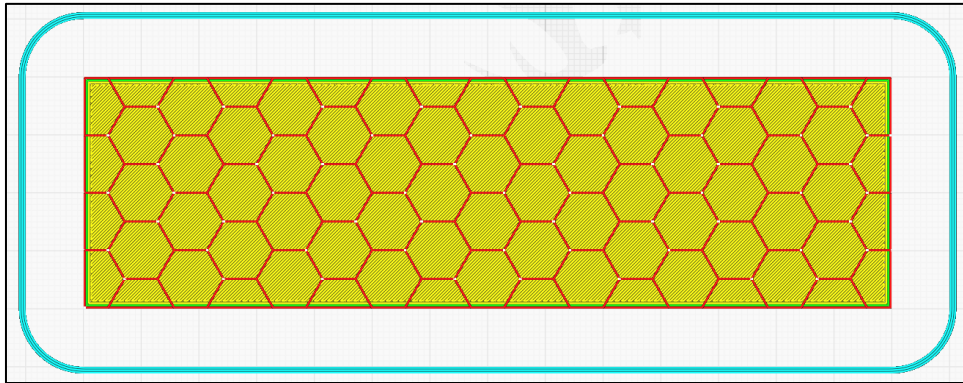


Figure 4.16: First sliced specimen with 9.5 mm cell size.

Finally, sliced specimen files were sent to the (Crealty Ender 3 V2) 3D printer provided with polylactic acid (PLA) filament to create the samples, as shown in Figures (4.19), (4.20), and (4.21).



Figure 4.17: First printed specimen with 9.5 mm cell size.

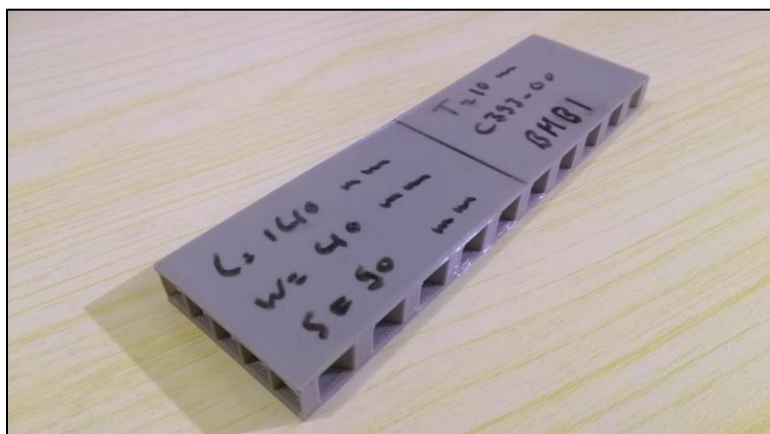


Figure 4.18: Second printed specimen with 7.52 mm cell size.



Figure 4.19: Third printed specimen with 6.2 mm cell size.

The samples are labeled with (BHA1, BHA2, and BHA3); (BHB1, BHB2, and BHB3); and (BHC1, BHC2, and BHC3) as illustrated in table (4.1) below:

Table 4.1: Samples of hexagonal type attributes

Specimen labeled code.		Number of cells in cross-section	Specimen weight (g)	Specimen core
First density 9.5mm Cell size	BHA1	4	19	
	BHA2	4	19	
	BHA3	4	19	
Second density 7.52mm Cell size	BHB1	5	20	
	BHB2	5	20	
	BHB3	5	20	
Third density 6.2mm Cell size	BHC1	6	21	
	BHC2	6	21	
	BHC3	6	21	

4.4.6.2 The Triangular Honeycomb Core Manufacturing

A triangular core means that all cell sides are equal, and all internal corners are equal too at 60° . So, manufacturing specimens with a core density of three different values will be dependent on their governing geometrical parameters, which are cell wall thickness and cell size. The cell walls in this study will have the same thickness (0.4 mm) for all manufactured and tested species with any configuration (regular hexagonal, triangular, or tetrahedral), while cell size will be the sole governing parameter of core density magnitude, as shown in Figure (4.22)

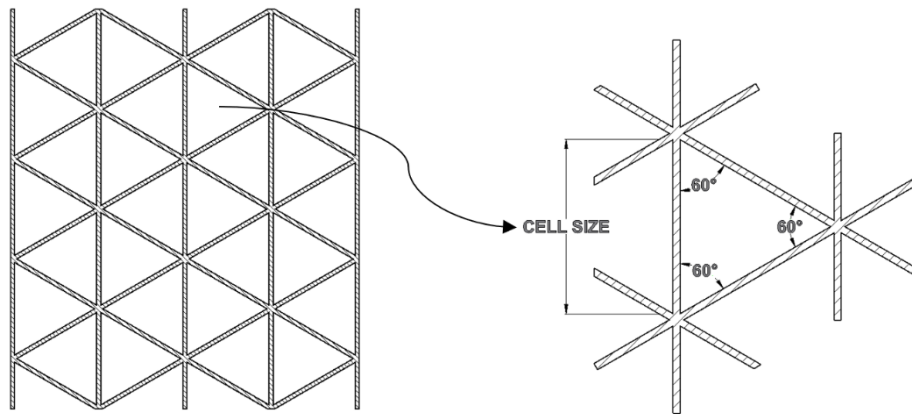


Figure 4.20: The triangular honeycomb core cell.

So, according to the intended experiment requirements of manufacturing sandwich panel specimens that have a triangular honeycomb core with three different values of density that are identical to those previously created for a regular hexagonal core, cell size would be the governing parameter for a density value while keeping other parameter values unchanged. Samples will be in three cell size values and, consequently, in three densities as follows: -

- The first specimen cell size value will be 16.45 mm, as shown in Figure (4.23).

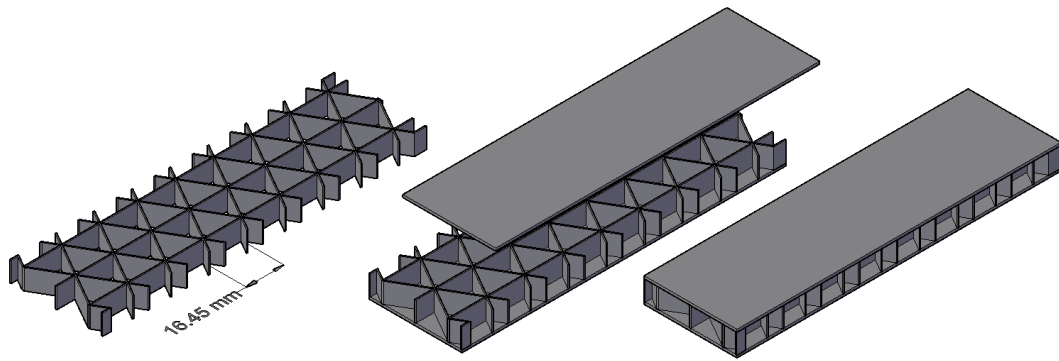


Figure 4.21: First specimen with 16.45 mm cell size.

- The second specimen cell size value will be 13 mm, as shown in Figure (4.24).

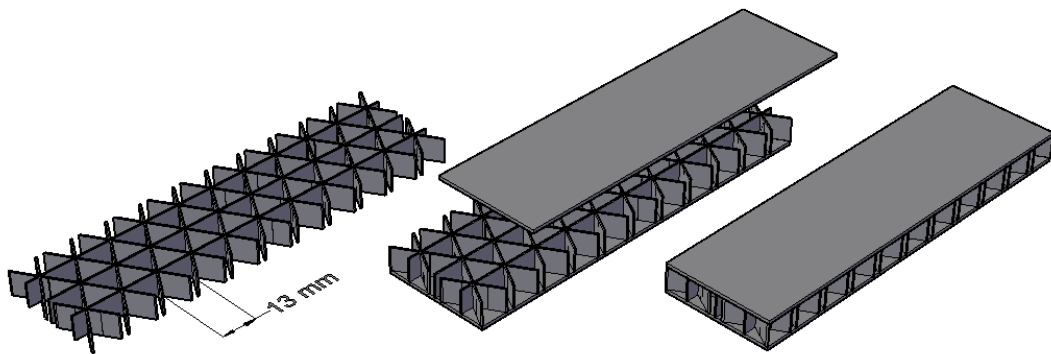


Figure 4.22: Second specimen with 13 mm cell size.

- The third specimen cell size value will be 10.74 mm, as shown in Figure (4.25).

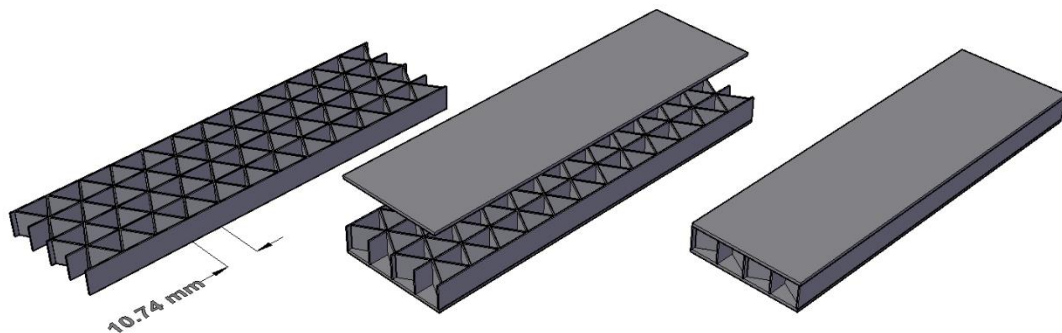


Figure 4.23: Third specimen with 10.74 mm cell size.

After utilizing AutoCAD Mechanical 2023 to draw the designed specimens, as illustrated in Figures (4.23), (4.24), and (4.25), 3D CAD files are exported to the (Ultimaker Cura) slicing program to convert 3D models to 2D printable slices with appropriate settings for PLA material printing, as shown in Figures (4.26).

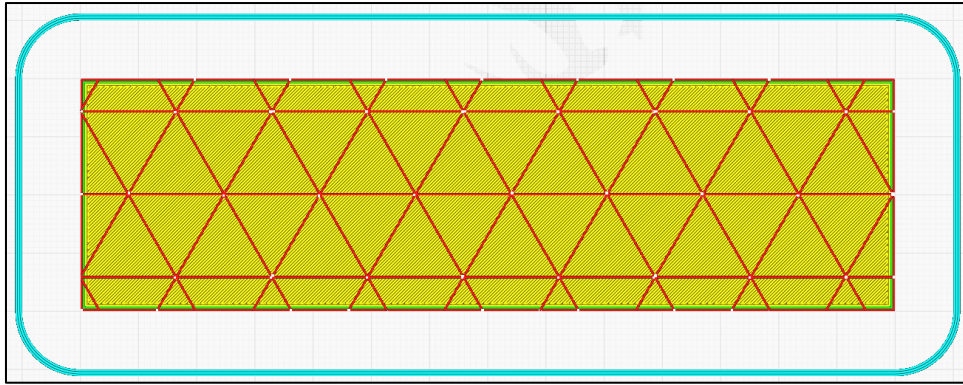


Figure 4.24: First sliced specimen with 16.45 mm cell size.

Finally, sliced specimen files were sent to the (Crealty Ender 3 V2) 3D printer provided with polylactic acid (PLA) filament to create the samples, as shown in Figures (4.29), (4.30), and (4.31).

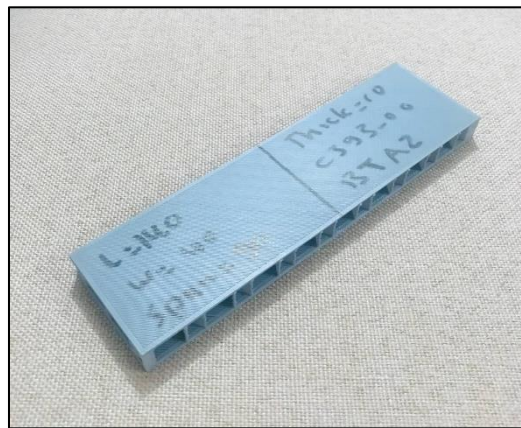


Figure 4.25: First printed specimen with 16.45 mm cell size.

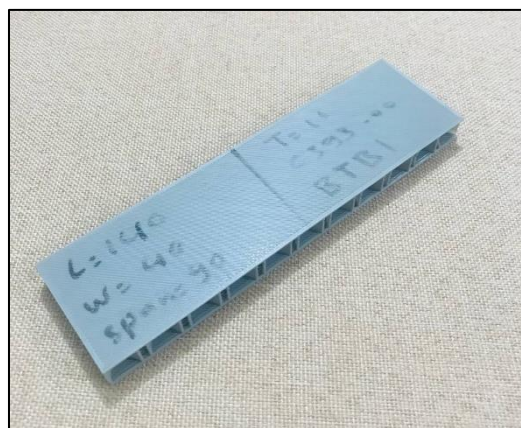


Figure 4.26: Second printed specimen with 13 mm cell size



Figure 4.27:Third printed specimen with 10.74 mm cell size.

The samples were labeled with (BTA1, BTA2, and BTA3); (BTB1, BTB2, and BTB3); and (BTC1, BTC2, and BTC3) as illustrated in table (4.2) below:

Table 4.2:Samples of triangular type attributes

Specimen labeled code.		Number of cells in cross section	Specimen weight (g)	Specimen core
First density 16.45mm Cell size	BTA1	2	19	
	BTA2	2	19	
	BTA3	2	19	
Second density 13 mm Cell size	BTB1	3	20	
	BTB2	3	20	
	BTB3	3	20	
Third density 10.74 mm Cell size	BTC1	4	21	
	BTC2	4	21	
	BTC3	4	21	

4.4.6.3 The Overlapped Octagonal Core Manufacturing

As shown in Figure (4.32), an overlapped octagonal core is the result of overlapping two patterns of octagonal configuration, which results in a new configuration consisting of squares and irregular hexagonal cells that predict adding extra stiffness. So, to explore stiffness, it would have to manufacture specimens with a core density of three different values, which will depend on their governing geometrical parameters: cell wall thickness and cell size. The cell walls in this study will have the same thickness (0.4 mm) for all manufactured and tested species with any configuration (regular hexagonal, triangular, or overlapped octagonal), and while cell size will be the sole governing parameter of core density magnitude, in the overlapped octagonal case, the cell size of the octagonal will be the governing parameter as dimensions of other produced shapes depend on it.

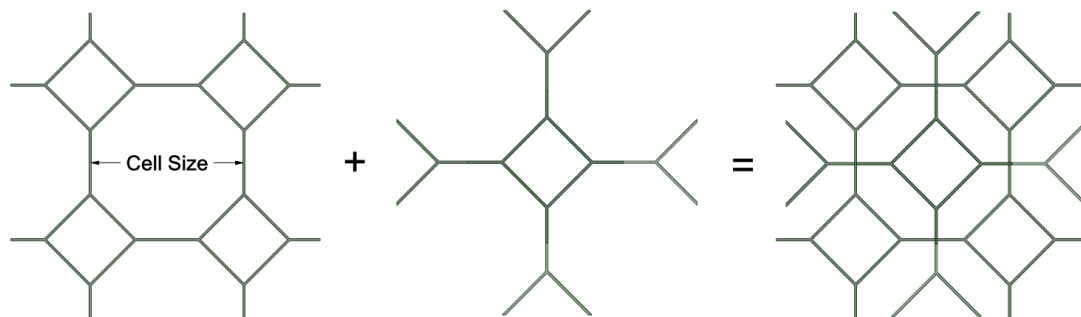


Figure 4.28: The Overlapped Octagonal Honeycomb Core.

Therefore, cell size would be the governing parameter for a density value while keeping other parameter values constant, in accordance with the intended experiment requirements of manufacturing sandwich panel specimens with an overlapped octagonal honeycomb core and three different values of density that are identical to those previously created for a regular hexagonal and triangular core. Samples will come in the following three densities and three cell size values: :

- The first specimen cell size value will be 23.6 mm, as shown in Figure (4.33).

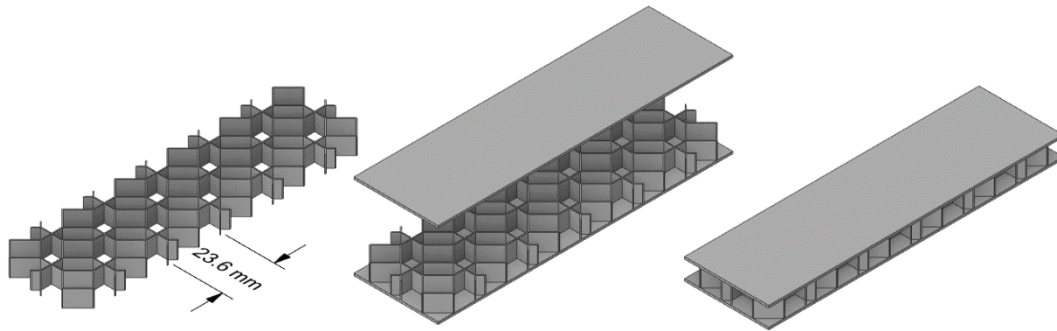


Figure 4.29: First specimen with 23.6 mm cell size.

- The second specimen cell size value will be 18.7 mm, as shown in Figure (4.34).

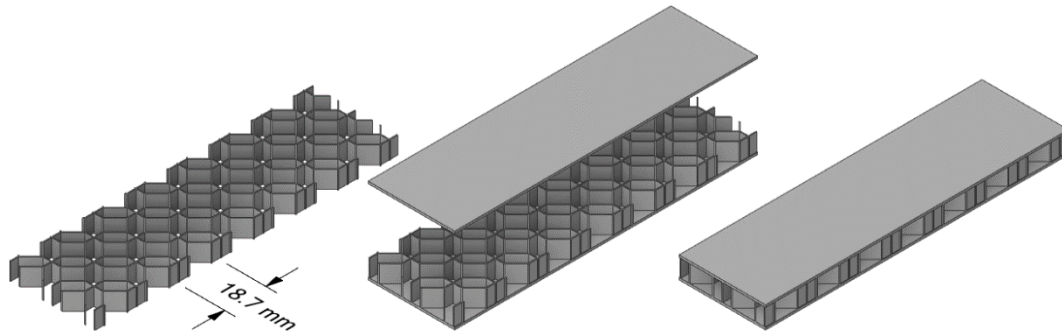


Figure 4.30: Second specimen with 18.7 mm cell size.

- The third specimen cell size value will be 15.4 mm, as shown in Figure (4.35).

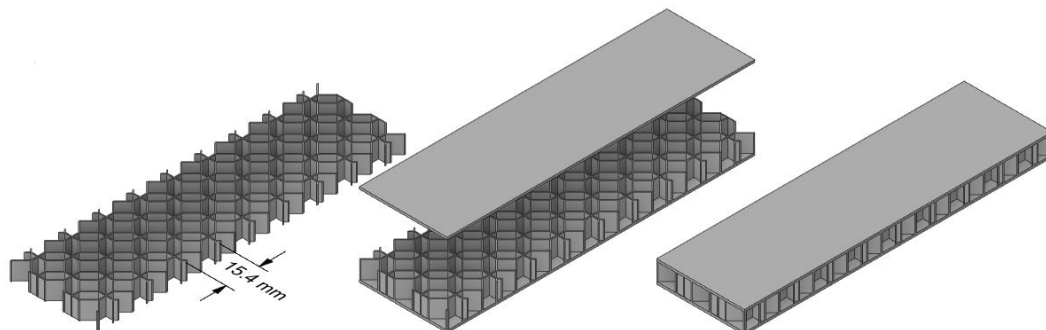


Figure 4.31: Third specimen with 15.4 mm cell size.

After utilizing AutoCAD Mechanical 2023 to draw the designed specimens, as illustrated in Figures (4.33), (4.34), and (4.35), 3D CAD files

are exported to the (Ultimaker Cura) slicing program to convert 3D models to 2D printable slices with appropriate settings for PLA material printing, as shown in Figures (4.36).

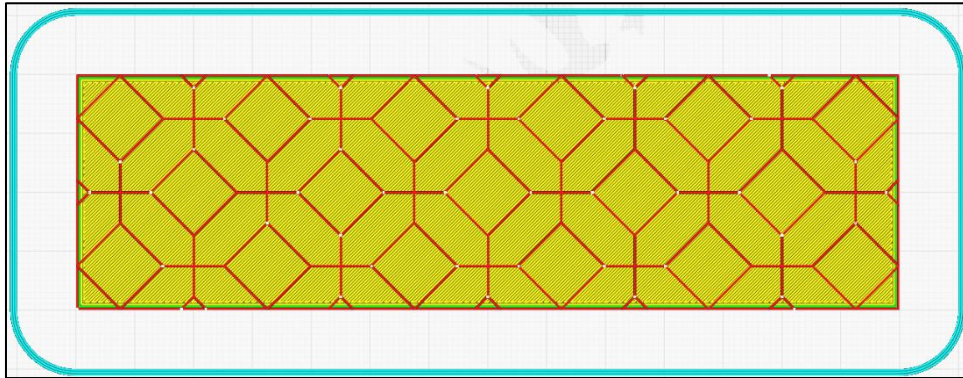


Figure 4.32: First sliced specimen with 23.6 mm cell size.

Finally, sliced specimen files were sent to the (Crealty Ender 3 V2) 3D printer provided with polylactic acid (PLA) filament to create the samples, as shown in Figures (4.39), (4.40), and (4.41).



Figure 4.33: First printed specimen with 23.6 mm cell size.



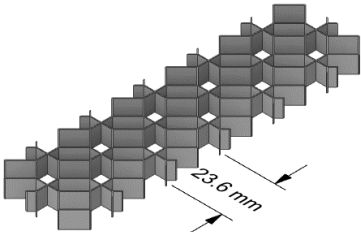
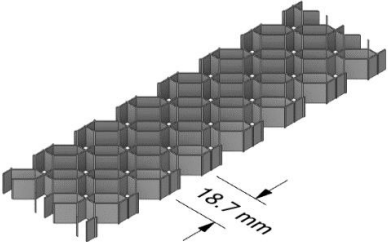
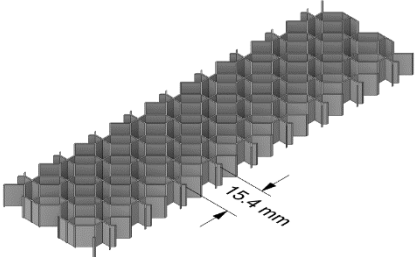
Figure 4.34: Second printed specimen with 18.7 mm cell size.



Figure 4.35: Third printed specimen with 15.4 mm cell size

The samples were labeled with (BOA1, BOA2, and BOA3); (BOB1, BOB2, and BOB3); and (BOC1, BOC2, and BOC3) as illustrated in table (4.3) below:

Table 4.3: Samples Attributes

Specimen labeled code.		Number of cells in cross-section	Specimen weight (g)	Specimen core
First density 23.6 mm Cell size	BOA1	2	19	
	BOA2	2	19	
	BOA3	2	19	
Second density 18.7mm Cell size	BOB1	2	20	
	BOB2	2	20	
	BOB3	2	20	
Third density 15.4 mm Cell size	BOC1	3	21	
	BOC2	3	21	
	BOC3	3	21	

4.5 Specimens testing

After the manufacturing processes are completed, specimens with varying core densities are ready to undergo the testing recommended by the standard (ASTM C393-00) [80]. The universal test machine (Max Load 5 KN) in the University of Babylon - Material Faculty labs is utilized to conduct flexural tests, as shown below in Figure (4.42).



Figure 4.36: The universal test machine (Max Load 5 KN)

The rollers with a diameter of 10 mm, as shown in Figure (4.43), were used to support and apply the central load at a selected constant speed of (3 mm/min). The computer attached to the testing machine tracks the movement of the central loading point and records displacement values according to the applied load magnitude.



Figure 4.37:The roller used with a universal test machine.

Finally, samples are subjected to the bending loads as illustrated in figure (4.44) at the recommended constant speed until they reach the peak load and fail while the attached computer records displacement and draws the load-deflection curve.

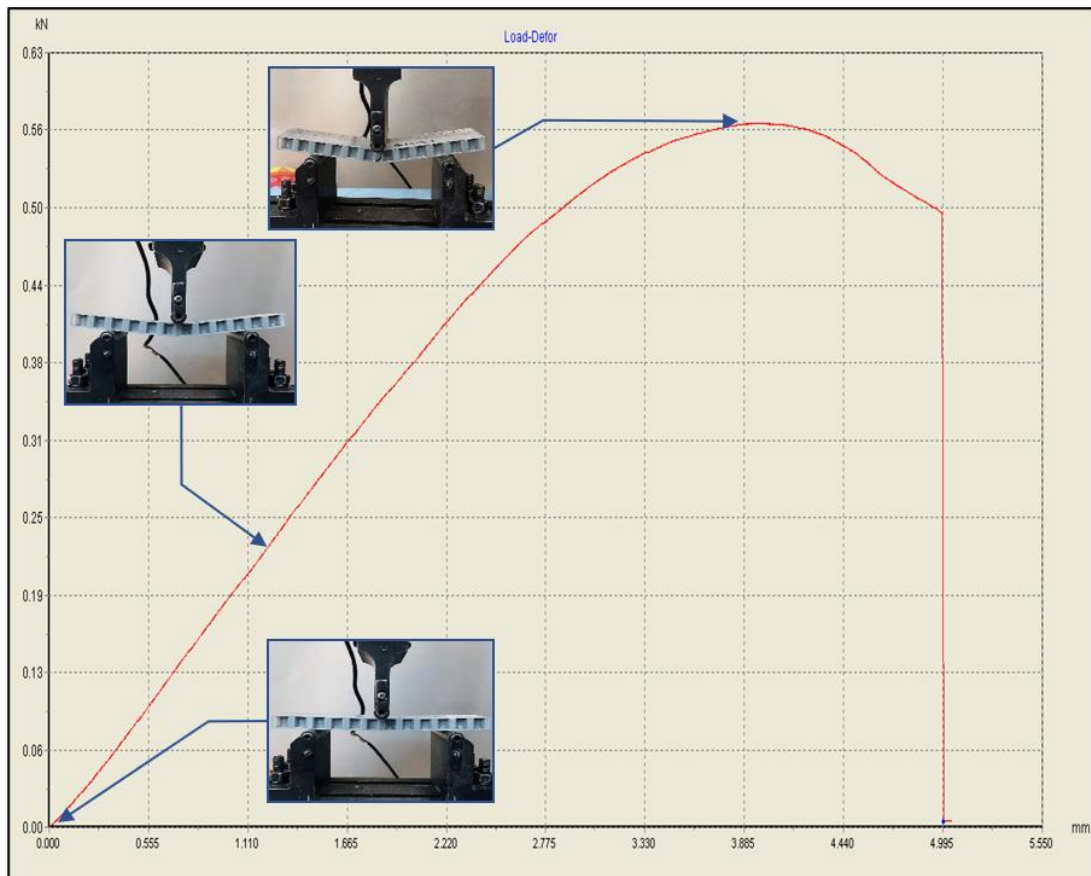


Figure 4.38:The load-deflection curve.

4.6 Filament Material Mechanical Properties

Polylactic acid (PLA) is a non-toxic and biodegradable polymer that is widely used in additive manufacturing with FDM technology (Fused Deposition Modeling) due to its low melting temperature, allowing it to be easily extruded to produce 3D printed objects. To evaluate their performance under loading, the mechanical properties should be known under realistic environmental conditions to decide whether they can be classified as mechanically efficient in conditions requiring tensile strength [73] On the other hand, the determination of those mechanical properties is important to simulate loading conditions with simulation software later.

4.6.1 Experimental Test

A tensile test is required for evaluating the mechanical properties of 3D-printed component material. So, under specified conditions of pretreatment, temperature, humidity, and testing machine speed, the Standard Test Method for Tensile Properties of Plastics (ASTM D638-14) test method covers the determination of the tensile properties of plastics by testing samples in the form of standard dumbbell-shaped specimens. [74].

4.6.1.1 Samples preparing

Dumbbell-shaped samples are prepared by utilizing the same 3D printer (Creality Ender 3 V2) in the same conditions and slicing settings in which honeycomb samples are printed. This 3D printer is supplied with PLA filament to print the required specimens with the recommended geometry that the ASTM D638-14 standard demands [74]. Firstly, the designed sample has to be drawn with CAD software (AutoCAD Mechanical 2023) as shown in Figure (4.45).

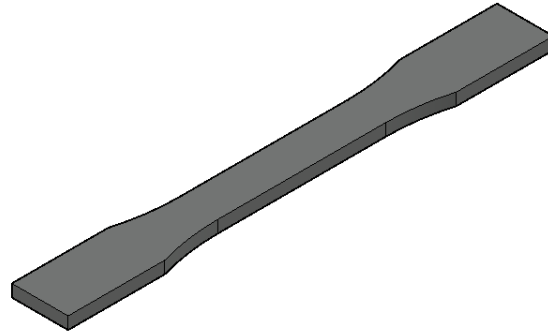


Figure 4.39:(Type I) specimen.

In this study, the specimen geometry will be as shown in Figure (4.46) in accordance with the (Type I) specimen, which is the preferred type by the (ASTM: D638-14) [74] standard recommendation for rigid and semi-rigid plastics, where PLA material has appropriate rigidity.

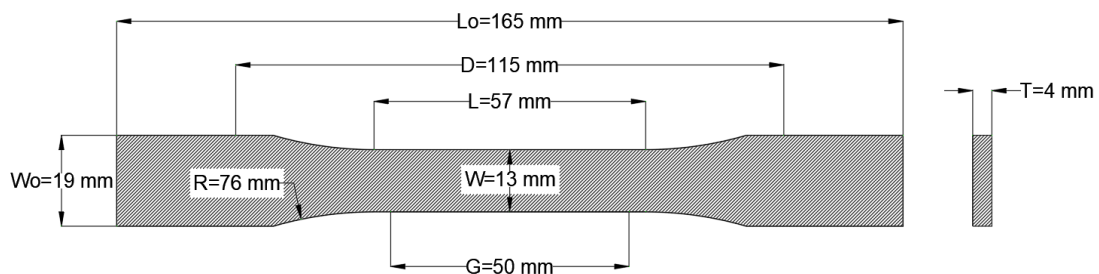


Figure 4.40:Dimension of the specimen.

Where, in accordance with (Type I) [74] :

- Specimen thickness (T) =4mm
- Width of narrow section (W)= 13 mm
- Length of narrow section (L)= 57mm
- Width overall (Wo)= 19mm
- Length overall (Lo)= 165mm
- Gage length (G)= 50mm
- Distance between grips (D) = 115 mm
- Radius of fillet (R) =76mm

Secondly, slicing using a slicing program (Ultimaker Cura) as shown in Figure (4.47).

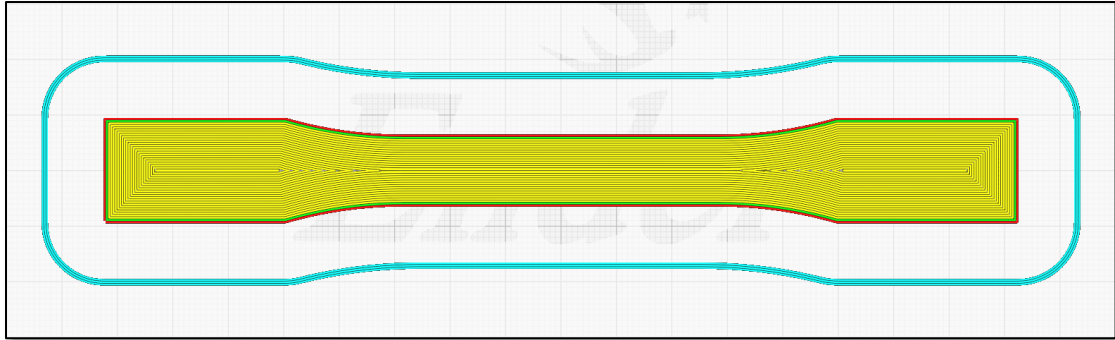


Figure 4.41:Sliced specimen via (Ultimaker Cura).

Finally, printing the required quantity of specimens by the (Creality Ender 3 V2) printer, as shown in Figure (4.48).



Figure 4.42:Printing samples by 3D printer.



Figure 4.43:Printed specimens before test.

The samples are labeled with (T1, T2, T3, T4, and T5), as shown in Figure (4.49), where the letter (T) indicates that they are tensile test samples, and the numbers follow the number of specimens required in the (ASTM D638-14)[74] standard.

4.6.2 Tensile Specimens testing

To perform the tensile test described in the (ASTM D638-14) standard , five specimens, as shown in Figure (4.49) should be tested using an appropriate tensile test machine [74] . In this study, the universal testing machine with a maximum load of 5 KN shown in Figure (4.50) is used.



Figure 4.44:The universal testing machine (Max Load 5 KN).

Jigs illustrated in Figure (4.51) hold and tension the samples at the recommended constant loading speed (5 mm/min) for specimens (Type I)

according to the ASTM D638-16 standard recommendation[74]. The computer attached to the testing machine records the elongation during the application of the tensile load.



Figure 4.45:Jigs of the testing machine.



Figure 4.46:Printed specimens after the test.

All samples have fracture positions near one of the jigs, as shown in figure (4.52).

4.7 Filament Material's Physical Properties

Certain physical attributes should be available to conduct the necessary numerical tests, and the most essential one is the density of the material utilized. Density magnitude is provided in various articles and on manufacturers' websites, but it needs to be measured experimentally for better accuracy.

4.7.1 Filament Material's Density

In order to calculate the density of the produced cores, the density of the polylactic acid (PLA) used to construct the samples is determined in a lab by ASTM D792 (Standard Test Methods for Density of Plastics) [75] by specifying the mass of a solid plastic specimen in air and then immersing it in a liquid to determine its mass in that liquid. As shown in fig (4.53).

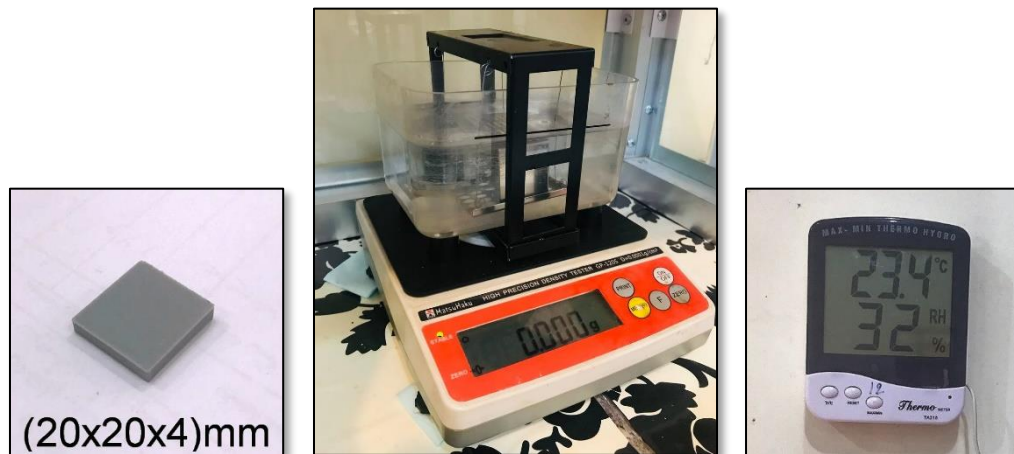


Figure 4.47: Specimen, Density Tester, and Lab Environment.

Finally, the density magnitude could be obtained by using the following formula.

$$\text{Density} = \frac{\text{mass in air}}{\text{mass in liquid}} * \text{liquid density}$$

Chapter Five: Results and Discussion

5.1 General

This chapter listed and discussed the theoretical, numerical, and experimental findings. Firstly, tensile test results for the polylactic acid (PLA) material were presented and examined to determine its mechanical properties so that it could be utilized in simulation software. Second, exhibit all of the results obtained from the available theoretical solutions to identify the effective parameters, then explore whether those theoretical or numerical results agree with the experimental ones.

5.2 Properties Results

5.2.1 Tensile Test Results

As previously described in experimental work, the stress-strain curves for five samples labeled T1, T2, T3, T4, and T5 were obtained by the tensile test according to ASTM D638-14, as shown in figures (5.1), (5.2), (5.3), (5.4), and (5.5).

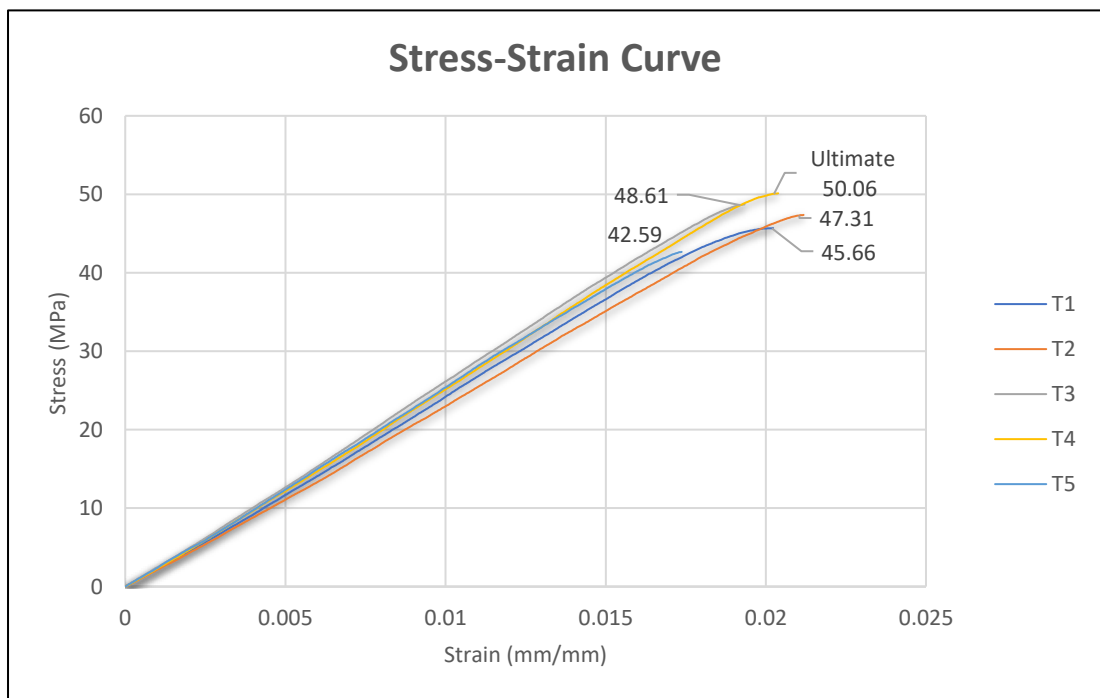


Figure 5.1: Tensile test results for samples.

The results shown in Table (5.1) are based on the curves shown above.

Table 5.1:Tensile test results for (PLA).


Sample	Ultimate stress (MPa)	Average Ultimate tensile stress (MPa)	Modulus of elasticity (MPa)	Average modulus of elasticity (MPa)
T1	45.60	46.842	1654.05	1802.48
T2	47.31		2303.964	
T3	48.64		1817.907	
T4	50.06		1593.893	
T5	42.60		1642.588	

These results agree with published research [76] so they were included as mechanical properties of the PLA material in the Ansys workbench software.

5.2.2 Density Determination Results

The density of the polylactic acid (PLA) used to make the samples was computed in a lab according to ASTM D792 to be used in determining the density of the created cores [75]. The automatically calculated result was (1241.6) kg/m³, as shown in Table (5.2).

Table 5.2:Density test results for (PLA).

Mass in Air (gram)	Mass in Water (gram)	Density (g/cm ³)	Automatic Results	Density (kg/m ³)
1.65	1.326	1.2416		1241.6

5.3 Results of Regular Hexagonal Honeycomb Core Tests

As previously described, to explore the effects of core density on sandwich behavior, a three-point bending test was conducted to determine the deflection under a specific load range to explore stiffness values. Fortunately, a theoretical solution is available for a regular hexagonal core to calculate the deflection and stiffness magnitude, as explained in Chapter 3. On the other hand, numerical solutions are also available by utilizing simulation software. Finally, the effects of core density on sandwich behavior would be obvious with experimental tests.

5.3.1 Theoretical Results of Regular Hexagonal Honeycomb Core

By utilizing Eq. (3.8) and (3.12) to calculate the deflection value for a specific load range (0 – 400 N) with identical experiment boundary conditions for each specimen of various densities (105, 132, and 160 Kg/m³), the results were as shown in Table (5.3).

Table 5.3: Deflections of (105, 132, and 160 Kg/m³) density specimens theoretically

Load (N)	Deflection (mm) for each sample		
	105 Kg/m ³	132 Kg/m ³	160 Kg/m ³
	Increasing ratio of density (%)	25.7 %	52.4 %
0	0	0	0
50	0.28193284	0.26779450	0.25681322
100	0.56386568	0.53558900	0.51362643
150	0.84579852	0.80338351	0.77043965
200	1.12773136	1.07117801	1.02725287
250	1.40966420	1.33897251	1.28406608
300	1.69159704	1.60676701	1.54087930
350	1.97352988	1.87456151	1.79769251
400	2.25546271	2.14235602	2.05450573
Stiffness (N/mm)	177.35	186.71	194.69
Increasing ratio of stiffness (%)		5.27 %	9.77%

Figure (5.6) depicts how the variation in core density affects the deflection value and, as a result, the stiffness value of each sample.

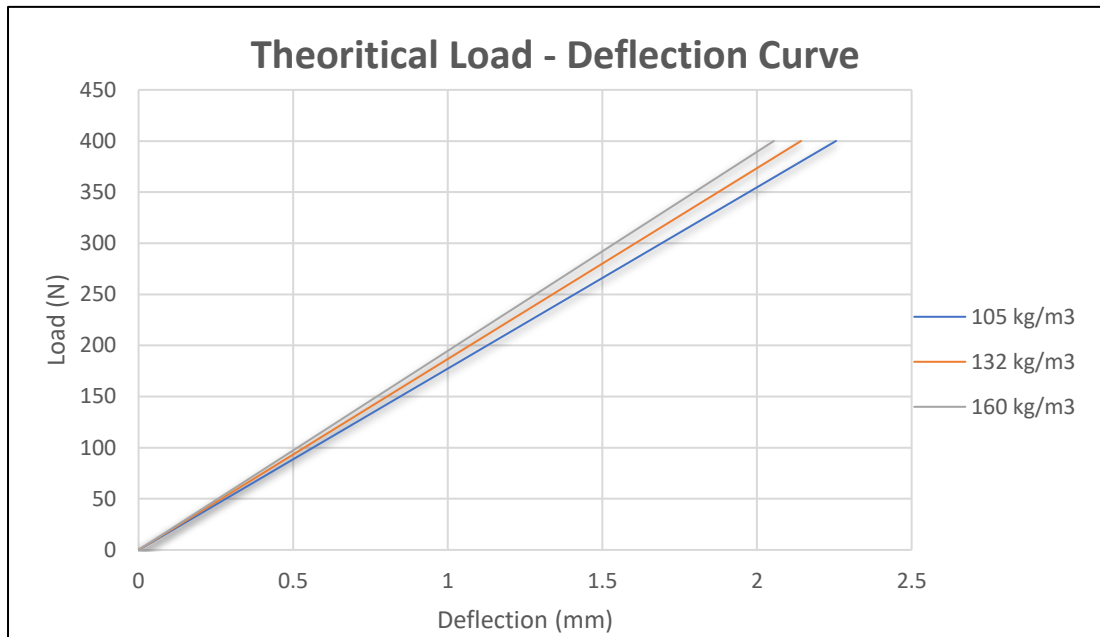


Figure 5.2: Theoretical Load-Deflection Curve

Based on these results, the effect of core density on stiffness can be represented in Figure (5.7).

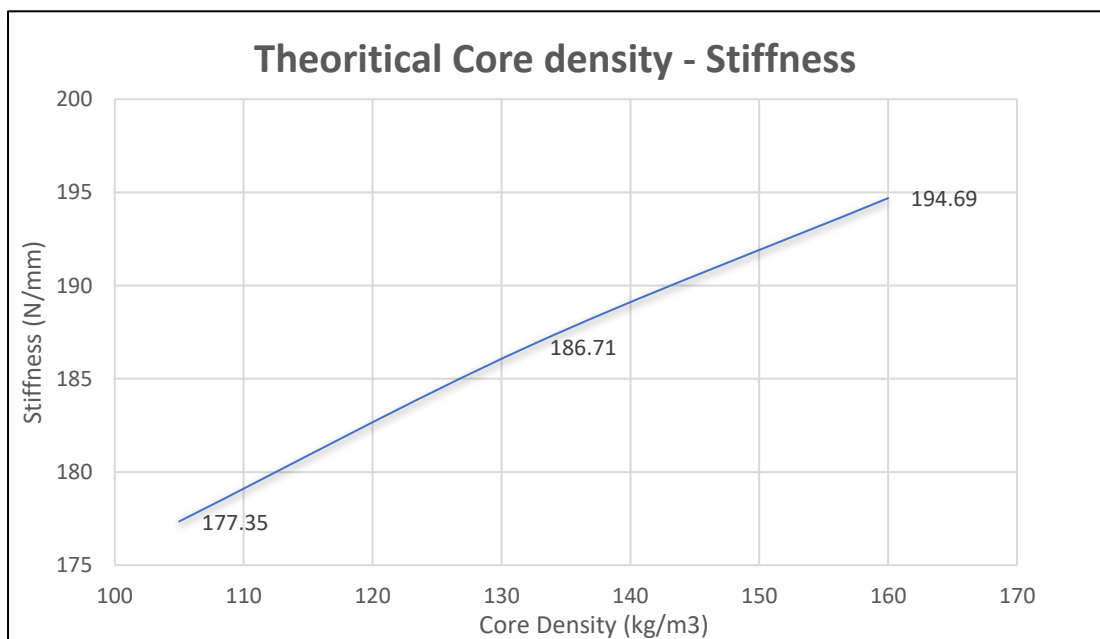


Figure 5.3: Theoretical Core density - Stiffness Curve

Increasing core density causes an increase in stiffness, as theoretically predicted in Chapter 3, because core density increases the shear modulus. Figure (5.8) shows the shear modulus increasing as calculated by Eq (3.13).

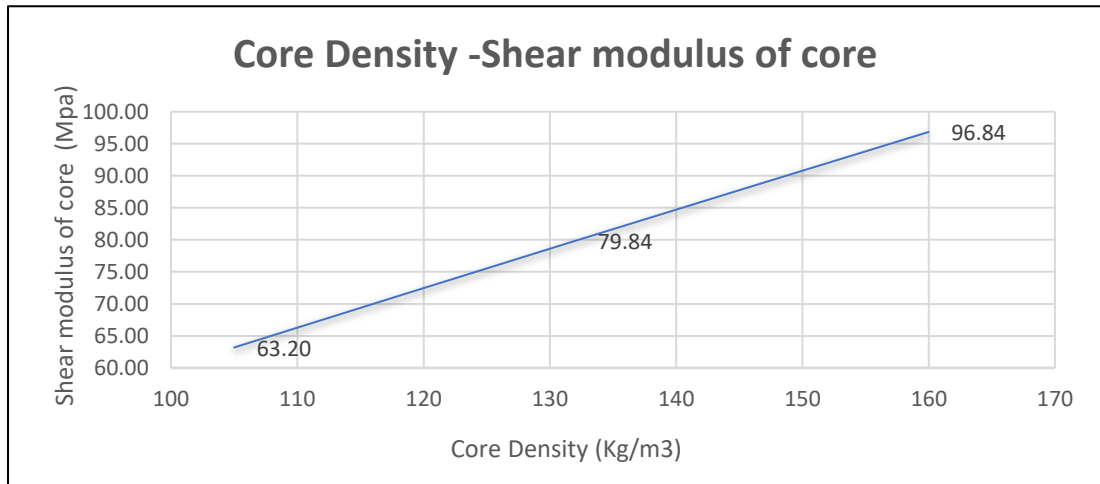


Figure 5.4:Relation Core density and Shear modulus of the core.

Consequently, increasing the shear modulus of the core would reduce deflection due to shear, according to Eq. (3.9), thus making samples stiffer as core density increases. Figure (5.9) depicts how increasing the shear modulus reduces deflection due to shear (deflection calculated at 400 N load).

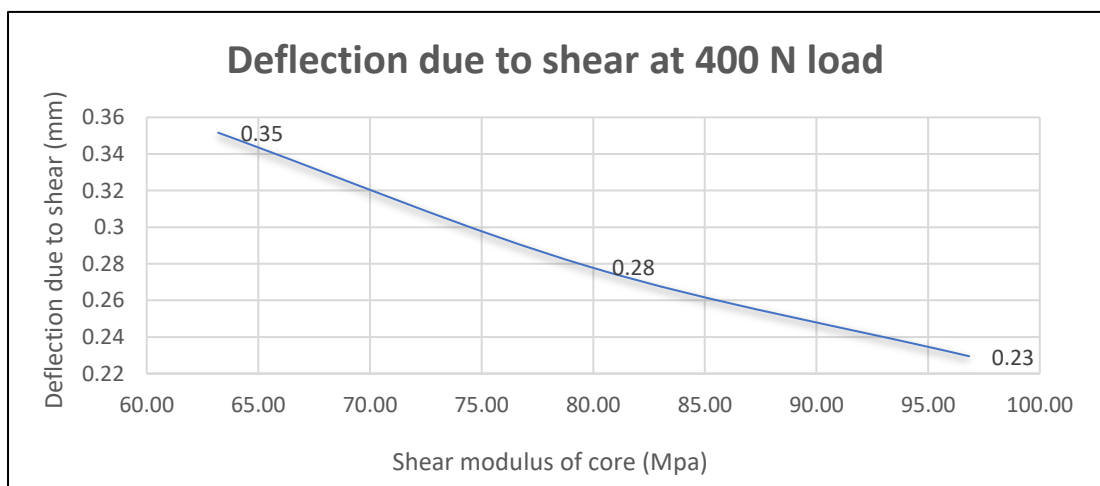


Figure 5.5:Shear modulus effect on the value of deflection due to shear

It is worth noting that the available theoretical solution for a regular hexagonal honeycomb core clearly states how core density affects

sandwich stiffness and provides a good indication of other core configurations.

5.3.2 Numerical Results of Regular Hexagonal Honeycomb Core

By utilizing Ansys 2021 R2 simulation software to calculate the deflection value for a specific load range (0 – 400 N) with identical experiment boundary conditions for each specimen of various densities (105, 132, and 160 Kg/m³), the results were as shown in Table (5.4).

Table 5.4: Deflections of (105, 132, and 160 Kg/m³) density specimens numerically with Ansys 2021 R2

Load (N)	Deflection (mm) for each sample		
	105 Kg/m ³	132 Kg/m ³	160 Kg/m ³
	Increasing ratio of density (%)	25.7 %	52.4 %
0	0	0	0
50	0.29009	0.26648	0.2473
100	0.57996	0.53274	0.49439
150	0.8695	0.79871	0.74122
200	1.1587	1.0644	0.9878
250	1.4477	1.3298	1.2341
300	1.7366	1.5952	1.4803
350	2.0258	1.8606	1.7265
400	2.3152	2.1264	1.973
Stiffness (N/mm)	172.77	188.11	202.73
Increasing ratio of stiffness (%)		8.87 %	17.34 %

Figure (5.10) depicts how the variation in core density affects the deflection value and, as a result, the stiffness value of each sample.

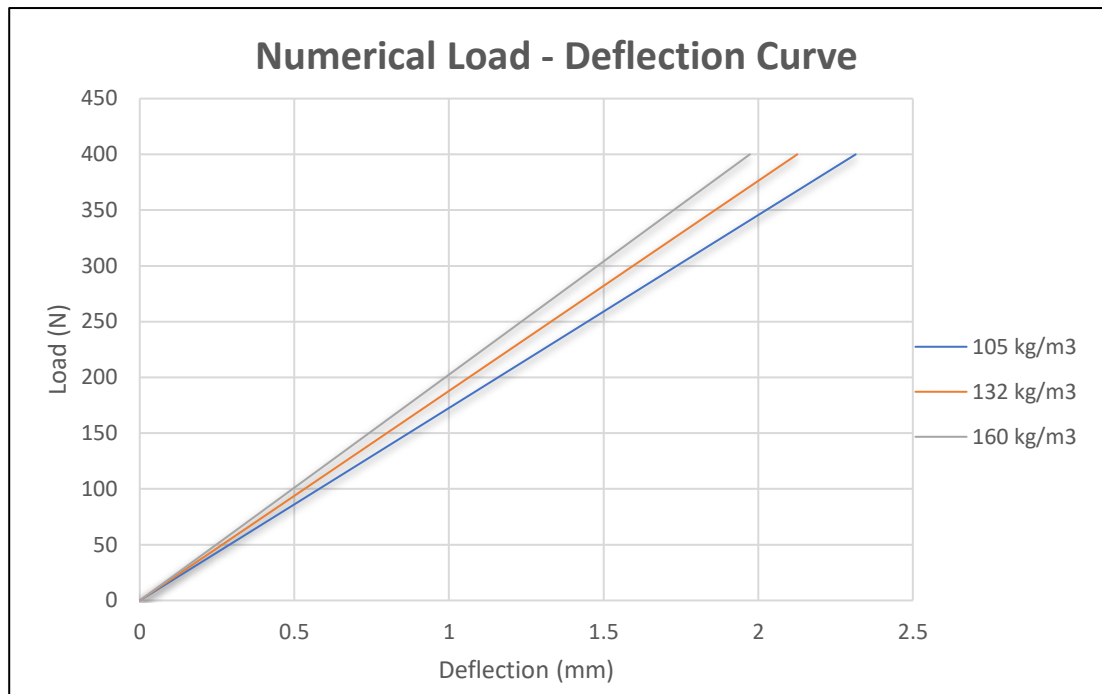


Figure 5.6: Numerical Load-Deflection Curve

Based on these results, the effect of core density on stiffness can be represented in Figure (5.11).

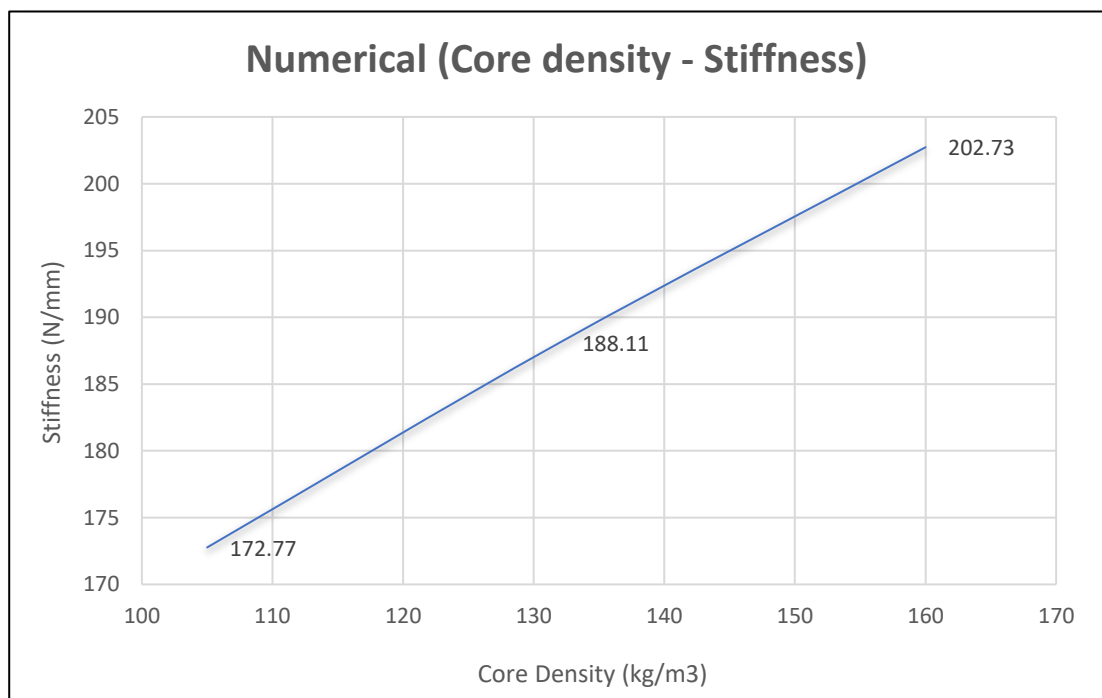


Figure 5.7: Numerical Core density - Stiffness Curve

As shown above, numerical results match theoretical ones in that increasing core density causes reduced deflection due to shear, which

increases sandwich stiffness magnitude. On the other hand, that also indicates the numerical solutions provided by simulation software provide acceptable solutions for any core configuration to predict its behavior under any loading conditions.

5.3.3 Experimental Results of Regular Hexagonal Honeycomb Core

By utilizing the Universal Test Machine (Max Load 5 KN) to conduct a 3-point bending test as explained in Chapter 4 to calculate the deflection value for a specific load range (0 – 400 N) with identical experiment boundary conditions for each specimen of various densities (105, 132, and 160 Kg/m³), the results were as shown in Table (5.5).

Table 5.5: Deflections of (105, 132, and 160 Kg/m³) density specimens Experimentally

Load (N)	Deflection (mm) for each sample		
	105 Kg/m ³	132 Kg/m ³	160 Kg/m ³
	Increasing ratio of density (%)	25.7 %	52.4 %
0	0	0	0
50	0.339466667	0.3048	0.2684
100	0.6007	0.56048	0.501833333
150	0.855033333	0.78373	0.732033333
200	1.111366667	1.01908	0.960866667
250	1.369066667	1.2606	1.1922
300	1.6324	1.5287	1.428233333
350	1.901033333	1.7944	1.6664
400	2.185466667	2.0284	1.911833333
Stiffness (N/mm)	175.33	189.61	204.70
Increasing ratio of stiffness (%)		8.14 %	16.75 %

Figure (5.12) depicts how the variation in core density affects the deflection value and, as a result, the stiffness value of each sample.

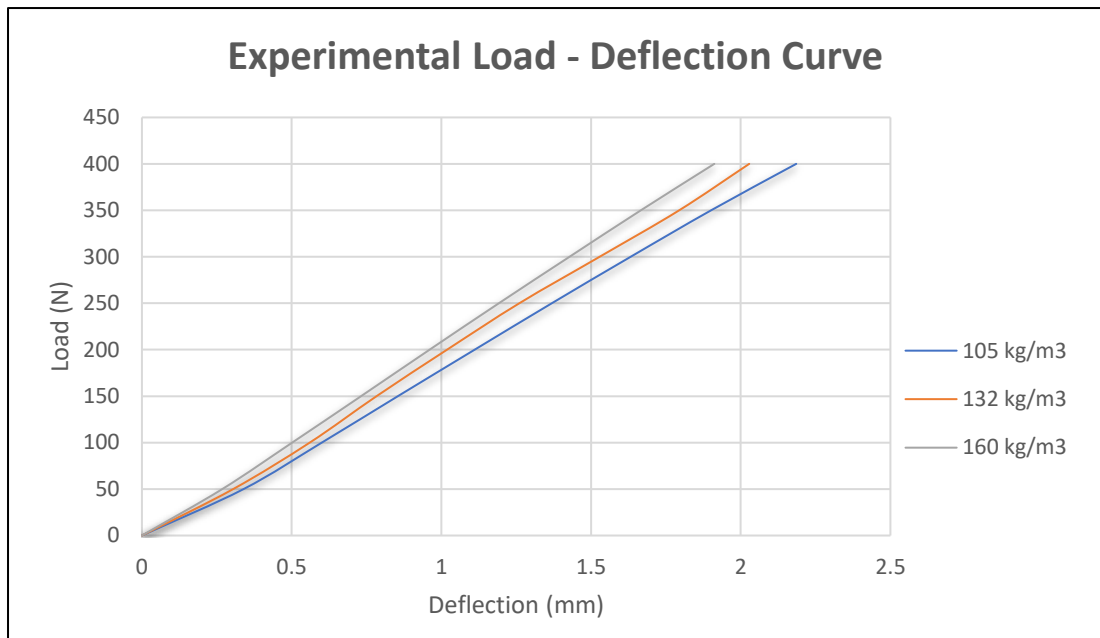


Figure 5.8: Experimental Load-Deflection Curve

Based on these results, the effect of core density on stiffness can be represented in Figure (5.13).

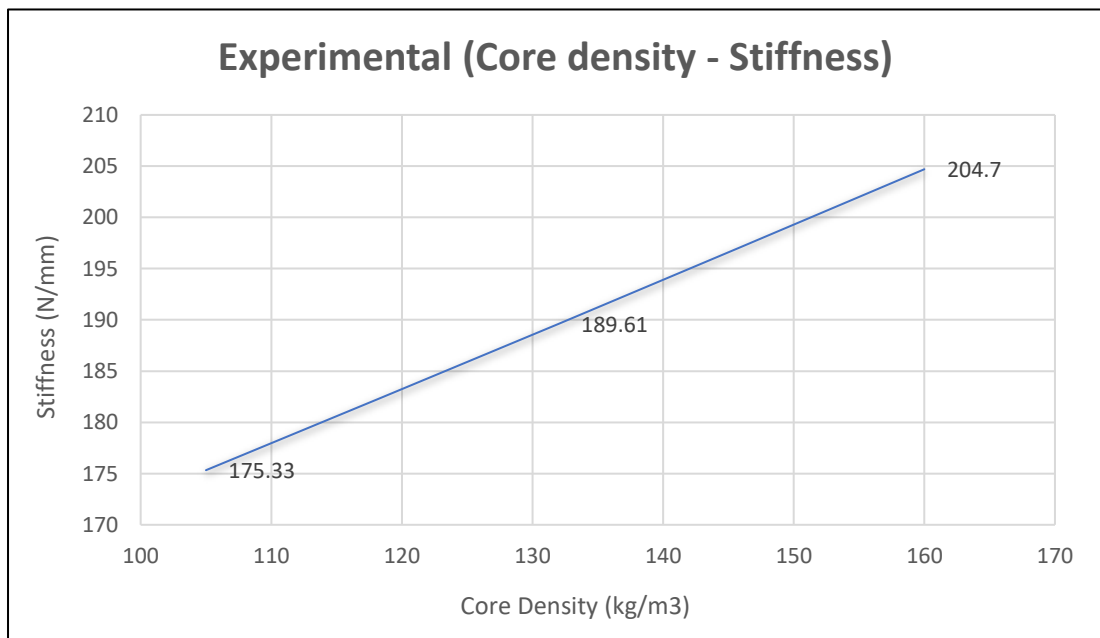


Figure 5.9: Experimental Core density - Stiffness Curve

Table (5.6) illustrates that experimental results are in good agreement with theoretical and numerical ones, with an acceptable deviation percentage ratio, in that increasing the density of a regular

hexagonal honeycomb core causes an increase in stiffness magnitude; figure (5.14) states that too.

Table 5.6: Theoretical, Numerical, and Experimental Stiffness values for each core density

Core Density (Kg/m ³)	Stiffness (N/mm) for each sample			Deviation ratio (%)		
	Theoretical	Numerical	Experimental	Theoretical to Numerical	Numerical to Experimental	Theoretical to Experimental
105	177.35	172.77	175.33	2.58	1.48	1.14
132	186.71	188.11	189.61	0.75	0.80	1.55
160	194.69	202.73	204.7	4.13	0.97	5.14

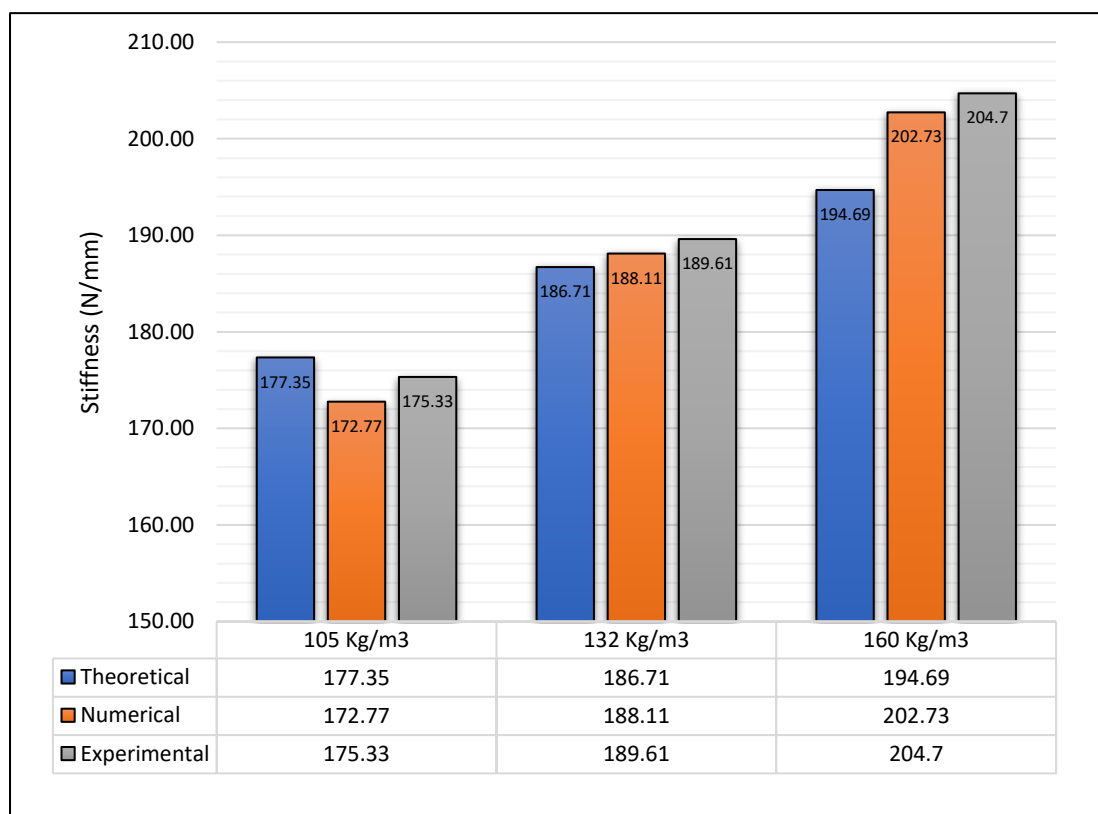


Figure 5.10: Theoretical, Numerical, and Experimental Stiffness Comparison

So, other core configurations are expected to have the same effect of increasing density on stiffness.

5.4 Results of Triangular Honeycomb Core Tests

Numerical and experimental solutions are available for triangular honeycomb cores to investigate sandwich behavior under various loading conditions with varying core densities, so the effect of core density

magnitude on sandwich stiffness would be obvious. Beginning with using simulation software to simulate test conditions and then comparing the results with the experimental test results.

5.4.1 Numerical Results of Triangular Honeycomb Core Tests

By utilizing Ansys 2021 R2 simulation software to calculate the deflection value for a specific load range (0 – 400 N) with identical experiment boundary conditions for each specimen of various densities (105, 132, and 160 Kg/m³), the results were as shown in Table (5.7).

Table 5.7: Deflections of (105, 132, and 160 Kg/m³) density specimens numerically with Ansys 2021 R2

Load (N)	Deflection (mm) for each sample		
	105 Kg/m ³	132 Kg/m ³	160 Kg/m ³
	Increasing ratio of density (%)	25.7 %	52.4 %
0	0	0	0
50	0.28566	0.2747	0.22574
100	0.57106	0.54917	0.45131
150	0.85616	0.82338	0.67671
200	1.141	1.0973	0.90193
250	1.4257	1.3711	1.127
300	1.7105	1.6446	1.352
350	1.9955	1.9182	1.5648
400	2.2755	2.1894	1.7729
Stiffness (N/mm)	175.32	182.31	222.44
Increasing ratio of stiffness (%)		3.98 %	26.87 %

Figure (5.15) depicts how the variation in core density affects the deflection value and, as a result, the stiffness value of each sample.

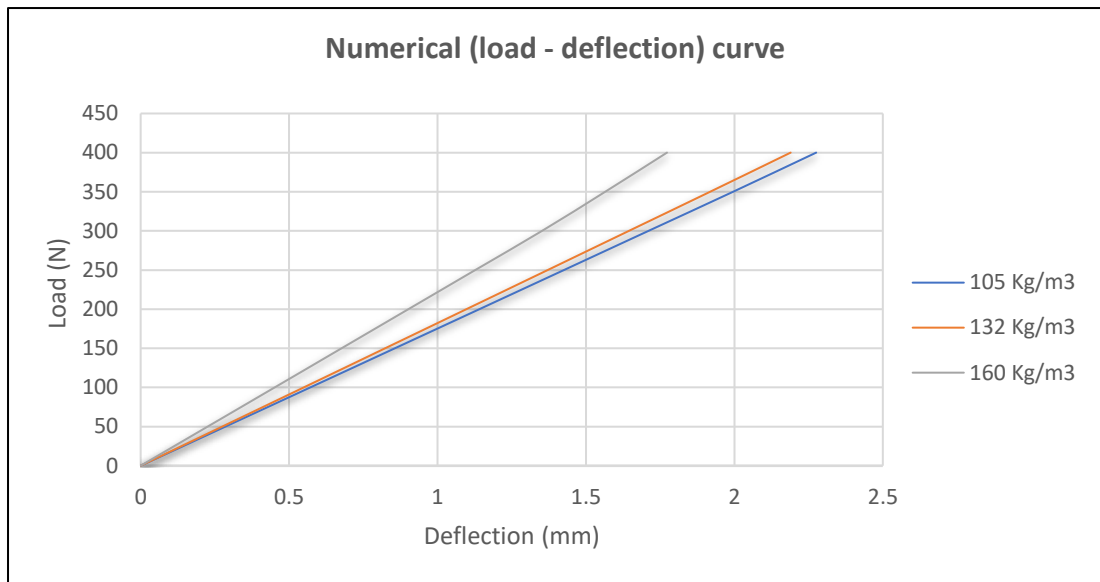


Figure 5.11: Theoretical Load-Deflection Curve

Based on these results, the effect of core density on stiffness can be represented in Figure (5.16).

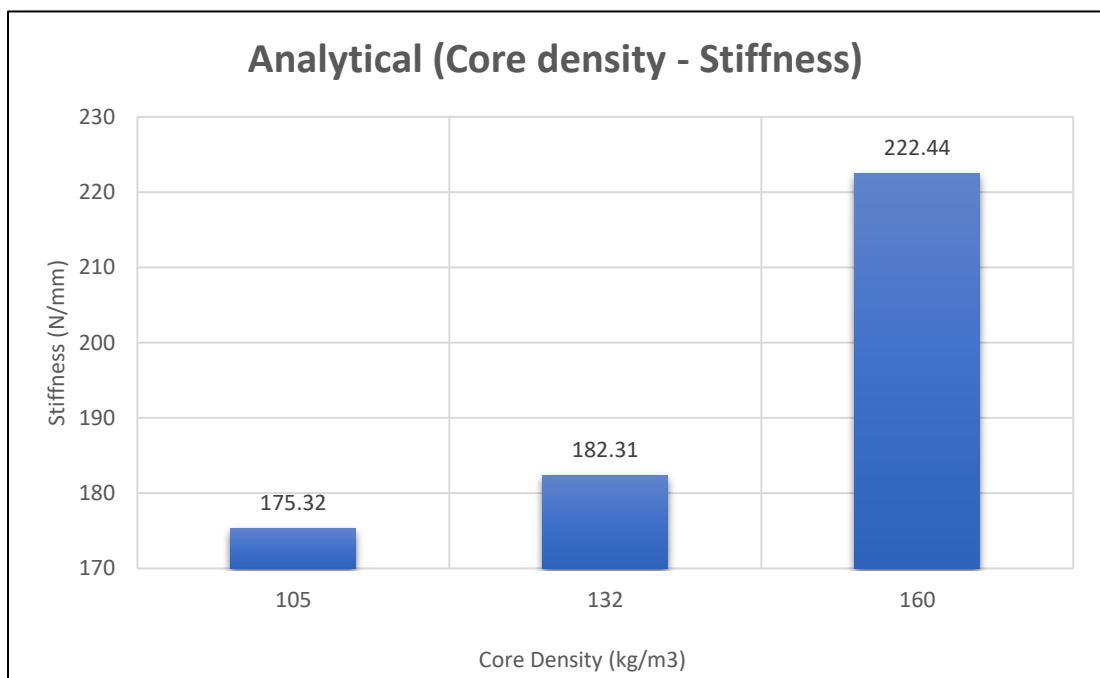


Figure 5.12: Numerical Core density - Stiffness Curve

As shown above, the numerical results state that increasing core density causes an increase in sandwich stiffness magnitude.

5.4.2 Experimental Results of Triangular Honeycomb Core Tests

By repeating the same steps of testing a regular hexagonal honeycomb core with the Universal Test Machine (Max Load 5 KN) to conduct a 3-point bending test as explained in Chapter 4 to calculate the deflection value for a specific load range (0 – 400 N) with identical experiment boundary conditions for each triangular core specimen of various densities (105, 132, and 160 Kg/m³), the results were as shown in Table (5.8).

Table 5.8: Deflections of (105, 132, and 160 Kg/m³) density specimens Experimentally

Load (N)	Deflection (mm) for each sample		
	105 Kg/m ³	132 Kg/m ³	160 Kg/m ³
	Increasing ratio of density (%)	25.7 %	52.4 %
0	0	0	0
50	0.297	0.2947	0.2432
100	0.5897	0.5442	0.49235
150	0.8874	0.7884	0.70855
200	1.184	1.0435	0.9281
250	1.5906	1.3048	1.1423
300	-	1.6058	1.3606
350	-	1.9698	1.5835
400	-	2.472	1.812
Stiffness (N/mm)	167.54	181.66	214.63
Increasing ratio of stiffness (%)		8.43 %	28.10 %

Figure (5.17) depicts how the variation in core density affects the deflection value and, as a result, the stiffness value of each sample.

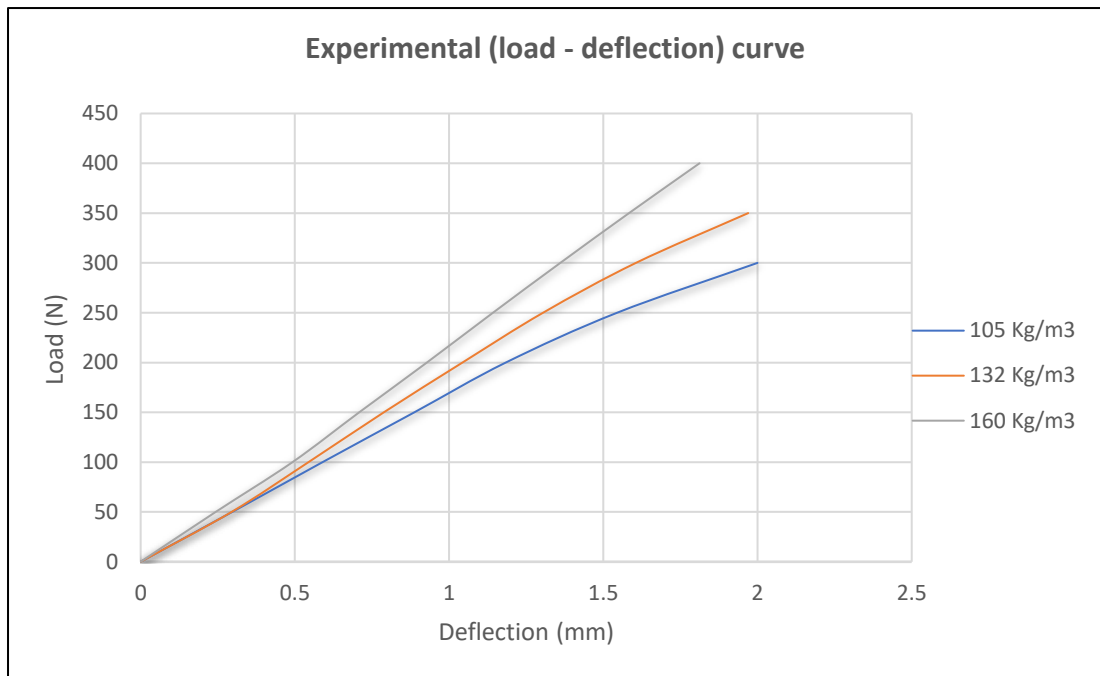


Figure 5.13: Experimental Load-Deflection Curve

Based on these results, the effect of core density on stiffness can be represented in Figure (5.18).

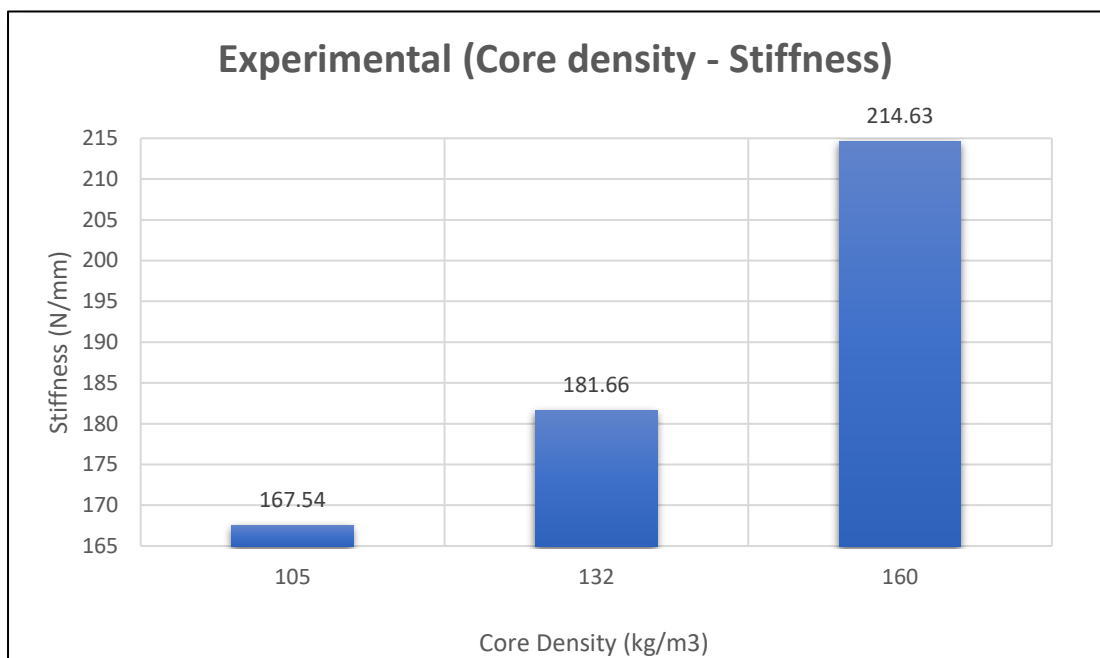


Figure 5.14: Experimental Core density - Stiffness Curve

Table (5.9) illustrates that experimental results have good agreement with numerical ones with an acceptable deviation percentage in that increasing

the density of a triangular honeycomb core causes an increase in stiffness magnitude; figure (5.19) states that too.

Table 5.9: Numerical, and Experimental Stiffness values for each core density

Core Density (Kg/m ³)	Stiffness (N/mm) for each sample		Deviation ratio (%)
	Numerical	Experimental	
105	175.32	167.54	4.44
132	182.31	181.66	0.36
160	222.44	214.63	3.51

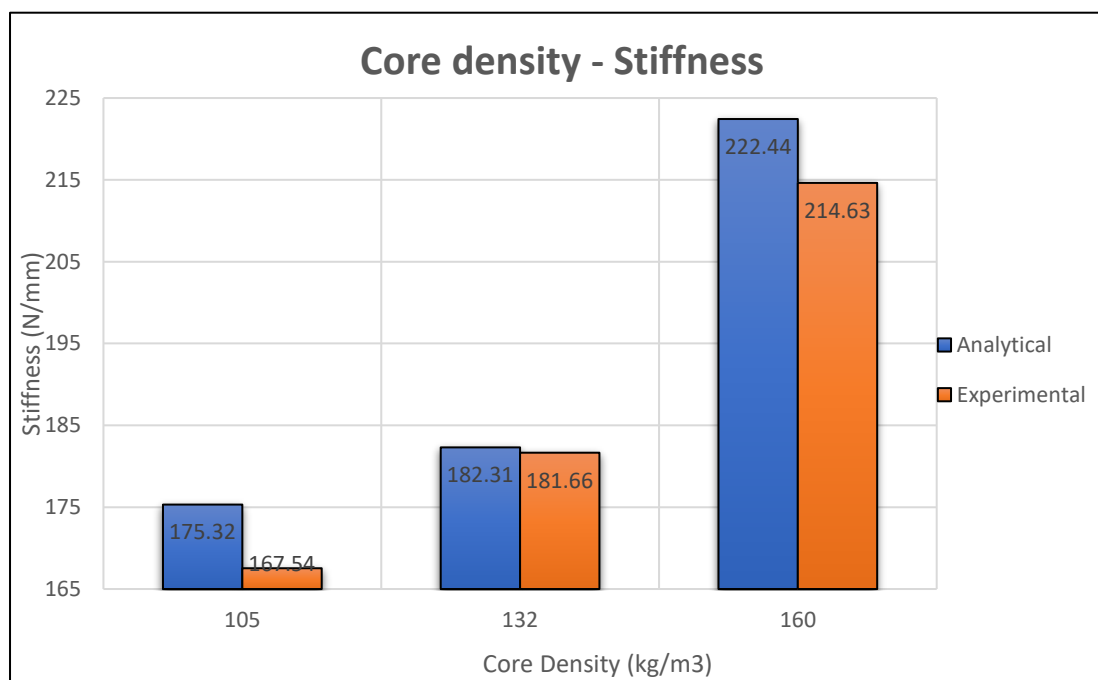


Figure 5.15: Numerical, and Experimental Core density - Stiffness Curves

5.5 Results of Overlapped Octagonal Core Tests

As a result of studying the effect of the core density values on the various mechanical properties, at least for the types included in this research, it became clear that to achieve higher stiffness, the core density must be increased, but it is possible to achieve this by choosing another type of core that guarantees higher stiffness without adding weight, In this

research, the overlapped octagonal core was proposed for study to verify its mechanical properties theoretically and experimentally to see if it meets the required criteria.

5.5.1 Numerical Results of Overlapped Octagonal Core Tests

By utilizing Ansys 2021 R2 simulation software to calculate the deflection value for a specific load range (0 – 400 N) with identical experiment boundary conditions for each specimen of various densities (105, 132, and 160 Kg/m³), the results were as shown in Table (5.10).

Table 5.10: Deflections of (105, 132, and 160 Kg/m³) Density Specimens Numerically

Load (N)	Deflection (mm) for each sample		
	105 Kg/m ³	132 Kg/m ³	160 Kg/m ³
	Increasing ratio of density (%)	25.7 %	52.4 %
0	0	0	0
50	0.28424	0.24432	0.22797
100	0.56794	0.48822	0.45558
150	0.85114	0.73173	0.68284
200	1.1341	0.97515	0.90991
250	1.4171	1.2185	1.137
300	1.6972	1.4617	1.3641
350	1.9697	1.69	1.588
400	2.2347	1.915	1.7988
Stiffness (N/mm)	176.80	205.75	220.11
Increasing ratio of stiffness (%)		17.25 %	24.49 %

Figure (5.20) depicts how the variation in core density affects the deflection value and, as a result, the stiffness value of each sample.

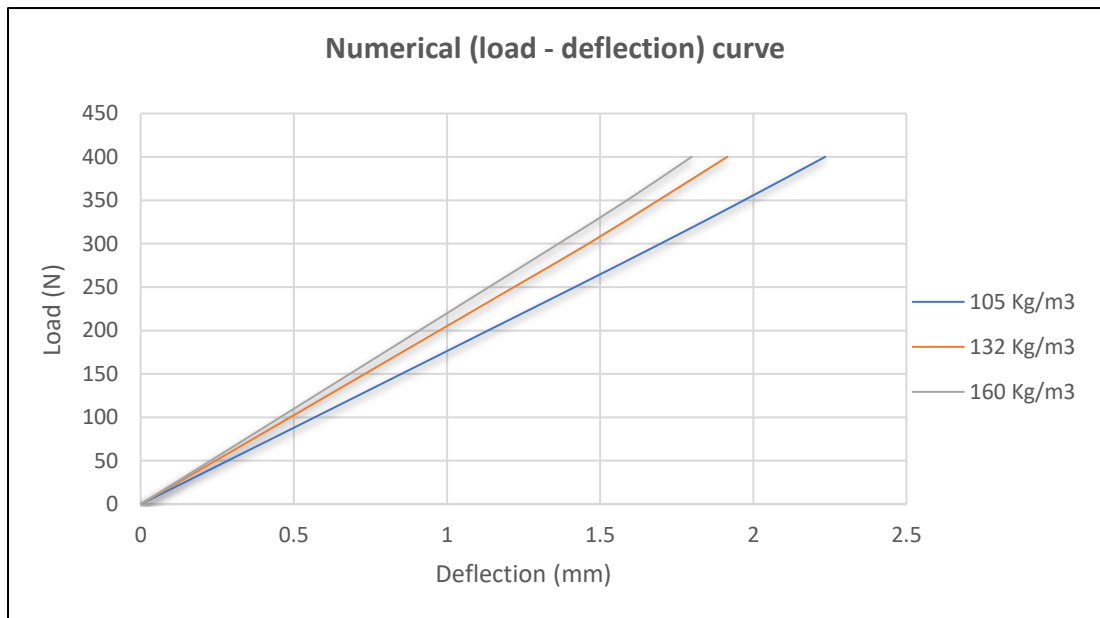


Figure 5.16: Numerical Load-Deflection Curve

Based on these results, the effect of core density on stiffness can be represented in Figure (5.21).

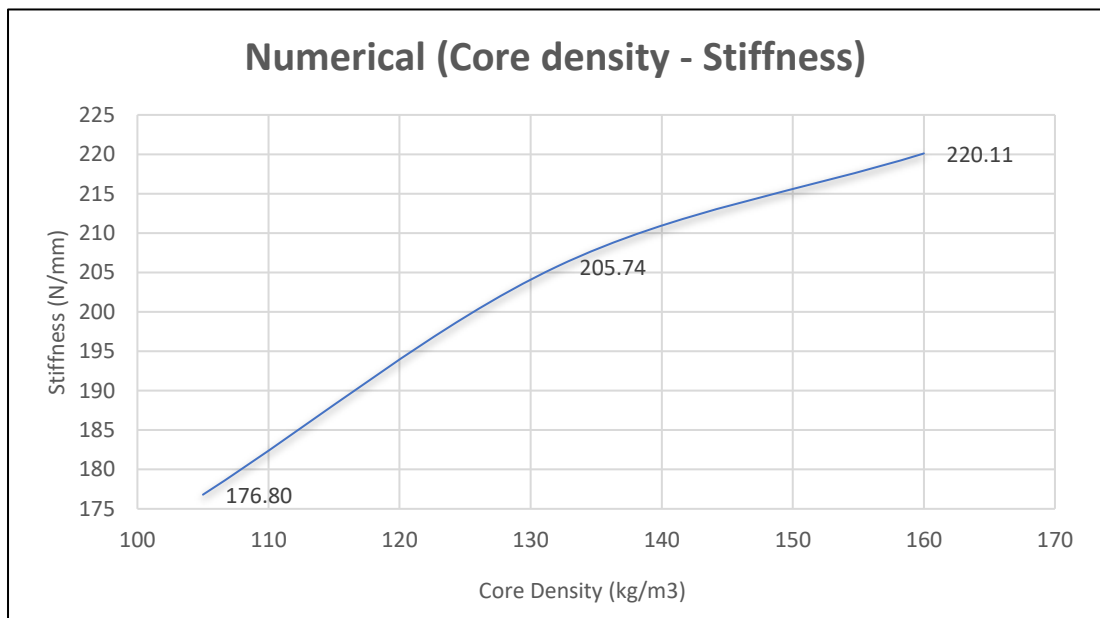


Figure 5.17: Numerical Core density - Stiffness Curve

As shown above, numerical results show that increasing core density causes reduced deflection due to shear, which increases sandwich stiffness magnitude.

5.5.2 Experimental Results of Overlapped Octagonal Core Tests

By repeating the same steps of testing a regular hexagonal and triangular honeycomb core with the Universal Test Machine (Max Load 5 KN) to conduct a 3-point bending test as explained in Chapter 4 to calculate the deflection value for a specific load range (0 – 400 N) with identical experiment boundary conditions for each Overlapped Octagonal Core specimen of various densities (105, 132, and 160 Kg/m³), the results were as shown in Table (5.11).

Table 5.11: Deflections of (105, 132, and 160 Kg/m³) density specimens Experimentally

Load (N)	Deflection (mm) for each sample		
	105 Kg/m ³	132 Kg/m ³	160 Kg/m ³
	Increasing ratio of density (%)	25.7 %	52.4 %
0	0	0	0
50	0.2858	0.2561	0.2452
100	0.5409	0.4891	0.4637
150	0.7897	0.7191	0.6745
200	1.0471	0.9527	0.888
250	1.3266	1.1906	1.1048
300	1.5909	1.4312	1.3243
350	1.8701	1.682	1.5437
400	2.1797	1.9473	1.7764
Stiffness (N/mm)	186.06	206.41	221.49
Increasing ratio of stiffness (%)		10.94%	19.04 %

Figure (5.22) depicts how the variation in core density affects the deflection value and, as a result, the stiffness value of each sample.

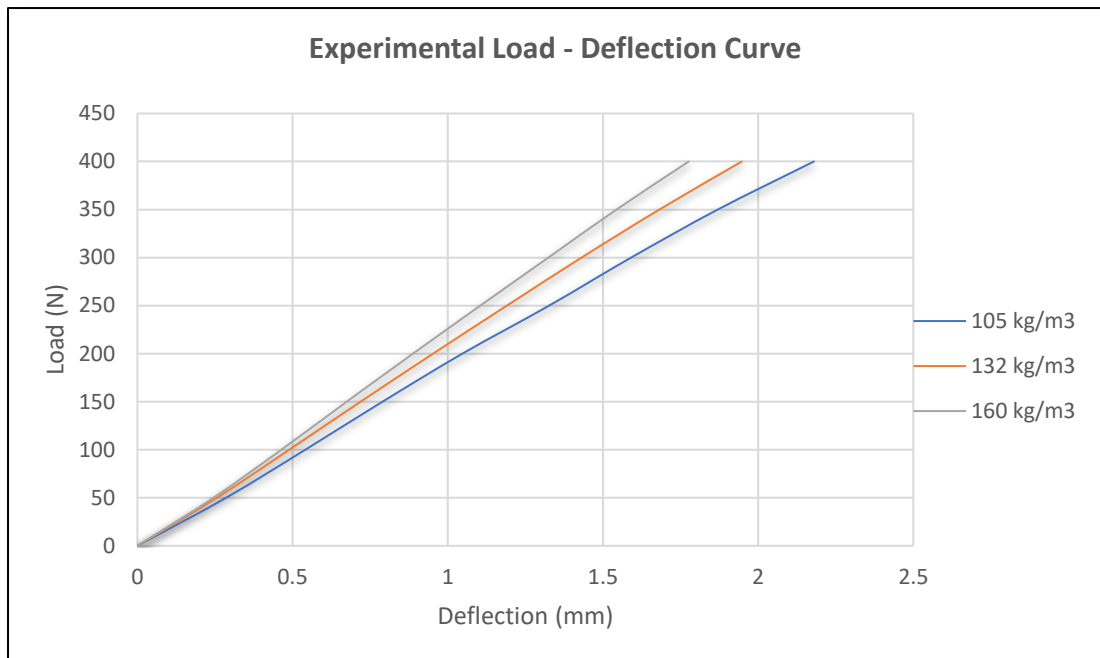


Figure 5.18: Experimental Load-Deflection Curve

Based on these results, the effect of core density on stiffness can be represented in Figure (5.23).

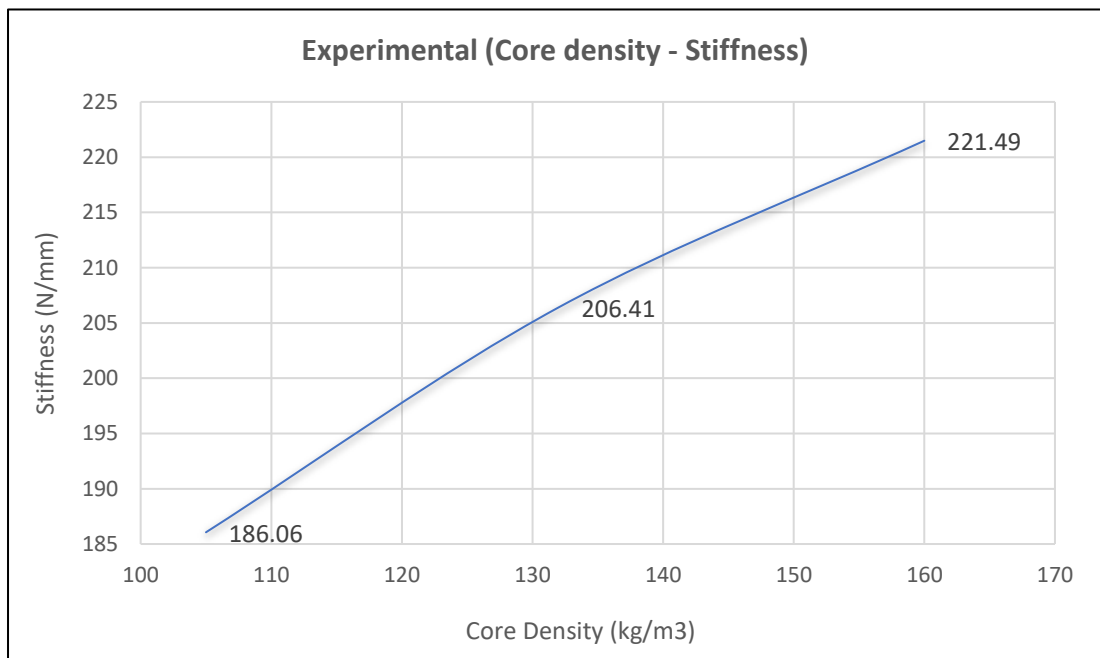


Figure 5.19: Experimental Core density - Stiffness Curve

Table (5.12) illustrates that experimental results have good agreement with numerical ones with an acceptable deviation percentage in that increasing

the density of an Overlapped Octagonal Core causes an increase in stiffness magnitude; figure (5.24) states that too.

Table 5.12: Numerical, and Experimental Stiffness values for each core density

Core Density (Kg/m ³)	Stiffness (N/mm) for each sample		Deviation ratio (%)
	Numerical	Experimental	
105	176.8	186.06	5.24
132	205.74	206.41	0.32
160	220.11	221.49	0.63

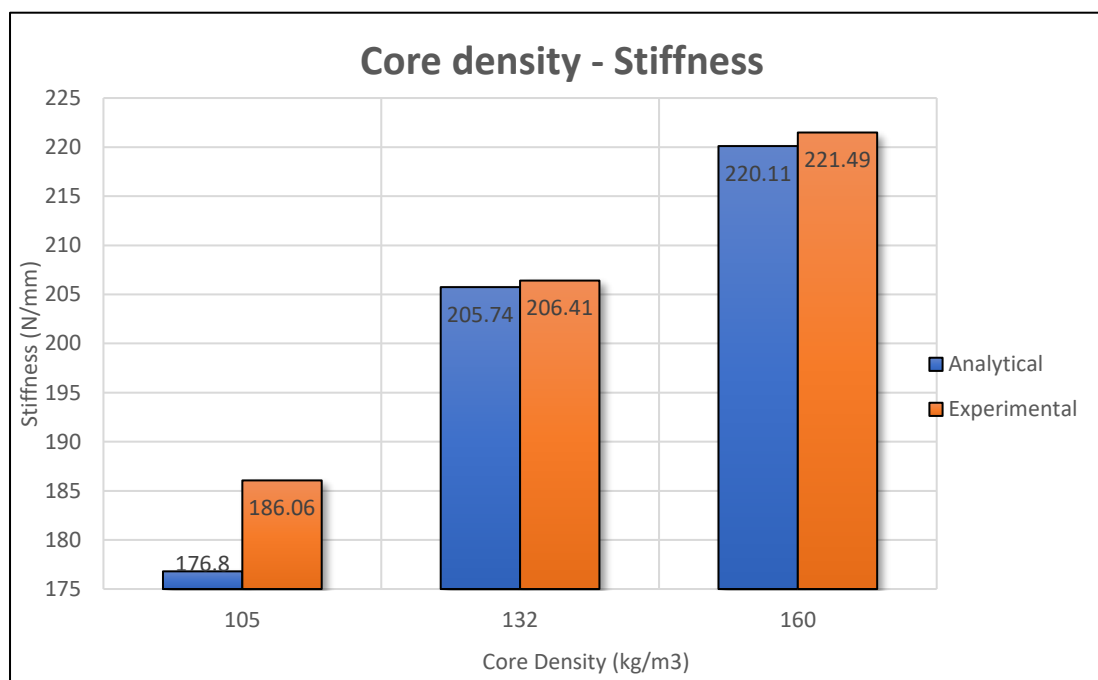


Figure 5.20: Numerical, and Experimental Core density - Stiffness Curves

Finally, the stiffness values for each investigated core type (Regular Hexagonal, Triangular, and Overlapped Octagonal Core) at different core densities may then be compared, as shown in figure (5.25), which demonstrates that the triangular and regular hexagonal cores often have less stiffness than the Overlapped Octagonal Core.

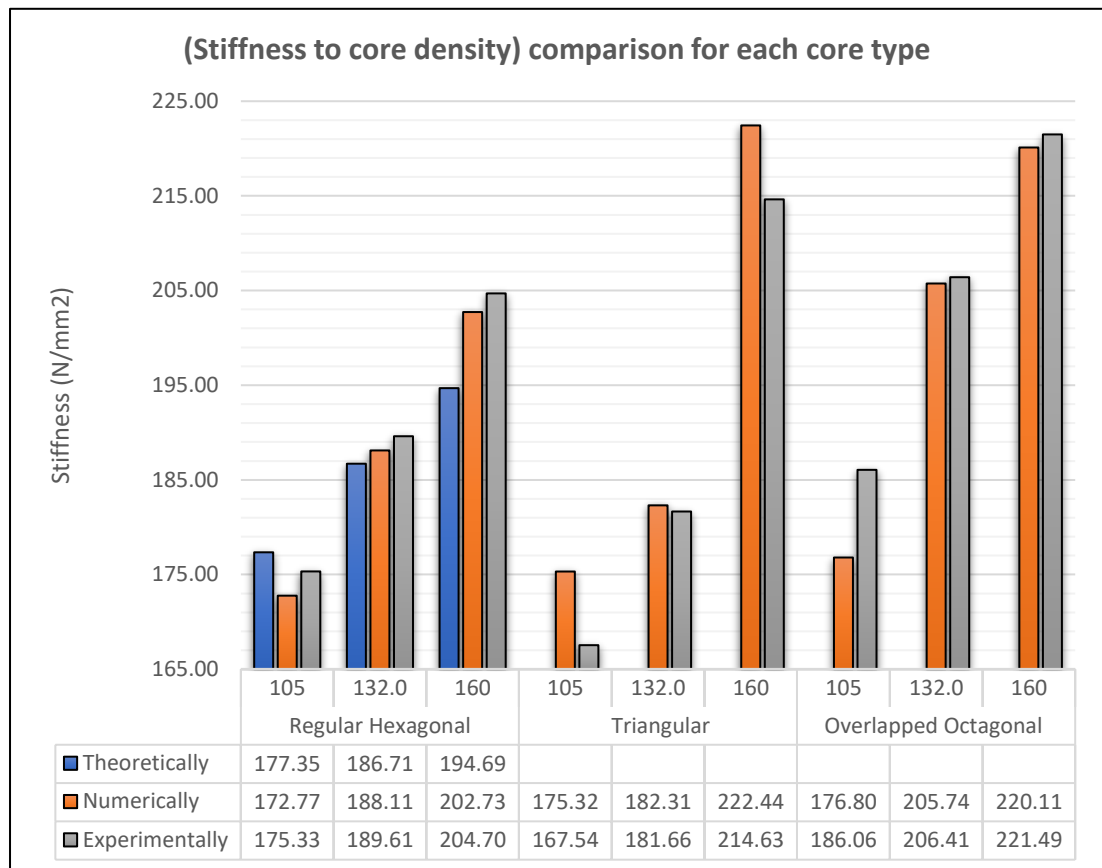


Figure 5.21: (Stiffness to core density) comparison for each core type

According to results from the comparison of hexagonal and triangular cores, the triangular core was the stiffest, which is in agreement with previous research [29], [77]. On the other hand, for an overlapping octagonal core stiffness, both numerical and experimental data indicate that it is often higher. Which indicates an increase in the shear modulus of the overlapped octagonal core.

5.6 Variation in mechanical properties according to the orientation

The honeycomb core has various mechanical properties, specifically the shear modulus, depending on the orientation of the applied load. As a result, that variation must be checked to specify the preferred loading

direction. So that it was necessary to perform an numerical check using Ansys simulation software for the tested configurations in this study.

5.6.1 Results of hexagonal core tests according to the orientation

Regular hexagonal honeycomb cores have two major loading directions (L and W). Simulation results listed in Table (5.13) show that stiffness in the W-direction was greater than stiffness in the L-direction. But, when the simulation was performed again with regular hexagonal honeycomb cores with doubled web thickness in the L-direction (as is common in industrial production), stiffness in the W direction was less than stiffness in the L direction, implying that shear modulus in the L-direction was greater than shear modulus in the W-direction. So, this agrees with most honeycomb manufacturers' publications [22]

Table 5.13: Numerically calculated stiffnesses specimens with single and double web thicknesses in various orientation loadings

Load (N)	Deflection (mm)			
	L-Direction	W-Direction	L-Direction Doubled web	W-Direction Doubled web
0	0	0	0	0
50	0.29009	0.25586	0.14938	0.20495
100	0.57996	0.51153	0.29877	0.40991
150	0.8695	0.76698	0.44815	0.61486
200	1.1587	1.0222	0.59754	0.81982
250	1.4477	1.2773	0.74692	1.0248
300	1.7366	1.5322	0.8963	1.2297
350	2.0258	1.7842	1.0457	1.4347
400	2.3152	2.0258	1.1951	1.6396
Stiffness (N/mm)	172.77	195.91	334.71	243.96

Figure (5.26) shows how a single web thickness sample loaded in the W direction would be stiffer than one loaded in the L direction, and how a double web thickness sample would have the reverse effect.

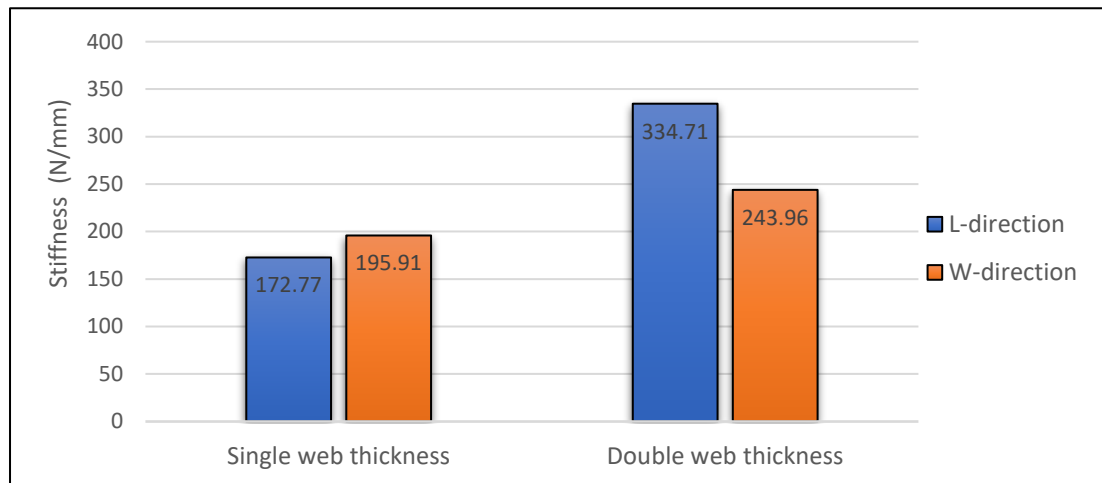


Figure 5.22: Stiffness in various orientations for single and double web thickness

5.6.2 Results of Triangular core tests according to the orientation

Triangular honeycomb cores have two major loading directions (L and W). Simulation results listed in Table (5.14) show that stiffness in the W-direction was greater than stiffness in the L-direction.

Table 5.14: Numerically calculated stiffnesses in various orientation loadings

Load (N)	Deflection (mm)	
	L-Direction	W-Direction
0	0	0
50	0.28566	0.25586
100	0.57106	0.51153
150	0.85616	0.76698
200	1.141	1.0222
250	1.4257	1.2773
300	1.7105	1.5322
350	1.9955	1.7842
400	2.2755	2.0258
Stiffness (N/mm)	175.32	181.01

Figure (5.27) shows how samples loaded in the W-direction would be stiffer than one loaded in the L-direction for a triangular honeycomb core.

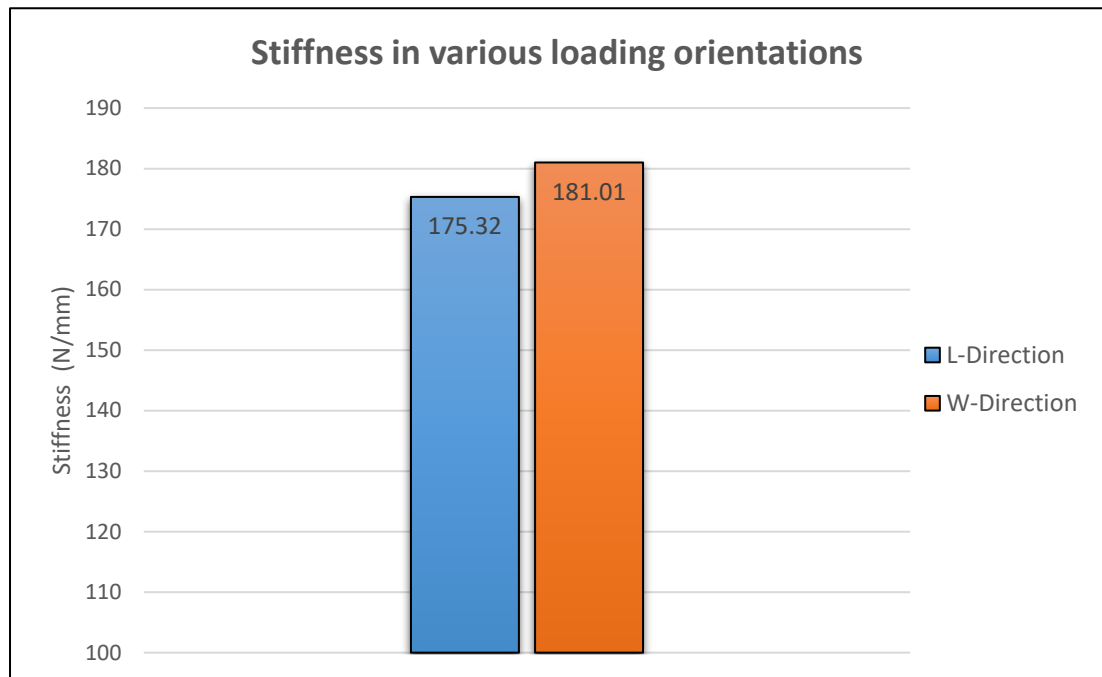


Figure 5.23: Stiffness in various loading orientations for Triangular core.

It is important to note that the properties of, say, the triangular or hexagonal cores differ relatively along the two perpendicular axes, L and W. Other core configurations, such as octagonal core configurations, have properties that are similar along perpendicular axes but distinct along diagonal axes, adding new criteria to honeycomb selection, design, and assembly regardless of density magnitude.

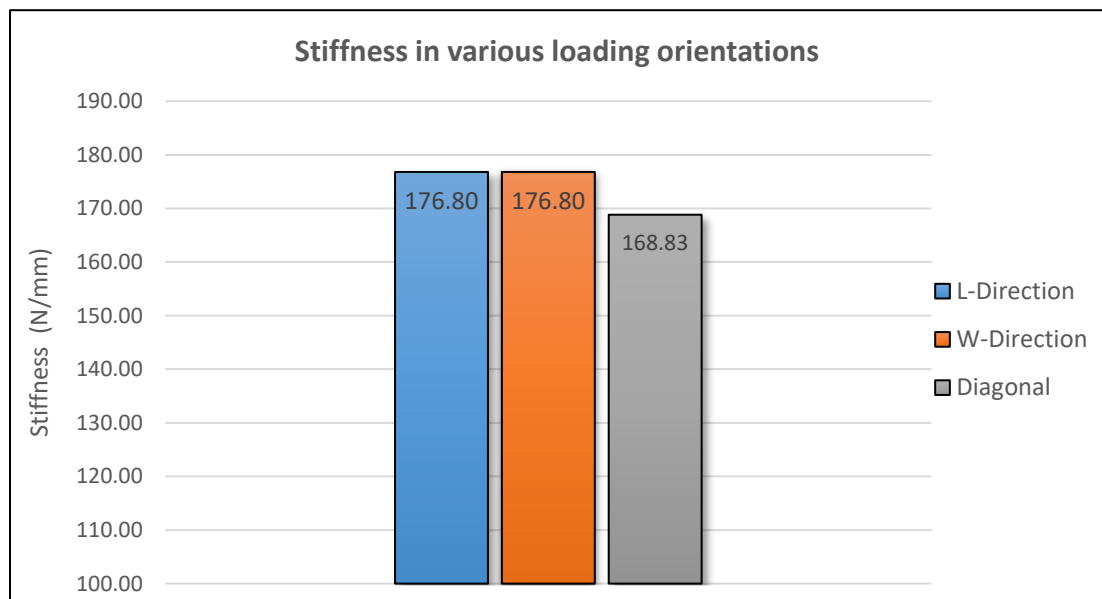
5.6.3 Results of Overlapped Octagonal Core tests according to the orientation

The Overlapped Octagonal Core has the same properties in the L and W directions. But on the diagonal, it has other properties. Simulation results listed in Table (5.15) show that stiffness in the W-direction was equal to stiffness in the L-direction. But diagonally, it was slightly less.

Table 5.15: Numerically calculated stiffnesses in various orientation loadings

Load (N)	Deflection (mm)		
	L-Direction	W-Direction	Diagonal-Direction
0	0	0	0
50	0.28424	0.28424	0.29716
100	0.56794	0.56794	0.59385
150	0.85114	0.85114	0.89035
200	1.1341	1.1341	1.1869
250	1.4171	1.4171	1.4835
300	1.6972	1.6972	1.7798
350	1.9697	1.9697	2.0665
400	2.2347	2.2347	2.3454
Stiffness (N/mm)	176.80	176.80	168.83

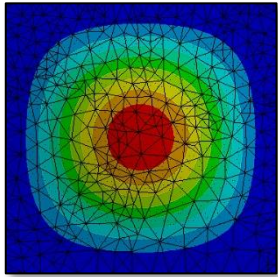
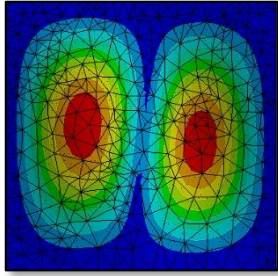
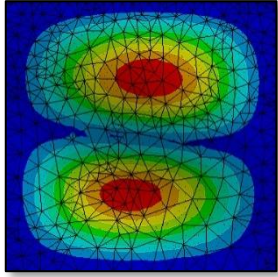
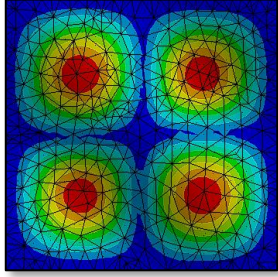
Figure (5.28) shows how a sample loaded in the L or W direction would be stiffer than one loaded in the diagonal direction for the Overlapped Octagonal Core.

**Figure 5.24: Stiffness in various loading orientations.**

5.7 Results of a Free Vibration Analysis

By conducting a simulation with Ansys software to estimate the first three natural frequencies for specimens with various core densities, the effect of the core density value on the natural frequency of a sandwich would be obvious. Table (5.16) shows the simulation results.

Table 5.16: Natural Frequencies for specimens with various core densities

Natural Frequency (Hz)	FVHA	FVHB	FVHC	FVHD	Mode shape
	105 (Kg/m ³) density	132 (Kg/m ³) density	160 (Kg/m ³) density	Sold Panel	
$\omega_{1,1}$	1232.6	1226.4	1212.9	962.48	
$\omega_{1,2}$	2370.9	2382.2	2370.7	1944.7	
$\omega_{2,1}$	2373.4	2389.9	2383	1944.7	
$\omega_{3,1}$	3347.1	3393.6	3388.6	2842.5	

According to the natural frequency values obtained from the analysis, the core density increase appears to slightly drop the value of natural frequencies, at least in the first natural frequencies, and that agrees with the literature [49], [53], [78]. However, when the results are compared to those obtained from analyzing a solid panel of the same size and material, we notice a slight effect of the cellular core usage on the value of the natural frequency, and that agrees with the literature [53].

5.8 Results of Impact Simulation Tests

As explained in the theoretical chapter, the results of the low-velocity impact test reveal the significant effect of core density magnitude on the sandwich's behavior under sudden dynamic loading, represented by dropping a cylindrical mass with a hemispherical head from a certain height; therefore, the mass would hit the sandwich surface at a specific velocity, leaving a trace whose depth depends on the sandwich's resistance to impact.

5.8.1 Results of Impact of Regular Hexagonal Honeycomb Core

In a simulation to meet ASTM D7766 [67] requirements, as illustrated in figure (5.31), sandwich panel samples after exposure to dropping that cylindrical object with the same velocity would have a specific dent, whose depth should indicate how that sandwich could resist impact.

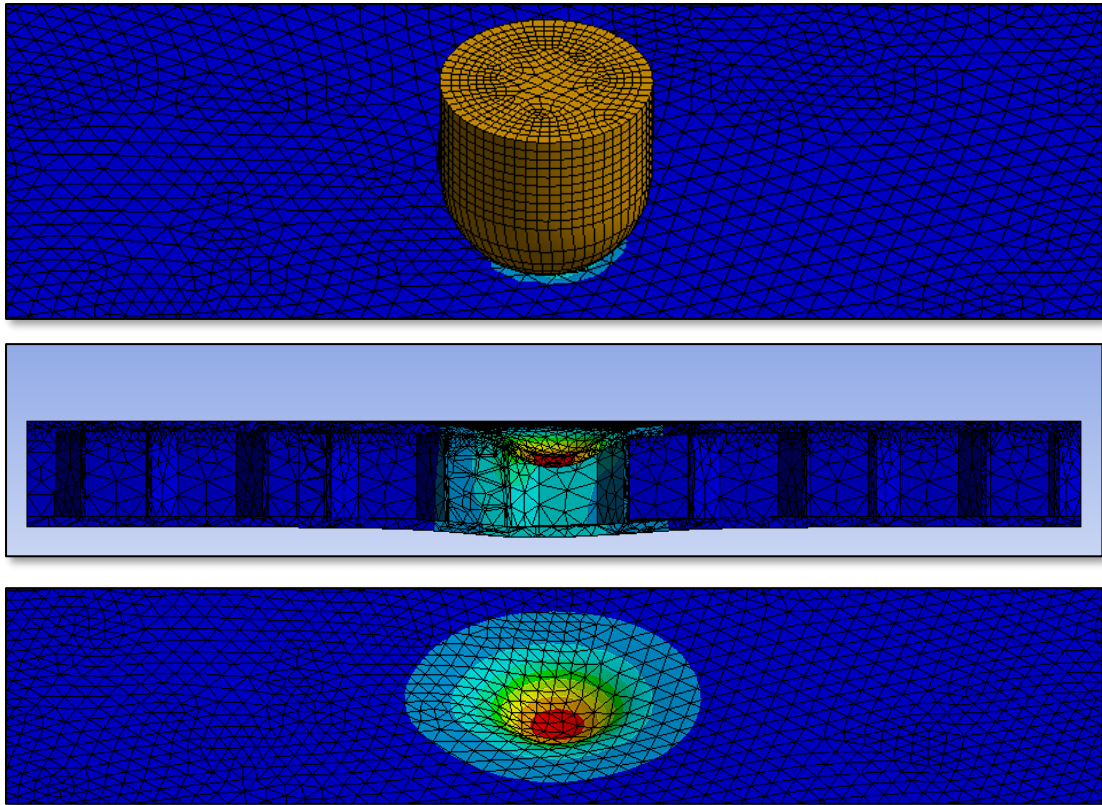
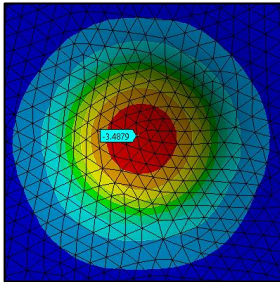
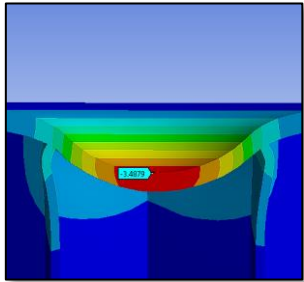
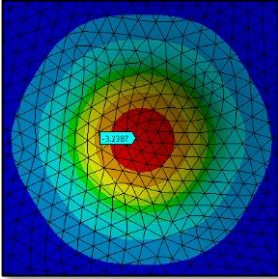
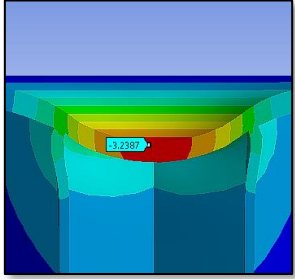
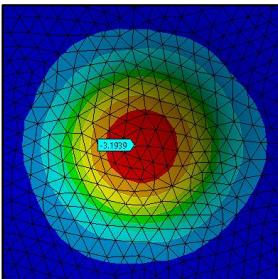
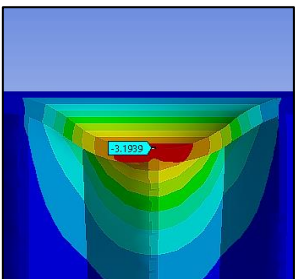


Figure 5.25:Simulation of the impact test.

Table (5.17) shows how cell size variation, or, in other words, the core density value, affects the produced dent depth due to impact.

Table 5.17:Core density effect on dent depth due to impact for Regular hexagonal honeycomb core sandwiches.

Cell size (mm)	Core Density (Kg/m ³)	Dent depth (mm)	Ansys results	
			Top view	Side view
9.5	105	3.48		

7.52	132	3.24		
6.2	160	3.19		

The table above shows that increasing core density by reducing cell size reduces dent depth due to impact and, as a result, increase of the impact resistance. Figure (5.32) depicts graphically how increasing the core density value reduced the impact dent depth.

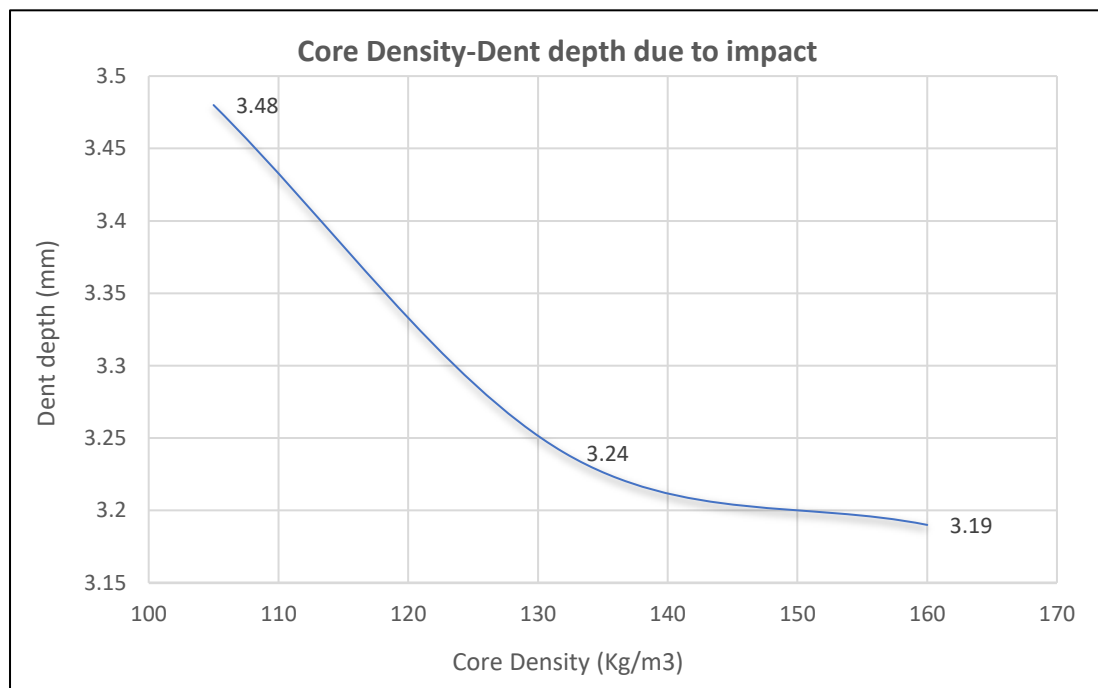
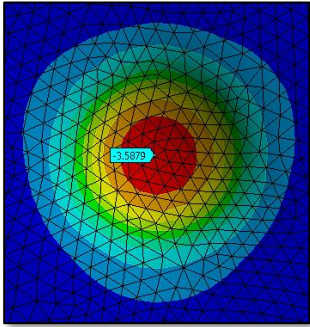
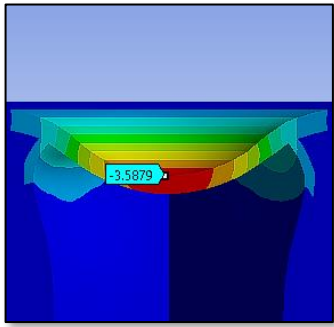
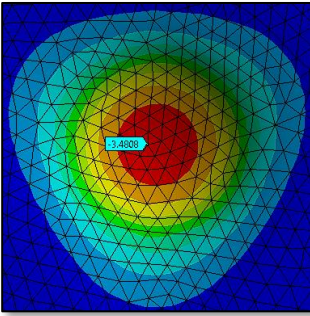
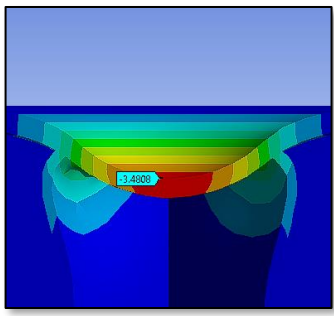
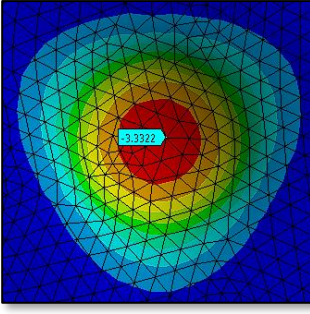
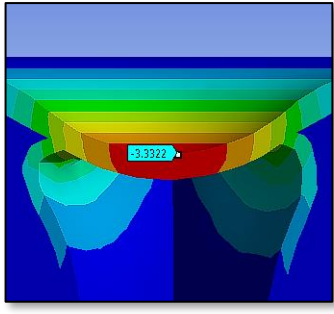


Figure 5.26:Relation between core density and dent depth due to impact for (Regular hexagonal honeycomb core).

5.8.2 Results of Impact Triangular Honeycomb Core

An impact test was numerically performed on a triangular honeycomb core with three sandwich samples, each with a different core density. In a simulation to meet ASTM D7766 [67] loading conditions, sandwich samples of triangular honeycomb core were also exposed to a dropped impactor. Table (5.18) shows how cell size variation, or, in other words, the core density value, affects the produced dent depth due to impact .

Table 5.18:Core density effect on dent depth due to impact for Triangular honeycomb core sandwiches.

Cell size (mm)	Core Density (Kg/m ³)	Dent depth (mm)	Ansys results	
			Top view	Side view
9.5	105	3.58		
7.52	132	3.48		
6.2	160	3.33		

The table above also shows that increasing the core density of the triangular core sandwich by reducing cell size reduces dent depth due to impact and, as a result, increasing impact resistance. Figure (5.33) depicts graphically how increasing the core density value reduced the impact dent depth.

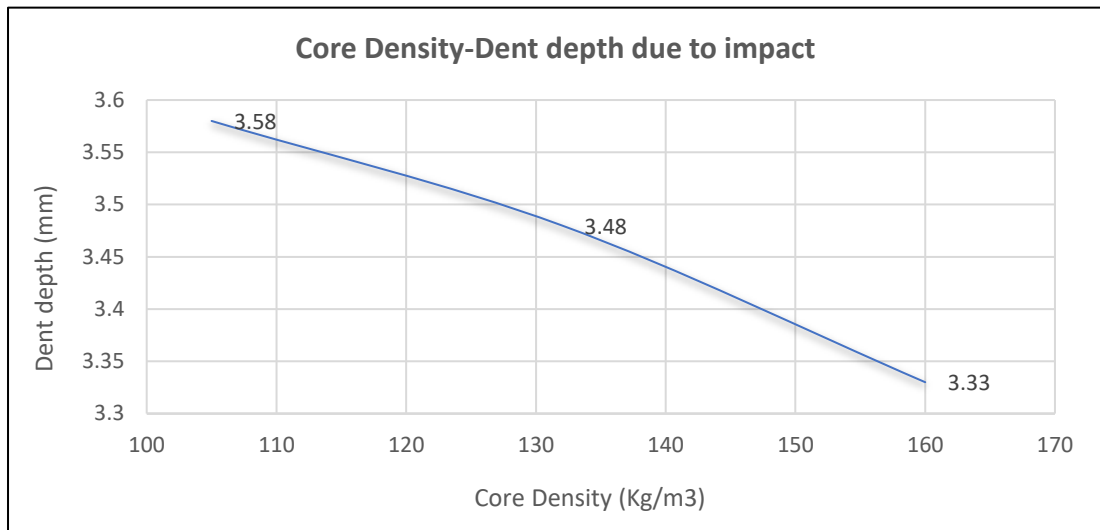


Figure 5.27:Relation between core density and dent depth due to impact for (Triangular honeycomb core).

Figure (5.34) shows that for regular hexagonal and triangular cores, the effect of core density on impact resistance is convergent, so the same effect might be predicted for a different core type.

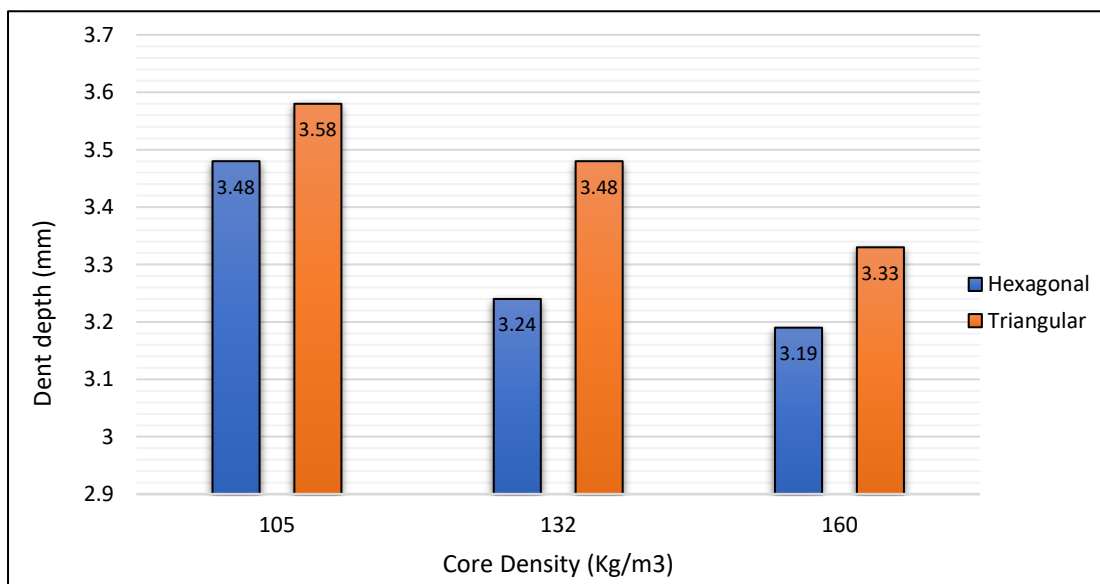


Figure 5.28:Comparison of (Core density - dent depth due to impact) for Hexagonal and Triangular honeycomb cores.

5.9 Wing Simulation

A simulation experiment has been designed to explore wing behavior under aerodynamic load conditions. Under these conditions, the wing would be exposed to distributed pressure, producing two main forces: lifting force and drag force, acting normally on its surface. Since the wing is fixed on one side, those forces would bend the wing, and the amount of that bend depended on its stiffness. So that by submitting wings with various core types and densities to that numerical simulation, the effect of core type and density would be clear and comparable. Table (5.19) shows the deflection of each case with a decreasing ratio of deflection results.

Table 5.19:Wing Deflection of Each Core Type and Density

Core Type	Core Density (Kg/m ³)	Deflection (mm)	Decreasing Ratio (%)
Regular Hexagonal	105	41.54	-
	132	40.97	1.37
	160	40.74	0.56
Triangular	105	42.27	
	132	40.89	3.26
	160	40.07	2.00
Overlapped Octagonal	105	41.76	-
	132	39.75	4.81
	160	39.5	0.63

It can be noted that with an increase in the value of the core density, the deflection decreases with it for all core types with the mentioned ratios, which indicates a higher stiffness as a result of the increase in the core density. On the other hand, the Overlapped Octagonal core often appears to be the stiffest, followed by the triangular, and then the hexagonal. Figure (5.35) shows the results of the comparison.

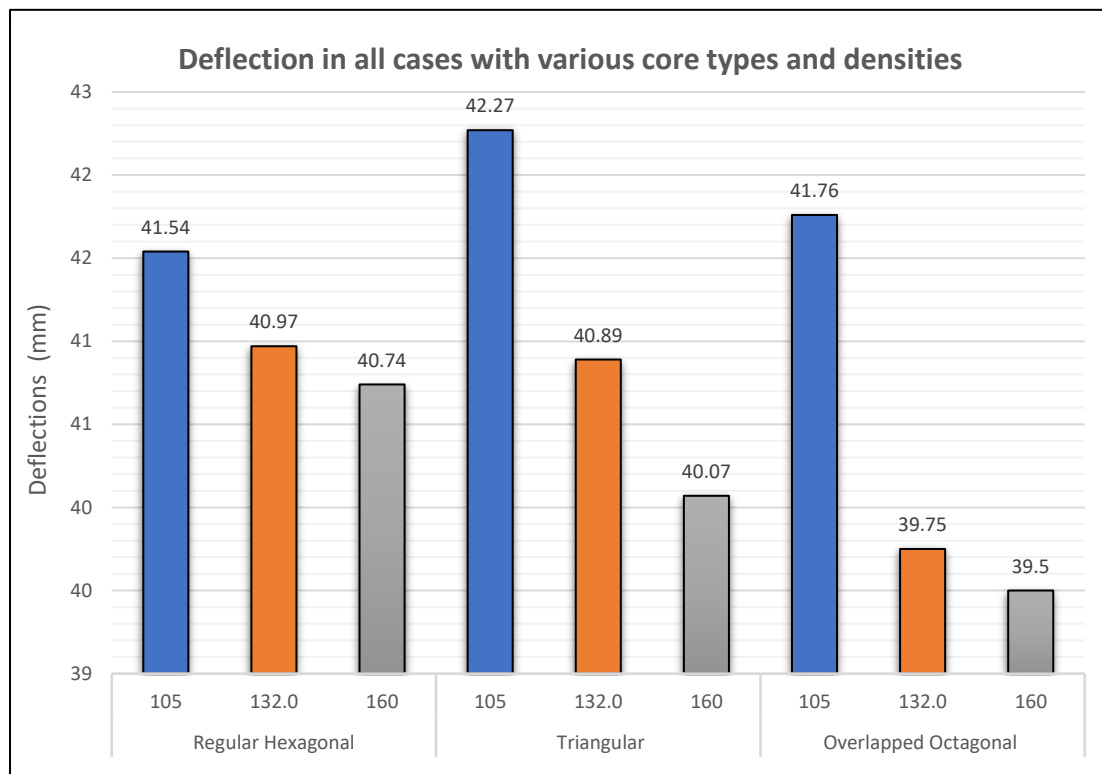


Figure 5.29: Deflection in all cases with various core types and densities

It is worth noting that the results of this simulation are compatible with the results of the previous tests shown and listed in Figure (5.25). That confirms the same previous conclusions that describe the effect of core density on the stiffness of the component involved in its manufacture, whether it is a sandwich panel board or a wing, as well as the effectiveness of the core type (at least the tested types) in overall sandwich structure behavior.

Chapter Six: Conclusions and Recommendations

The conclusions are described in this chapter. It also gives recommendations for further research.

6.1 Core density effects on the stiffness

- Increasing the magnitude of core density by 25.7% and 52.4% contributes to a 5.27% and 9.77% increase in stiffness (theoretically), 8.87% and 17.34% (numerically), and 8.14 % and 16.75% (experientially) for regular hexagonal honeycomb.
- Increasing the magnitude of core density by 25.7% and 52.4% contributes to a 3.98 % and 26.87% increase in stiffness (numerically), and 8.43% and 28.1% (experientially) for triangular honeycomb.
- Increasing the magnitude of core density by 25.7% and 52.4% contributes to a 17.25% and 24.49 increase in stiffness (numerically), and 10.94% and 19.04% (experientially) for overlapped octagonal honeycomb.
- Finally, without a doubt, it can be said that for the investigated configurations, an increase in core density, particularly when controlled by geometrical parameters (reducing cell size), results in an increase in sandwich stiffness.

6.2 Core density effects on the natural frequencies

- The core density increases by 25.7% and 52.4% seems to somewhat reduce the value of natural frequencies, at least in the first mode, according to the values of natural frequencies obtained numerically from the analysis.

6.3 Core density effects on the impact resistance (Numerically)

- It can be concluded that increasing the density of the core led to increasing the impact resistance of the sandwich. Also, the regular hexagonal core has more resistance to impacts than the triangular core.

6.4 Core type effect on results

- The stiffness results (theoretically, numerically, and experimentally) showed that the overlapped octagonal core stiffness was superior to the triangular core, and the hexagonal core had the lowest stiffness.
- The hexagonal and triangular cores have different properties on two perpendicular axes, but the octagonal core has equal properties on two perpendicular axes.

6.5 Suggestions for Future Work

- Studying samples with the same density but different cell sizes, cell wall thicknesses, and core materials might reveal the impact of each core density parameter and determine which one has the greatest impact on the strength and stiffness of sandwiches.
- Investigate the impact of core density on the performance of sandwiches under explosive load.
- Calculating the shear modulus of the core using the shear test method instead of the three-point bending method.
- Manufacture and test larger samples with a higher cell size-to-specimen size ratio to obtain more accurate results.
- Subjecting sandwich samples with various core densities to torsional loads to explore their performance and core density effect on it.

References

- [1] Adrian P. Mouritz, *Introduction to aerospace materials*. Woodhead Publishing Limited, 2012.
- [2] J. P. Nunes and J. F. Silva, “Sandwiched composites in aerospace engineering,” in *Advanced Composite Materials for Aerospace Engineering*, Elsevier, 2016, pp. 129–174. doi: 10.1016/b978-0-08-100037-3.00005-5.
- [3] Y. Okabe, S. Minakuchi, N. Shiraishi, K. Murakami, and N. Takeda, “Smart honeycomb sandwich panels with damage detection and shape recovery functions,” *Advanced Composite Materials*, vol. 17, no. 1, pp. 41–56, Mar. 2008, doi: 10.1163/156855108X295645.
- [4] B. CASTANIE, C. BOUVET, and M. Ginot, “Review of composite sandwich structure in aeronautic applications,” *Composites Part C: Open Access*, vol. 1. Elsevier B.V., Aug. 01, 2020. doi: 10.1016/j.jcomc.2020.100004.
- [5] A. S. Herrmann, P. C. Zahlen, and I. Zuardy, “*Sandwich Structures Technology In Commercial Aviation Present Applications And Future Trends*,” 2005.
- [6] “*Aviation Maintenance Technician Handbook-Airframe Volume 1*,” 2012. Accessed: May 07, 2023. [Online]. Available: <https://www.faa.gov/>
- [7] T. Megson, *Aircraft Structures for engineering students*. Butterworth-Heinemann is an imprint of Elsevier, 2017.
- [8] Michael Chun-Yu Niu, *Composite Airframe Structures*. Connilit Press LTD, 1992.
- [9] T. Bitzer, *Honeycomb Technology*. Springer Netherlands, 1997. doi: 10.1007/978-94-011-5856-5.

- [10] Z. Chen and N. Yan, “Investigation of elastic moduli of Kraft paper honeycomb core sandwich panels,” *Compos B Eng*, vol. 43, no. 5, pp. 2107–2114, Jul. 2012, doi: 10.1016/j.compositesb.2012.03.008.
- [11] “HexWeb ® Honeycomb Selector Guide HexWeb ® honeycomb provides exceptional stiffness and strength with little added weight for aerospace and industrial applications.”
- [12] Ehsan Kharrazi, “Structural FEM analysis of innovative sandwich configuration for automotive application,” Polytechnic of Turin, TORINO, 2020.
- [13] J. M. Davies, *Lightweight sandwich construction*. Manchester: International Council for Building Research, , 2001.
- [14] Y. Du, N. Yan, and M. T. Kortschot, “Light-weight honeycomb core sandwich panels containing biofiber-reinforced thermoset polymer composite skins: Fabrication and evaluation,” *Compos B Eng*, vol. 43, no. 7, pp. 2875–2882, Oct. 2012, doi: 10.1016/j.compositesb.2012.04.052.
- [15] J. Pflug and I. Verpoest, “Sandwich materials selection charts,” *Journal of Sandwich Structures & Materials*, vol. 8, no. 5, pp. 407–421, 2006.
- [16] R. A. Staal, G. Mallinson, D. Horrigan, and J. Krishnan, “Failure of Sandwich Honeycomb Panels in Bending,” 2006.
- [17] E. Oterkus, C. Diyaroglu, D. De Meo, and G. Allegri, “Fracture modes, damage tolerance and failure mitigation in marine composites,” in *Marine Applications of Advanced Fibre-Reinforced Composites*, Elsevier Inc., 2016, pp. 79–102. doi: 10.1016/B978-1-78242-250-1.00004-1.
- [18] D. Zenkert, *The handbook of sandwich construction*. Engineering Materials Advisory Services, 1997.

- [19] M. M. William, *Design of composite sandwich panels for lightweight applications in air cargo containers*. West Virginia University, 2016.
- [20] J. Vinson, *The behavior of sandwich structures of isotropic and composite materials*. Routledge, 2018.
- [21] Sudharsan, “*Structural Design And Analysis Of A Lightweight Composite Sandwich Space Radiator Panel*,” 2003.
- [22] hexcel, “HexWeb ® *Honeycomb Attributes and Properties*,” 2016. [Online]. Available: <http://www.hexcel.com/contact/salesoffice>
- [23] F. A. Fazzolari, “Sandwich Structures,” in *Stability and Vibrations of Thin-Walled Composite Structures*, Elsevier, 2017, pp. 49–90. doi: 10.1016/B978-0-08-100410-4.00002-8.
- [24] N. Amsc and A. A. CMPS, “Composite materials handbook,” *Polymer matrix composites materials usage, design, and analysis*, 2002.
- [25] M. Tauhiduzzaman, “Design optimization of sandwich core,” University of Texas, El Paso, 2016. [Online]. Available: https://digitalcommons.utep.edu/open_etd/970
- [26] L. J. Gibson and F. Ashby, “Cellular Solids: Structure, Properties and Applications,” 1997.
- [27] A. Nazir, K. M. Abate, A. Kumar, and J. Y. Jeng, “A state-of-the-art review on types, design, optimization, and additive manufacturing of cellular structures,” *International Journal of Advanced Manufacturing Technology*, vol. 104, no. 9–12, pp. 3489–3510, Oct. 2019, doi: 10.1007/s00170-019-04085-3.
- [28] Alaa Abdulzahra Deli Al-Fatlawi, “*Minimum Weight And Cost Design Optimization Of Honeycomb Sandwich Structures*,” UNIVERSITY OF MISKOLC, Miskolc, 2021. doi: 10.14750/ME.2021.026.

- [29] H. E. Soliman, R. K. Kapania, R. C. Batra, J. T. Black, and A. J. Brown, “*Mechanical Properties of Cellular Core Structures*,” 2016.
- [30] Hexcel, “HexWeb™ *Honeycomb Attributes and Properties*,” 1999.
- [31] “A/C - What does A/C stand for? The Free Dictionary.” <https://acronyms.thefreedictionary.com/A%2fC> (accessed Apr. 07, 2023).
- [32] “*NASA BOEING 727 EXPERIMENTAL COMPOSITE / CARBON FIBER ELEVATOR ASSEMBLY FILM 45864 - YouTube*.” <https://www.youtube.com/watch?v=ZIsAzQgo0tk> (accessed Apr. 07, 2023).
- [33] “*Historical Snapshot: 727 Commercial Transport*.” <https://www.boeing.com/history/products/727.page> (accessed Apr. 07, 2023).
- [34] K. K. Rao, K. J. Rao, A. G. Sarwade, and M. S. Chandra, “Strength analysis on honeycomb sandwich panels of different materials,” *International Journal of Engineering Research and Applications (IJERA)*, vol. 2, no. 3, pp. 365–374, 2012.
- [35] H. R. Ali, B. Manafi, V. Shatermashhadi, and A. Salimi, “*Analysis and investigation of honeycomb sandwich panel parameters under Static three-point bending*,” *Cell*, vol. 11, no. 10mm, p. 9mm, 2013.
- [36] K. Seto *et al.*, “*Analytical prediction of bending stiffness of honeycomb sandwich panels bonded adhesively*,” Tokyo, 2014.
- [37] A. S. Navi, A. Ehsan, and A. G. Sayyad, “*Effect of Core Geometry on Shear Moduli in Cellular Core Sandwich Structures*,” *Indian J Sci Technol*, vol. 8, no. 12, Jun. 2015, doi: 10.17485/ijst/2015/v8i12/70709.
- [38] N. Bruffey and W. Shiu, “*Predicting Flexural Strength Of Composite Honeycomb Sandwich Panels Using Mechanical Models Of Face Sheet Compressive Strength*,” 2016.

- [39] D. Fadhel Mohammed, “*Experimental And Numerical Study Of Bending Behavior For Honeycomb Sandwich Panel With Different Core Configurations,*” 2016.
- [40] H. E. Soliman, R. K. Kapania, R. C. Batra, J. T. Black, and A. J. Brown, “*Mechanical Properties of Cellular Core Structures,*” 2016.
- [41] Małgorzata and Dorota, “*Comparative Study Of Bending Stiffness Of Sandwich Plates With Cellular Cores,*” 2017.
- [42] C. Kaboglu, L. Yu, I. Mohagheghian, B. R. K. Blackman, A. J. Kinloch, and J. P. Dear, “*Effects of the core density on the quasi-static flexural and ballistic performance of fibre-composite skin/foam-core sandwich structures,*” *J Mater Sci*, vol. 53, no. 24, pp. 16393–16414, Dec. 2018, doi: 10.1007/s10853-018-2799-x.
- [43] S. Raeisi and A. Tovar, “*The Effect of the Cell Shape on Compressive Mechanical Behavior of 3D Printed Extruded Cross-sections,*” in *SAE Technical Papers*, SAE International, 2018. doi: 10.4271/2018-01-1384.
- [44] L. Azzouz *et al.*, “*Mechanical properties of 3-D printed truss-like lattice biopolymer non-stochastic structures for sandwich panels with natural fibre composite skins*”, doi: 10.1016/j.compstruct.2019.01.103i.
- [45] Assmaa Sattar Hamzah, “*Numerical and Experimental Study of the Parameters affected on the Honeycomb Structures Properties Supervised by,*” University of Babylon, Babylon, 2020.
- [46] A. Farrokhbadi, S. Ahmad Taghizadeh, H. Madadi, H. Norouzi, and A. Ataei, “*Experimental and numerical analysis of novel multi-layer sandwich panels under three point bending load,*” *Compos Struct*, vol. 250, Oct. 2020, doi: 10.1016/j.compstruct.2020.112631.
- [47] P. Dhananandh*, Dr. V. R. Mamilla, and K. S. R. Murthy, “*Design and Analysis of Hexagonal and Octagonal Honey Comb Structures*

- with Various Materials and FEM Analysis.,” International Journal of Innovative Technology and Exploring Engineering*, vol. 9, no. 7, pp. 669–677, May 2020, doi: 10.35940/ijitee.E2254.059720.
- [48] H. Abedzade Atar, M. Zarrebini, H. Hasani, and J. Rezaeepazhand, “*The effect of core geometry on flexural stiffness and transverse shear rigidity of weight-wise identical corrugated core sandwich panels reinforced with 3D flat spacer knitted fabric,*” *Polym Compos*, vol. 41, no. 9, pp. 3638–3648, Sep. 2020, doi: 10.1002/pc.25662.
- [49] S. E. Sadiq, M. J. Jweeg, and S. H. Bakhy, “*Strength Analysis of an Aircraft Sandwich Structure with a Honeycomb Core: Theoretical and Experimental Approaches,*” *Engineering and Technology Journal*, vol. 39, no. 1A, pp. 153–166, Jan. 2021, doi: 10.30684/etj.v39i1a.1722.
- [50] D. Sridhar and D. Shashikala, “*Effect of Foam and Epoxy on Aluminium Honeycomb structure for an Automobile Applications,*” 2021.
- [51] D. Pereira *et al.*, “*Cellular lattice cores of sandwich panels fabricated by additive manufacturing: Effect of dimensions and relative density on mechanical behaviour,*” *Proceedings of the Institution of Mechanical Engineers, Part L: Journal of Materials: Design and Applications*, 2022, doi: 10.1177/14644207221138003.
- [52] R. A. Staal, G. Mallinson, D. Horrigan, and J. Krishnan, “*Failure of Sandwich Honeycomb Panels in Bending,*” 2006.
- [53] B. Amit Kumar Jha, “*FREE VIBRATION ANALYSIS OF SANDWICH PANEL,*” 2007.
- [54] E. A. Flores-Johnson and Q. M. Li, “*Experimental study of the indentation of sandwich panels with carbon fibre-reinforced polymer face sheets and polymeric foam core,*” *Compos B Eng*, vol. 42, no. 5, pp. 1212–1219, Jul. 2011, doi: 10.1016/j.compositesb.2011.02.013.

- [55] Y. Parikh and P. Mahamuni, “*Study of Modal Analysis and Testing of Hexagonal Honeycomb Plates,*” *International Journal of Applied Engineering Research*, 2015, [Online]. Available: <http://www.ripublication.com>
- [56] S. B. Loganathan and H. K. Shivanand, “*Effect of Core Thickness and Core Density on Low Velocity Impact Behavior of Sandwich Panels with PU Foam Core,*” *Journal of Minerals and Materials Characterization and Engineering*, vol. 03, no. 03, pp. 164–170, 2015, doi: 10.4236/jmmce.2015.33019.
- [57] M. J. Jweeg, “*A Suggested Analytical Solution for Vibration of Honeycombs Sandwich Combined Plate Structure,*” *International Journal of Mechanical & Mechatronics Engineering IJMME-IJENS*, vol. 16, 2016.
- [58] C. Pimenta, S. Morris, and A. Dear, “*The influence of different types of core materials on the impact behaviour of sandwich composites,*” 2017. [Online]. Available: www.propaas.eu
- [59] R. Kumar and S. Patel, “*Failure analysis on octagonal honeycomb sandwich panel under air blast loading,*” in *Materials Today: Proceedings*, Elsevier Ltd, 2019, pp. 9667–9672. doi: 10.1016/j.matpr.2020.07.525.
- [60] J. Qi, C. Li, Y. Tie, Y. Zheng, and Y. Duan, “*Energy absorption characteristics of origami-inspired honeycomb sandwich structures under low-velocity impact loading,*” *Mater Des*, vol. 207, Sep. 2021, doi: 10.1016/j.matdes.2021.109837.
- [61] A. Castellanos and P. Prabhakar, “*Elucidating the Mechanisms of Damage in Foam Core Sandwich Composites under Impact Loading and Low Temperatures,*” Apr. 2021, doi: 10.1177/1099636221993848.

- [62] G. R. Rayjade, R. V Bhaskar, and A. D. Bhagure, “*International Journal of Current Engineering and Technology Honeycomb Sandwich panel analysis-Analytical and FEA approach,*” 500/*International Journal of Current Engineering and Technology*, vol. 9, no. 4, doi: 10.14741/ijcet/v.9.4.1.
- [63] L. Wahl, S. Maas, D. Waldmann, A. Zürbes, and P. Frères, “*Shear stresses in honeycomb sandwich plates: Analytical solution, finite element method and experimental verification,*” *Journal of Sandwich Structures and Materials*, vol. 14, no. 4, pp. 449–468, Jul. 2012, doi: 10.1177/1099636212444655.
- [64] H. G. Allen, “*Analysis And Design Of Structural Sandwich Panels Pergamon Press Ox Ford-London-Edinburgh-New York Toronto-Sydney · Paris · Braunschweig,*” 1969.
- [65] “17. Sandwich Panels - YouTube.” <https://www.youtube.com/watch?v=4zpQwirFsbk&t=2047s> (accessed Apr. 04, 2023).
- [66] B. Sadiq Emad Sadiq and A. H. Sadeq Bakhy Muhsin J Jweeg, “*Investigation of Static and Dynamic Analysis of Aluminum Honeycomb Plate Using Resistance Spot Welding,*” University of Technology, 2016.
- [67] “*Standard Practice for Damage Resistance Testing of Sandwich Constructions.*” https://www.astm.org/d7766_d7766m-16.html (accessed Apr. 04, 2023).
- [68] “NACA-0009 9.0% smoothed (n0009sm-il).” <http://airfoiltools.com/airfoil/details?airfoil=n0009sm-il> (accessed Apr. 04, 2023).
- [69] “*Astm C393 Testing Fixture Core Shear Properties Of Sandwich Constructions By Beam Flexure* 1 ASTM D393 Testing Fixture.”

- [70] “*Standard Test Method for Core Shear Properties of Sandwich Constructions by Beam Flexure.*” https://www.astm.org/c0393_c0393m-20.html (accessed Apr. 04, 2023).
- [71] R. T. L. Ferreira, I. C. Amatte, T. A. Dutra, and D. Bürger, “*Experimental characterization and micrography of 3D printed PLA and PLA reinforced with short carbon fibers,*” *Compos B Eng*, 2017, doi: 10.1016/j.compositesb.2017.05.013.
- [72] A. L. Woern, D. J. Byard, R. B. Oakley, M. J. Fiedler, S. L. Snabes, and J. M. Pearce, “*Fused particle fabrication 3-D printing: Recycled materials’ optimization and mechanical properties,*” *Materials*, vol. 11, no. 8, Aug. 2018, doi: 10.3390/ma11081413.
- [73] B. M. Tymrak, M. Kreiger, and J. M. Pearce, “*Mechanical properties of components fabricated with open-source 3-D printers under realistic environmental conditions,*” *Mater Des*, vol. 58, pp. 242–246, 2014, doi: 10.1016/j.matdes.2014.02.038.
- [74] “*Standard Test Method for Tensile Properties of Plastics.*” <https://www.astm.org/d0638-14.html> (accessed Apr. 04, 2023).
- [75] “*Standard Test Methods for Density and Specific Gravity (Relative Density) of Plastics by Displacement.*” <https://www.astm.org/d0792-20.html> (accessed Apr. 04, 2023).
- [76] P. Breunig *et al.*, “*Dynamic-impact-behavior-of-syntactic-foam-core-sandwich-composites,*” *J Compos Mater*, 2018.
- [77] U. B. Shah and R. K. Kapania, “*Alternate sandwich panel core for space structures,*” in *2018 AIAA SPACE and Astronautics Forum and Exposition*, American Institute of Aeronautics and Astronautics Inc, AIAA, 2018. doi: 10.2514/6.2018-5352.
- [78] “*The-Free-Vibration-Analysis-of-Honeycomb-Sandwich-Beam-Using-3D-and-Continuum-Model*”.

الخلاصة

الألواح الطباقية ، والتي تتكون غالبًا من لوحين وجهتين متصلتين بقرص العسل أو نواة رغوية. تم استخدام الألواح الطباقية في مجموعة متنوعة من التطبيقات ، مثل أنظمة طاقة الرياح والسفن والطائرات. في هذه الدراسة ، تمت دراسة النواة من نوع قرص العسل السداسي المنتظم باستخدام الحلول التحليلية المتاحة التي تتضمن إيجاد العلاقة بين كثافة النواة والانحراف الكلي للألواح تحت أحمال الانحناء. بينما ، في دراسة عملية ، تم تصنيع عينات الواح ذات كثافات نواة مختلفة في توى بتكوينات سداسية وثلاثية وثمانية الأضلاع متداخلة ، باستخدام تقنية الطباعة ثلاثية الأبعاد مع مادة PLA (حمض polylactic) عن طريق ضبط قيمة كثافة النواة إلى ثلاثة مقادير (105) كجم / م³ ، 132 كجم / م³ ، و 160 كجم / م³ باستخدام حجم الخلية كمعلمة تحكم وحيدة في قيمة الكثافة. تخضع هذه العينات لاختبار الانحناء وفقًا للمعيار (ASTM C393-00) لإيجاد الانحراف والصلابة وبالتالي تأثير التباين في كثافة النوى لكل نوع. ثم يتم مقارنة الاستنتاجات النظرية ، متبوعة بنتائج الاختبارات التجريبية ، مع النتائج العددية الناتجة عن برنامج المحاكاة "Ansys" لتقديم فكرة واضحة عن كيفية تأثير كثافة النوى على الخصائص الميكانيكية للألواح وكشف عن نوع النواة المتفوقة. بالإضافة إلى ذلك ، تتأثر مقاومة الصدمات بشكل كبير بتغير كثافة النواة ، ومن أجل استكشاف ذلك ، تعرضت العينات ذات الكثافة النوى المختلفة لمحاكاة اختبار الاسقاط من برج. علاوة على ذلك ، تم إجراء تقييم عددي لتحديد تأثير كثافة النوى على الترددات الطبيعية واستكشاف سلوك الألواح تحت الأحمال المتكررة. أخيرًا ، أظهرت النتائج التجريبية أن الزيادة في كثافة النواة بنسبة 25.7% و 52.4% تؤدي إلى مزيد من الصلابة بنسبة 8.14% و 16.75% في النوى السداسية ، و 8.43% و 28.1% في النوى الثلاثية ، و 10.94% و 19.04% في النوى المثلثة. إلى جانب ذلك ، فإن النوى المثلثة والمثلثة أكثر صلابة من النوى السداسية. فيما يتعلق باستكشاف تأثير الاصطدام ، يمكن استنتاج أن زيادة كثافة النوى زادت من مقاومة الألواح للصدمات وأن النوى السداسية المنتظمة لها مقاومة صدمة أكبر من النوى الثلاثية. بالإضافة إلى ذلك ، أظهرت النتائج أن الزيادة في كثافة النوى بنسبة 25.7% و 52.4% تؤدي إلى انخفاض طفيف في قيمة الترددات الطبيعية ، على الأقل في المود الأول.



جمهورية العراق
وزارة التعليم العالي و البحث العلمي
جامعة كربلاء
كلية الهندسة
قسم الهندسة الميكانيكية

التحقيقات النظرية والتجريبية لألواح الطباقية المطبوعة ثلاثية الأبعاد المستخدمة في هيكل الطائرة

رسالة مقدمة الى مجلس كلية الهندسة / جامعة كربلاء وهي جزء من متطلبات نيل درجة الماجستير في
علوم الهندسة الميكانيكية

المؤلف:

حيدر عبد الجبار صباح

بكالوريوس في علوم الهندسة الميكانيكية لسنة 2002

باشراف :

الأستاذ الدكتور محسن جبر جويج

المدرس الدكتور احمد قاسم حسين